EXPERIMENTAL INVESTIGATION OF FAILURE IN THIN RINGS SUBJECTED TO UNIFORM EXTERNAL PRESSURE

Jules Henry Demyttenaere
and
William Joseph Norris

EXPERIMENTAL INVESTIGATION OF FAILURE IN THIN RINGS SUBJECTED TO UNIFORM EXTERNAL PRESSURE

by

JULES HENRY DEMYTTENAERE, LTJG., U.S.NAVY
B.S., United States Naval Academy
(1949)

8854
on spine:

DEMYTTENAERE U.S.NAVY
Academy

1954

THESIS
D3

IENT OF THE

REE OF

Letter on front cover:

EXPERIMENTAL INVESTIGATION OF
FAILURE IN THIN RINGS SUBJECTED
TO UNIFORM EXTERNAL PRESSURE

ECHNOLOGY

JULES HENRY DEMYTTENAERE
and
WILLIAM JOSEPH NORRIS

8854
on spine:

DEMYTTENAERE

1954

THESIS
D3

Letter on front cover:

EXPERIMENTAL INVESTIGATION OF
FAILURE IN THIN RINGS SUBJECTED
TO UNIFORM EXTERNAL PRESSURE

JULES HENRY DEMYTTENAERE
and
WILLIAM JOSEPH NORRIS

'IGATION OF FAILURE IN THIN
'FORM EXTERNAL PRESSURE

.AERE, LTJG., U.S.NAVY
cates Naval Academy
(1949)

and

WILLIAM JOSEPH NORRIS, LTJG., U.S.NAVY
B.S., United States Naval Academy
(1949)

SUBMITTED IN PARTIAL FULFILLMENT OF THE

REQUIREMENTS FOR THE DEGREE OF

NAVAL ENGINEER

at the

MASSACHUSETTS INSTITUTE OF TECHNOLOGY

May, 1954

EXPERIMENTAL INVESTIGATION OF FAILURE IN THIN RINGS SUBJECTED TO UNIFORM EXTERNAL PRESSURE

by

JULES HENRY DEMYTTENAERE, LTJG., U.S.NAVY
B.S., United States Naval Academy
(1949)

TITLE: EXPERIMENTAL INVESTIGATION OF FAILURE IN THIN RINGS SUBJECTED TO UNIFORM EXTERNAL PRESSURE

AUTHORS: J. H. Demyttenaere, LTJG., U.S.N., and
W. J. Norris, LTJG., U.S.N.

Submitted to the Department of Naval Architecture and Marine Engineering on May 24, 1954, in partial fulfillment of the requirements for the degree of Naval Engineer.

ABSTRACT

The object of this thesis was to investigate experimentally the strain distributions and ultimate failures in thin circular and non-circular aluminum rings subjected to uniform external pressure.

A test apparatus was designed to permit the application of hydraulic pressure to the outer circumference of a ring placed between two sheets of Plexiglas. The small clearance between the edges of the ring and the Plexiglas was sealed by a continuous rubber gasket of slightly greater width fitted around the outer circumference of the ring. Except for friction at the gasket-Plexiglas interface, the ring was free of restraint.

Nine rings of aluminum alloy, 61S-T6, were tested to collapse; the variable in this series was out-of-roundness. Correlation between measured and predicted strains was obtained in five of the six rings in which the assumptions of the prediction were valid. A somewhat arbitrary strain distribution was observed in the two most circular rings. The four rings of moderate out-of-roundness collapsed very near predictions based upon a criteria related to the maximum stress level in the outer fibers while the three rings of relatively large out-of-roundness failed at pressures somewhat higher than predicted. The two most circular rings collapsed near a computed pressure when the minimum rather than average section thickness was used in the calculation. Collapse pressures were predicted most accurately when the stress used in conjunction with the failure criteria was defined by the point on the stress-strain curve at which marked non-linearity occurred.

An analysis of the results indicates that strain distributions in an out-of-round ring loaded by uniform external pressure can be predicted with satisfactory

AUTHORS: 1. A. Departmaster, USAO., U.S.A., and
E. J. Works, CPIO., U.S.A.

Submitted to the Department of Navy Aeronautics and Marine Engineering on May 24, 1954, in partial fulfillment of the requirements for the degree of Naval Engineer.

ABSTRACT

The object of this thesis was to investigate whether the structural characteristics and ultimate failure of thin circular and non-circular plates subjected to uniform external pressure.

A test structure was designed to permit the application of uniform pressure to any curved circumference of a flat plated between two sheets of Plexiglas. The result clearance between the edges of the flat and the Plexiglas was sealed by a continuous rubber gasket of slightly greater width than the flat around the outer circumference of the flat. Except for fixation of the Plexiglas interfaces, the flat was free of restraint.

Four flats of aluminum alloy, 61S-T6, were tested to collapse; the ellipse is only tested was out-of-specification. Correlation between observed and predicted strains was obtained in five of the six cases in which the deformations were measured at the center of the flat. A numerical solution of the Navier-Stokes equations was developed in the two dimensional plane. The time-cycle of loading and out-of-roundness collapse was near predicted using a criteria related to the maximum stress level in the outer fibers while this factor was found at times of initially local out-of-roundness failed at pressures somewhat higher than predicted. The two most effective criteria for failure were a combined pressure and strain criterion based on the maximum strain theory and a modified Southwell coefficient. Oscillographic recordings were used in the majority of the tests. Oscillographic recordings were used in the majority of the tests. Oscillographic recordings were used in the majority of the tests

accuracy provided the assumptions made in the prediction are satisfied; namely, that the thickness to diameter ratio be the order of 0.0285 and that the initial configuration assumed is actually predominate. A failure criteria based upon the stress level in the outer fibers will, when the assumptions above are fulfilled, predict collapse quite accurately in rings of out-of-roundness to thickness ratio between 0.10 and 0.30. At larger values of out-of-roundness the criteria is conservative but not over cautious.

It is recommended that the experimentation be extended to include a quantitative investigation of the effects of deviations from a basic two lobe out-of-roundness such as might be obtained in a practical situation. Such an investigation should be conducted using rings of constant thickness in order to avoid many of the unnecessary complications encountered in the analysis of data obtained in this thesis.

Cambridge, Massachusetts
May 24, 1954

Professor Leicester F. Hamilton
Secretary of the Faculty
Massachusetts Institute of Technology
Cambridge, Massachusetts

Dear Sir:

In accordance with the requirements for the degree of Naval Engineer, we submit herewith a thesis entitled, "Experimental Investigation of Failure in Thin Rings Subjected to Uniform External Pressure."

ACKNOWLEDGMENTS

The authors wish to express their appreciation to those individuals at the Massachusetts Institute of Technology, Boston Naval Shipyard, and the David Taylor Model Basin, who so generously gave their time and advice so that the objectives of this thesis might be accomplished.

Specifically the authors wish to thank Dr. E. Wenk, Jr., of the David Taylor Model Basin, who originally posed many of the problems involved; Dr. W. W. Murray, of the Massachusetts Institute of Technology, and his assistant Mr. Peter Stein for their most helpful advice on a multitude of details.

The authors are particularly grateful to their Thesis Supervisor, J. H. Evans, Assistant Professor of Naval Architecture, Massachusetts Institute of Technology, for his encouragement and advice during the progress of the thesis.

ACKNOWLEDGMENTS

The authors wish to express their appreciation to those individuals at the Massachusetts Institute of Technology, Boston Naval Shipyard, and the David Taylor Model Basin, who so generously gave their time and advice to make the objectives of this thesis more accomplished.

Specifically the authors wish to thank Dr. S. Yeh, Jr., of the David Taylor Model Basin, who originally posed many of the problems investigated; Dr. W. Murray, of the Massachusetts Institute of Technology, and his assistant Mr. Peter Stein for their helpful advice on a multitude of details.

The authors are particularly grateful to their thesis supervisor, A. D. Bruns, Associate Professor of Naval Architecture, Massachusetts Institute of Technology, for his encouragement and advice during the progress of the thesis.

SYMBOLS AND ABBREVIATIONS

The following symbols and abbreviations are used throughout this report:

b = Width of ring, in inches

D = Mean diameter measured to neutral axis, in inches

E = Modulus of elasticity - initial slope of stress-strain curve, psi.

ε = Compressive strain, inches/inch or micro-inches/inch.

h = Thickness of ring, in inches.

I = Moment of inertia of ring cross-section about neutral axis, in $in.^4$

P = Pressure, psi.

$P_{crit.}$ = Collapse pressure of a circular ring, psi.

psi. = Pounds per square inch.

R = Mean radius to neutral axis of ring, in inches.

R_o = Mean radius to outer circumference of ring, in inches.

σ = Compressive stress, psi.

σ_y = 0.2% proof stress, psi.

θ = Angular coordinate to designate positions on ring, in degrees.

u_o = Two-lobe out-of-roundness, maximum deviation from a true circle of the same perimeter as the two-lobe configuration, in inches.

u_1 = Three-lobe out-of-roundness, inches

u_2 = Four-lobe out-of-roundness, inches

SYMBOLS AND ABBREVIATIONS

The following symbols and abbreviations are used throughout this report:

β = angle of ring, in radians

λ = mean diameter measured to neutral axis, in inches

μ = modulus of elasticity - initial slope of stress-strain curve, psi.

ξ = compressive strain, inches/inch or micro-inches/inch.

ρ = curvature at crot, in inches.

ΣI = moment of inertia of ring cross-section about neutral axis, in in.^{4}

Σ = pressure, psi.

$\Sigma_{crit.}$ = collapse pressure of a circular ring, psi.

$\sigma_{cl.}$ = tensile per square inch.

θ = mean radius to neutral axis of ring, in inches.

R_o = mean radius to outer circumference of ring, in inches.

σ_c = compressive stress, psi.

σ_2 = 0.2% proof stress, psi.

θ = angular coordinate to designate positions in ring, in degrees.

θ_0 = two-lobe out-of-roundness, maximum variation from a true circle of the centre position of the centre-line configuration, in inches.

θ_1 = three-lobe out-of-roundness, inches

θ_2 = four-lobe out-of-roundness, inches

Experimental Investigation of Failure in Thin Rings Subjected to Uniform External Pressure

TABLE OF CONTENTS

Experimental Investigation of Buffets in Jets
Study Supported by Jaffee Aerospace Laboratory

TABLE OF CONTENTS

TABLE OF CONTENTS (Continued)

I.

INTRODUCTION

Objective

The objective of this thesis is to investigate experimentally the strain distributions and ultimate failures obtained in thin circular and non-circular aluminum rings subjected to uniform external pressure.

Background

The slender column in axial compression is generally cited as the classic example of a buckling failure. The behavior of such axially loaded columns was subjected to an early theoretical analysis, and at the same time numerous investigators supplied experimental data relevant to the problem. The experimentation served two purposes. First, the conclusions substantiated the basic concepts and accuracy of the theoretical analysis. Second, certain practical aspects of the problem were magnified. Thus, through an analysis of experimental data and an appreciation of the difficulty in obtaining a perfectly loaded column, Moncrieff (1) was able to propose a practical criteria for column strength which included the assumption of an inherent eccentricity.

The failure of thin rings subjected to uniform external pressure is analogous to the buckling of columns.

I.

INTRODUCTION

Objective

The objective of this thesis is to investigate experimentally the static characteristics and ultimate failures obtained in thin circular and non-circular plywood tube subjected to uniform external pressure.

Background

The slender column in axial compression is commonly cited as the classic example of a buckling failure. The behavior of such axially loaded columns was observed to be early theoretical analysis, and at the same time numerous investigators supplied experimental data relevant to the problem. The circumscription marked the beginning. First, the conclusions established the basic concepts and accuracy of the theoretical analysis. Second, certain practical aspects of the problem were neglected. That, through an analysis of experimental data and by extrapolation of the difficulty in obtaining a perfectly formed column, Donovan (1) was able to propose a practical criteria for column strength which included the consideration of an inherent eccentricity.

The failure of thin shells subjected to uniform external pressure is analogous to the buckling of columns.

The buckling of such uniformally loaded rings has been treated theoretically by investigators as early as Levy (2) and as recent as Boresi (3). In addition a clear presentation of the problem is given by Timoshenko (4). Despite the extensive theoretical analysis, experimentation has been lacking. In a search of the literature, the authors found no instance of a ring being collapsed experimentally under a uniform external load.

The lack of experimental data relative to the ring problem may be partially explained by the following:

1. The use of the ring as a structural member is not so widespread as the column. Hence the need for usable data was not pressing.
2. Many of the conclusions formulated as a result of column analysis were applicable to the ring problem.
3. The buckling of a cylinder subjected to external pressure is closely related to the buckling of a ring. Obviously much of the data gleaned from failure of cylinders also applies to rings. The collapse of a cylinder may be effected simply and conveniently in the laboratory.
4. A free ring loaded with uniform external pressure offers a difficult problem in the design of a test apparatus.

The buckling of such unsymmetrically loaded rings was treated theoretically by Timoshenko as early as 1913 (2) and as recent as Bureau (3). In addition a clear presentation of the problem is given by Timoshenko (4). Despite the extensive theoretical analysis, experimentation has been lacking. In a search of the literature, the authors found no instance of a ring being collapsed experimentally under a uniform external load.

The lack of experimental data relative to the ring problem may be partially explained by the following:

1. The use of the ring as a structural member is not as widespread as the column. Hence the need for usable data was not pressing.
2. Many of the conclusions formulated as a result of column analysis were applicable to the ring problem.
3. The buckling of a cylinder subjected to external pressure is closely related to the buckling of a ring. Obviously much of the data gleaned from tests of cylinders also applies to rings.
4. The collapse of a cylinder may be effected simply and conveniently in the laboratory.
5. A ring ring loaded with uniform external pressure offers a difficult problem in the design of a test apparatus.

Despite the apparent validity of the theoretical analysis of ring buckling and the availability of related experimental data, there is a need for experimentation devoted specifically and directly to the collapse of a thin ring. This need arises not merely from the satisfaction to be gained by proving the validity of the concepts or assumptions of the pertinent theory but from a desire to obtain a practical perspective. Thus, some peculiarity of the ring problem may yet be unrecognized; practical expedients such as the assumption of an inherent out-of-roundness may be necessary. Furthermore, there is need for a substantial and tested criteria of failure which may or may not be related to the stress level at the inner or outer surface of the ring. It is to be appreciated that in out-of-round rings, failure results when stable equilibrium is not possible between an internal and external bending moment and is not a direct result of some specified stress in the outer fibers. In addition, the ring provides a convenient means of studying and evaluating out-of-roundness not only in rings but also in cylinders. In a theoretical approach out-of-roundness may be represented very simply by a Fourier series; there is need for a simple, yet reliable, measure of out-of-roundness which has a practical value.

Problem

The authors have undertaken the task of obtaining and

evaluating experimental data of the type referred to above.

Implied in this assignment are the following specific problems:

1. The design and construction of a test apparatus which will permit the application of a uniform external load to an essentially free ring.
2. The instrumentation of a ring such that the strain distribution may be determined.
3. A comparison of measured strain distribution and failure loads with theoretical predictions.
4. A review of experimental results for the purpose of pointing out the practical aspects of the ring buckling problem.

II.

PROCEDURE

Outline

The procedure followed in this thesis is to be presented under the following subheadings:

(a) Selection of Material for Construction of Rings

(b) Manufacture of Rings

(c) Ring Dimensions and Instrumentation

(d) Design and Manufacture of Test Apparatus

(e) Proof Test of Apparatus

(f) Test of Rings

(g) Test of Compression Specimens

(h) Evaluation of Data

(i) Correlation of Data

11.

PROCEDURE

Outline

The procedure followed in this thesis is to be presented under the following subheadings:

(a) Selection of Material for Construction of Rings

(b) Manufacture of Rings

(c) Ring Dimensions and Instrumentation

(d) Design and Manufacture of Test Apparatus

(e) Proof Test of Apparatus

(f) Test of Rings

(g) Test of Compression Specimens

(h) Evaluation of Data

(i) Correlation of Data

Selection of Material for Construction of Rings

Rings were machined from a length of 9" aluminum alloy (61S-T6)tubing of 1/4" wall thickness. The actual outside diameter as determined by the authors was 9.016".

The decision to use aluminum alloy test rings was based upon the following considerations:

1. To properly correlate measured and predicted strain distributions it was necessary to select a material in which the stress-strain relationship was essentially linear over a considerable range of stress. Aluminum alloy 61S-T6 was suitable in this respect since the estimated 0.2% proof stress was 40,000 psi. (5).
2. The predicted failure pressures for rings of reasonable diameter and thickness were satisfactory. Reasonable dimensions were defined as any diameter and thickness of tubing or pipe which was available and which could be accommodated by the facilities in the testing laboratory. A relatively high failure pressure was desirable in that sufficient accuracy could be obtained without the use of an extremely sensitive pressure measuring device. Yet the maximum pressure should not be so high as to require an excessively complicated and expensive test apparatus.

Selection of Material for Cryogenic Service

Rings were machined from a length of 3" diameter alloy (Ti-6Al-4V)tubing or 1/4" wall thickness. The actual outside diameter was determined by the relation mm 3.048".

The decision to use aluminum alloy test rings was based upon the following considerations:

1. To properly correlate measured and predicted strain distributions it was necessary to select a material in which the stress-strain relationship was essentially linear over a considerable range of stress. Aluminum alloy 6Al-4V was suitable in this respect since the estimated 0.2% proof stress was 40,000 psi. (5).

2. The predicted failure pressures for rings of reasonable diameter and thickness were unsatisfactory. Reasonable dimensions were defined as any diameter and thickness of tubing or pipe which was available and which could be accommodated by the facilities in the testing laboratory. A relatively high failure pressure was desirable in that auxiliary equipment would be operated without the use of an extremely sensitive pressure measuring device. Yet the maximum pressure should not be so high as to require an excessively configured and expensive test apparatus.

Manufacture of Rings

The aluminum alloy tubing as received was cut into sections of 2 1/2" to 3 1/2" lengths. Out-of-roundness was then intentionally introduced in the majority of these pieces by placing the individual sections in a loading machine and applying a load. When the desired permanent set had been obtained the load was removed. Since essentially circular rings were to be machined from the remainder of the sections no deformation was introduced. In this manner a range of out-of-roundness was obtained which varied from u_o = 0.007" in the tubing as received to u_o = 0.296" in the section with the greatest intentional deformation.

As a result of the permanent set imposed, there existed an unknown residual stress at points stressed above the elastic limit. To insure linearity of measured strains over a maximum range, the sections were subjected to a solution heat treatment followed by the precipitation heat treatment required to obtain alloy 61S-T6. Uniformity of properties was insured by heat treating, as a group, all sections plus the material from which compression specimens were to be manufactured.

Wooden plugs about 1 inch in thickness were tailored to fit into one end of each section in order to facilitate final machining and to avoid distortion caused by the clamping jaws of the lathe. Rings of specified width were

Manufacture of Rings

The aluminum alloy tubing as received was cut into
sections of 7 1/2" to 9 1/2" length. Out-of-roundness
was then intentionally introduced in the majority of these
pieces by placing the individual sections in a loading
machine and applying a load. When the desired permanent
set had been obtained the load was removed. Since essentially
circular rings were to be machined from the remainder of the
sections no deformation was introduced. In this manner a
range of out-of-roundness was obtained which varied from
u_o = 0.002" in the tubing as received to u_o = 0.250" in
the section with the greatest intentional deformation.

As a result of the heat-treatment set imposed, there existed
an unknown residual stress at points stressed above the
elastic limit. To insure linearity of measured strains over
a maximum range, the sections were subjected to a modified
heat treatment followed by the precipitation heat treatment
required to obtain alloy 6ln-T6. Uniformity of properties
was insured by heat treating, as a group, all sections plus
the material from which compression specimens were to be
manufactured.

Wooden plugs about 1 mm to thickness were cemented
to the ends and a seam section in order to restrict the
final machining and to avoid distortion caused by the
clamping jaws of the lathe. Rings of specified width were

then cut from the sections; this width was determined by a direct measurement of the clearance between the surfaces of the annular test chamber in the completed test apparatus. The rings as cut were generally 0.444" to 0.446" in width, the maximum deviation for a single ring being 0.001". The thickness of the rings remained the same as received.

Ring Dimensions and Instrumentation

The outside diameter of each ring was found by fitting a wire 0.01" in diameter around the outer circumference. The wire was scribed and then measured between the scribe marks on a 36" steel rule. An outside radius was computed by dividing the measured circumference by 2π and correcting for the thickness of the measuring wire. All radii thus determined were averaged to give a mean outside radius (4.508") for use in the computations.

The measuring wire was scribed at intervals of 30 degrees of arc length and again fitted around each ring. The scribe marks were transferred to the aluminum alloy. For those rings in which deformation had been introduced care was taken to locate one of the scribe marks as close as possible to the point of maximum diameter. The twelve stations so determined were designated 0° through 330° in 30° increments, with 0° at a point of maximum diameter. The thickness and width at each station were measured with small micrometers

while the outside diameter was measured at stations and half stations with large outside micrometers.

Baldwin SR-4, type A-7, strain gages were cemented to the inner surface of the ring at each station with the gage length along the circumference. Photograph No. 1 shows the strain gages in position on the ring after the leads had been soldered in place. The leads were passed through the bottom of the test apparatus and connected to the multiple selector switchbox which in turn was connected to the strain indicator. The dummy gage was attached to a scrap piece of aluminum alloy which was placed in the vicinity of the test apparatus. Leads from the dummy were connected to the switchbox.

Design and Manufacture of Test Apparatus

The design of the apparatus and its associated equipment can be understood from photographs Nos. 2, 3, 4 and Figures I and II. The bucket pump had been previously tested up to a pressure of 1600 psi and was considered to be of sufficient capacity to supply oil to the pressure chamber enclosing the ring.

The test apparatus was made by the Mechanical Engineering Department machine shop at the Massachusetts Institute of Technology to plans and specifications furnished by the authors. It is to be noted that provision was made for a

made the outside diameter was measured at various and fait
sections with large outside micrometers.

Holders RH-4, type B-7, strain gages were cemented to
the inner surface of the ring at each station with the gage
leads along the circumference. Photograph No. 1 shows the
strain gages in position on the ring after the leads had
been soldered in place. The leads were passed through the
bottom of the test apparatus and connected to the multiple
selector switchbox which in turn was connected to the strain
indicator. The dummy gage was attached to a scrap piece of
aluminum alloy which was placed in the vicinity of the test
apparatus. Leads from the dummy were connected to the
switchbox.

Design and Manufacture of Test Apparatus

The design of the apparatus and its associated equipment
can be understood from photographs Nos. 2, 3, 4 and
Figures I and II. The bucket pump had been previously tested
up to a pressure of 1600 psi and was considered to be of
sufficient capacity to supply oil to the pressure chamber
enclosing the ring.

The test apparatus was made by the Mechanical Engineer-
ing Department machine shop at the Massachusetts Institute
of Technology to plans and specifications furnished by the
author. It is to be noted that perfection was made for a

Photograph No. 1

RING WITH STRAIN GAGES AND LEADS

Photograph No. 2

TEST APPARATUS

Photograph No. 3

TEST APPARATUS

Photograph No. 4

TEST APPARATUS WITH CATHETOMETER MOUNTED

FIGURE I

TEST APPARATUS

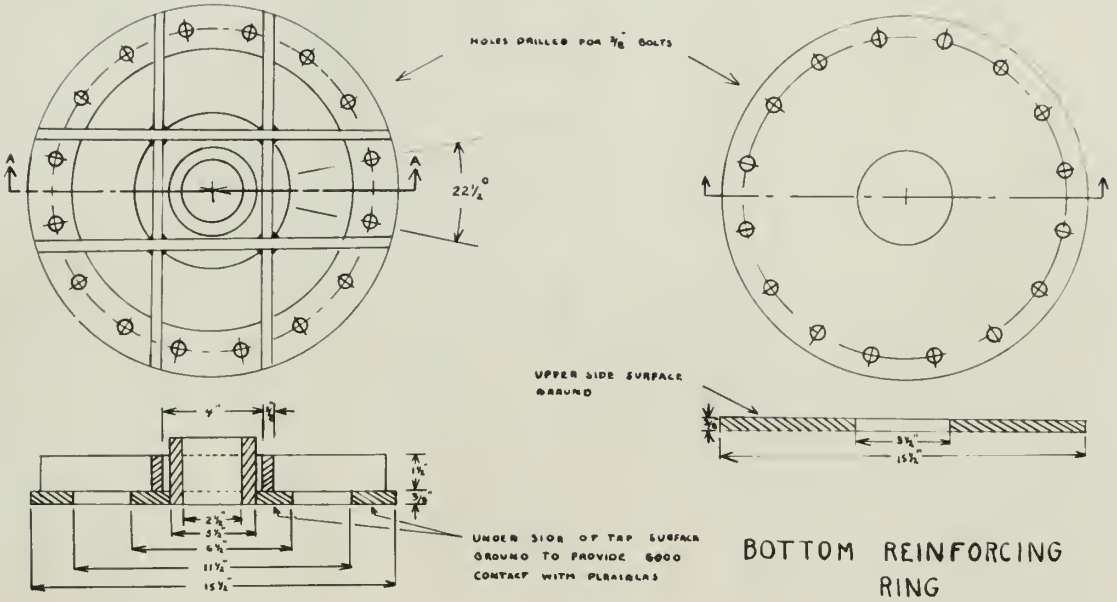

TOP ASSEMBLY

BOTTOM REINFORCING RING

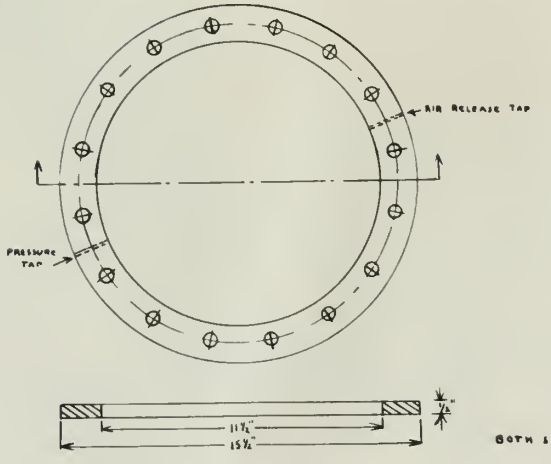

SPACER RING

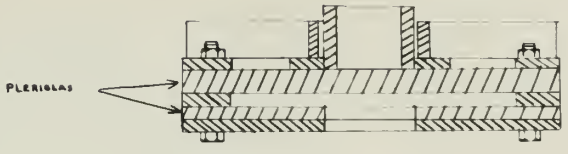

CROSS SECTION OF ASSEMBLED TEST APPARATUS

4/13/54 YHD -297

FIGURE II

CATHETOMETER MOUNTING

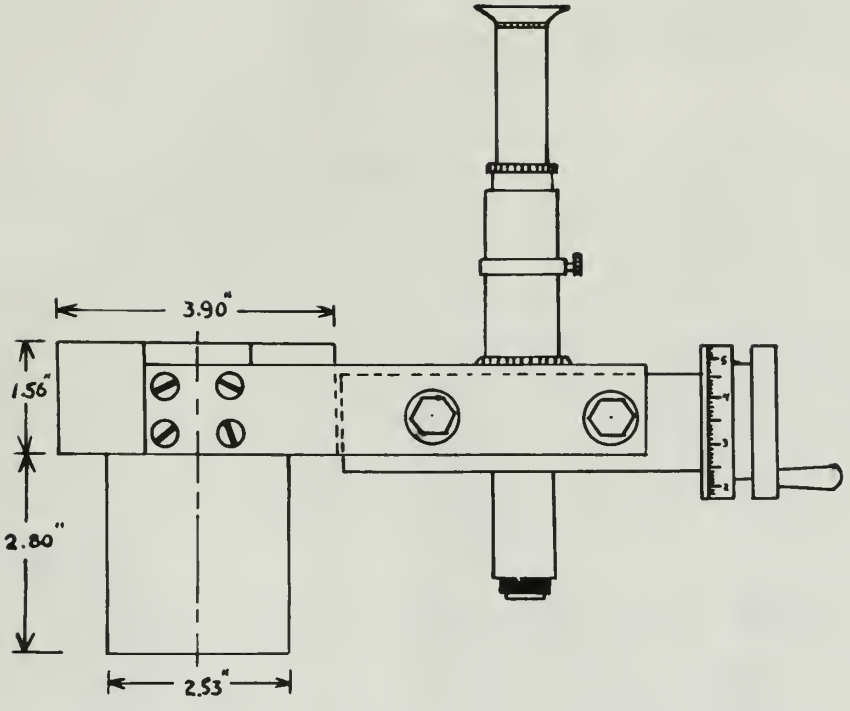

SIDE VIEW

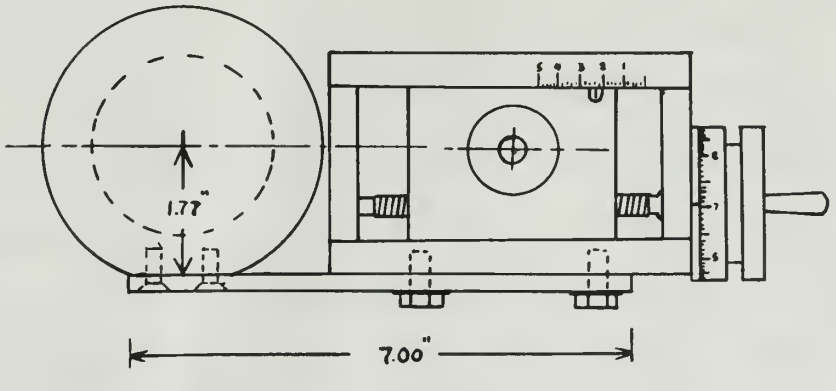

TOP VIEW

4/24/54 MD - WJM

viewing chamber which would permit inspection of the rings during application of pressure. The pressure gage was furnished by the Department of Mechanical Engineering, MIT, and calibrated by the authors.

Proof Test of Apparatus

Upon completion of the test chamber by the machine shop, the complete test apparatus as indicated in Photographs Nos. 2, 3, and 4 was assembled and proof tested by the authors. Two preliminary test rings were machined from a section of the original aluminum tubing for use in this phase of the testing.

To maintain pressure in the test chamber behind the aluminum rings, a gasket of width slightly greater than 1/2" was placed around the outer circumference of the ring; several types of gasket material were tried. In each case the gasket material was cut to size, glued to the outer surface of the ring, and bound lightly by several strands of light string lying along the circumference. The ring was then placed in the test apparatus and the upper Plexiglas surface and top web assembly were bolted down. Oil was pumped into the test chamber with the bucket pump and the air vented through the air release tap. Pressure was built up behind the ring in the test chamber until, in most cases, the gasket material extruded between the Plexiglas surfaces

the general material adopted between the Invictus materials
on hauled the ring in the test chamber until, in most cases,
air evacuated through the air release tap. Pressure was built
up by pumping into the test chamber with the bucket pump and the
burnose and top was assembly were bolted down. Oil was
then placed to the test apparatus and the other Invictus
pipe return joint close the circumference. The ring was
marked of the ring, and pumping lightly by several strokes of
the pump material was cut to size, fixed to the outer
several types of gasket material were tried. In each case
was placed around the outer circumference of the ring;
flushing rings, a gasket of width slightly greater than 1/2"
the original aluminum tubing for use in this phase of the
testing.

To maintain pressure in the test chamber during the
Two preliminary test rings were machined from a section of
the complete test apparatus as indicated in Photographs
Nos. 2, 3, and 4 was assembled and proof tested by the authors.

Upon completion of the test chamber by the machine shop,
and delivered to the authors.

Proof Test of Apparatus

Turbines by the Department of Mechanical Engineering, MIT,
during application of pressure. The pressure gage was
viewing chamber which permit inspection of the rings

and the edges of the ring. As a result of these trials, the best gasket material for sealing the ring edges appeared to be a rubber gasket cut from an ordinary truck tire inner tube approximately 9" in diameter. This type of gasket was used throughout the remainder of the proof tests and the final tests. Pressures up to 875 psi. were maintained in the test chamber using this gasket.

An Ames dial gage was mounted on the steel web assembly midway between the top inner and outer backing up rings to determine the maximum deflection of the Plexiglas surface as pressure was applied. A maximum deflection of 0.007" occurred at 875 psi. The deflection occurring at 500 psi. was of the order of 0.004".

It became apparent during these tests that some type of lubricant was necessary to eliminate or reduce to a minimum the friction between the rubber gasket and the Plexiglas surfaces. Several types of lubricant were tried and the best found to be black rubber-to-metal cement. Strains at a particular station were found to vary with the lubricant and gasket material when the same pressure was applied.

The cathetometer was mounted during the preliminary test phase and attempts were made to take deflection readings. Unfortunately the cathetometer proved impractical as a means

of reading deflection for several reasons, viz.

1. The slight deflection of the upper Plexiglas surface distorted the ring as seen through the eye piece of the cathetometer.
2. The use of black rubber-to-metal cement as a lubricant obscured the aluminum ring in the test chamber when oil was introduced.

The proof testing period was of infinite value to the authors in planning and carrying out the final tests of the circular and non-circular rings.

Test of Rings

One result of the proof testing was the formulation of a standard test procedure. As a consequence, the remainder of the tests were made in a minimum amount of time and with little difficulty.

Nine rings were tested in accordance with the following steps:

1. Leads were soldered to strain gages, threaded through the bottom of the test chamber, and connected to terminals on the back of the multiple selector switchbox.
2. Black rubber-to-metal cement was applied to the rubber gasket and outer circumference of the ring. (Cement allowed to dry 3-5 minutes).
3. The rubber gasket was slipped around the outer

circumference of the ring and secured in place by four strands of light string. The gasket was adjusted so that the bevels extended an equal distance beyond the edges of the ring.

4. A thin film of #40 S.A.E. motor oil was applied to the inner Plexiglas surfaces.
5. The ring was centered in the test chamber.
6. The upper Plexiglas plate was slipped over the bolts and held down firmly by hand while the top web assembly was lowered into place.
7. All bolts were tightened.
8. Initial zero readings were set on all strain gages by adjusting switchbox set screws.
9. Air was vented through the air release tap while the test chamber was being filled with oil from the bucket pump.
10. Pressure in the chamber was increased in increments of 50 to 100 psi. depending upon the expected collapse pressure of the particular ring, 100 psi. increments being used for the more circular rings and 50 psi. increments for the more out-of-round rings. Strain gage readings were taken at each pressure increment.
11. Because the collapse of the more circular rings occurred rather quickly, the pressure was maintained

operated machine quickly, the pressure was maintained
at 50 psi. Increments for the more out-of-round
items. Static wear readings were taken at each
pressure increment.

11. Observe the readings of the wear gitometer after
completing wear test, the pressure was maintained
at 50 psi. Increments for the more out-of-round
items. Static wear readings were taken at each
pressure increment.

12. Observe the readings of the wear gitometer after
completing wear test, the pressure was maintained
at 50 psi. Increments for the more out-of-round
items. Static wear readings were taken at each
pressure increment.

momentarily at 5 psi. increments when the ring was near collapse. The collapse of a significantly out-of-round ring generally proceeded at a very slow rate. In this case the strain indicator was connected to read the maximum strain. Pressure was then increased in steps of 5 psi. or smaller, each pressure being maintained until the strain indication steadied.

12. When the strain indicator needle did not steady, failure occurred. Failures in the more circular rings were evidenced by an immediate drop in pressure and obvious deformations.

Collapse pressure was thus defined as that pressure at which static strains could not be maintained. Complete failure of all rings was characterized by large, visible deflections regardless of the rate at which collapse proceeded; once complete failure occurred the ring would not again sustain collapse pressure.

Test of Compression Specimens

The stress-strain curve for the material used in the fabrication of the rings for this investigation was determined by means of the "Single Thickness" compression test method. Three specimens of the aluminum alloy (61S-T6) were tested in the compression block as indicated in photographs Nos. 5 and 6. A complete description and

Photograph No. 5

HUGGENBERGER TENSOMETERS MOUNTED
ON SPECIMEN IN COMPRESSION BLOCK

Photograph No. 6

COMPRESSION BLOCK IN LOADING MACHINE

bibliography for this method is given in reference (6). Compression tests in general are also discussed in reference (5).

Evaluation of Data

All data obtained during the testing period can be grouped as follows:

1. Dimensions
2. Pressure at which strains were recorded
3. Pressure at which ring collapsed
4. Strain readings
5. Compression Specimen test data.

With one exception all dimensions recorded were taken with micrometers and can be considered accurate to 0.0005". The circumference, as determined by the scribed wire, was read to the nearest 1/128" on the steel rule. However, the authors felt that the accuracy was of the order of 1/64", one scale division. The accuracy of the average outside radius then becomes 0.0025".

The pressure gage was calibrated by the authors prior to the tests using a dead-weight tester. Two calibration runs were made using increasing pressures and two with decreasing pressures. The maximum deviation from true was found to be 4 psi.; the largest difference between an up reading and a down reading for the same true pressure was also 4 psi. Used in conjunction with a calibration curve

.(6) ɐuɐuǝɟǝɹ ɹo ɹǝʇʇɐɯ ɐ uǝʌǝƃ ɯoɹɟ ǝuᴉʌɐ ǝq ʇnqɯ ʇɐɥʇ ɹo ʇsǝʇ ɹǝʇʇɐɯ ɐ

Compression tests to deform pre-fired specimens to failure (5).

Evaluation of Data

All data obtained during the testing period can be grouped as follows:

1. Dimensions
2. Pressure at which strains were measured
3. Pressure at which ring collapsed
4. Strain readings
5. Compression specimen test data.

With one exception all dimensions recorded were taken with micrometers and can be considered accurate to 0.0005". The circumference, as determined by the scribed mark, was read to the nearest 1/128" on the steel rule. However, the extreme fact that the accuracy was of the order of 1/64", one scale division. The accuracy of the average diameter reading then becomes 0.0025".

The pressure gage was calibrated by the manufacturer prior to its being used a dead-weight tester. Two calibrations were made using increasing pressures and two using decreasing pressures. The maximum deviation from this was found to be 4 psi; the factory difference between an increasing and decreasing pressure for the same true pressure was testing and a dead reading for the same true pressure was also 4 psi. Used in conjunction with a centrifugal pump

the gage was considered to be accurate to ± 2 psi. althougn the accuracy was considerably better over most of the pressure range. During the tests the indicated pressure could be held fairly constant. An accuracy of plus or minus one half a scale division (±2 1/2 psi.) is probably conservative but will be assumed. The accuracy of the recorded pressures at which strain readings were taken then becomes ±5 1/2 psi.

With one additional consideration the above remarks also apply to the accuracy of the recorded collapse pressures. The collapse of rings with significant amounts of out-of-roundness occurred rather slowly. It would seem that the pressure could be inadvertently increased above the true collapse pressure, the only effect being an accelerated failure. However, in these instances the strain gage indicating the greatest strain was checked at small increments of pressure when the ring was near collapse. The pressure was not increased further until the strain gage reading steadied. In the authors' opinion the point of collapse was accurate to - 5 psi. for the very non-circular rings. On the otherhand, failure of the more circular rings occurred rather quickly. During the latter portion of a test run it was customary to pause momentarily at each 5 psi. increment of pressure. Again the authors estimate that the point of collapse was accurate to - 5 psi.

Considering both the accuracy of the pressure reading and the point of failure, the recorded collapse pressure is believed to be within - 10-1/2 psi. or + 5-1/2 psi. of true.

The accuracy of the strain gages used, as stipulated by the manufacturer, was ± 2%. The transverse sensitivity correction was insignificant, being of the order of - 0.05%. An accuracy of one half the smallest scale division on the strain indicator, ± 5 micro-inches per inch , is generally assigned to the switchbox-indicator combination.

As a practical expedient plots of out-of-roundness which are presented in the RESULTS were derived in the following manner; the average diameter was subtracted from the measured diameter at stations and half stations; the difference was divided by two and plotted at diametrically opposite stations. It is to be appreciated that this method will define a symmetrical out-of-roundness curve but is truly representative of the initial configuration only when a symmetrical two lobe pattern predominates.

Correlation of Data

The experimental data is compared to theoretical predictions based upon the following formula:

$$\sigma = \frac{P R}{h} - \frac{6 P R u_o \cos 2\theta}{h^2 (1 - P/P_{crit.})} \qquad (1)$$

Equation (1) was developed for the case of circular tubes in reference (4) but applies equally well to rings; the

Considering both the accuracy of the pressure reading and the point of failure, the recorded collapse pressure is believed to be within - 10-1/2 pct. or + 5-1/2 pct. of true.

The accuracy of the strain gages used, as stipulated by the manufacturer, was ± 2%. The transverse sensitivity correction was insignificant, being of the order of - 0.05%. An accuracy of one half the smallest scale division on the strain indicator, ± 5 micro-inches per inch, is generally assigned to the switchbox-indicator combination.

As a practical alphabet plots of out-of-roundness which are presented in the RESULTS were derived in the following manner; the average diameter was subtracted from the measured diameter at stations and half stations; the difference was divided by two and plotted at diametrically opposite stations. It is to be appreciated that this method will derive a symmetrical out-of-roundness curve but is only representative of the initial modification only when a symmetrical two lobe pattern predominates.

Correlation of Data

The experimental data is compared to theoretical predictions based upon the following formula:

$$\frac{p}{p_0} = \frac{1}{1 - \frac{6 p R n_0^2 \cos 2\theta}{E t (n^2 - 1)^2}} \qquad (1)$$

Equation (1) was developed for the case of elastic tubes in reference (4) but applies equally well to steel; the

assumptions made in the derivation may be found in the same reference. The major qualifications are that the ring be thin and that the initial configuration be given by $(R + u_o \cos 2\theta)$.

For purposes of computation the authors found it convenient to rearrange and modify equation (1)

$$\sigma = \frac{PR_o}{h} + \frac{6\ P\ Ru_o\ h\ E \cos 2\theta}{Eh^3 - 4PR^3} \qquad (2)$$

$$\varepsilon = \frac{PR_o}{Eh} + \frac{6\ P\ Ru_o\ h \cos 2\theta}{Eh^3 - 4PR^3} \qquad (3)$$

Equation (2) was derived directly from equation (1) by the substitution of $3\ Eh^3/12$ for $P_{crit.}$, R_o for R, and rearranging. Equation (3) is obtained by dividing equation (2) by E. The use of the outside radius, R_o, instead of the radius to the neutral axis, R, in the hoop stress term seemed well taken but changed the predicted strains an insignificant amount.

A common criteria for failure is yielding of the outer fibers due to the addition of hoop stress and the maximum bending stress. Then as a basis for comparison of experimental and theoretical collapse pressures in those cases where the out-of-roundness pattern is $u_o \cos 2\theta$, equation (2) can be reduced to

$$\sigma_{max.} = \frac{PR_o}{h} + \frac{6\ PR\ u_o\ h\ E}{Eh^3 - 4PR^3} \qquad (4)$$

assumptions made in the derivation may be found in the same reference. The major qualifications are that the ring be thin and that the initial configuration be given by ($R = R^o \cos 2\theta$).

For purposes of comparison the authors found it convenient to rearrange and modify equation (1)

$$\frac{\sigma}{E^o} = \frac{R}{R^o} + \frac{6\,(1-\mu^2)\,R \cos 2\theta}{Eh^2 - 4Rh^2} \qquad (2)$$

$$\frac{\varepsilon}{\varepsilon^o} = \frac{R}{R^o} + \frac{6\,r\,R^o \cos 2\theta}{Eh^2 - 4Rh^2} \qquad (3)$$

Equation (2) was derived directly from equation (1) by the substitution of $3\,Rh^2/12$ for $I^{orig.}$, R^o for R, and rearranging. Equation (3) is obtained by dividing equation (2) by E. The use of the outside radius, R^o, instead of the radius to the neutral axis, R, in the hoop stress term caused well taken but changed the predicted strains an insignificant amount.

A common criteria for failure is reaching of the outer fibers due to the addition of hoop stress and the bending stress. Then as a basis for comparison of equivalent and theoretical collapse pressures in shells cause where the out-of-roundness defined as R^o over θ, equation (2) can be reduced to

$$\sigma_{max.} = \frac{p}{t}R^o + \frac{6\,(1-\mu^2)}{Eh^2-4Rh^2}\,p\,R^o \qquad (4)$$

When $\sigma_{max.}$ is assumed to be equal to σ_y, the pressure as determined by equation (4) is then the theoretical collapse pressure.

d_{max}. is assumed to be equal to d_2, the clearance between the two adjacent (#1 is when the piston is at the top dead center position).

III

RESULTS

All results presented in this section were derived from data obtained by the authors.

Figure III is a plot of the data obtained during the compression tests of the aluminum alloy specimens and from which the value of Young's Modulus and the yield stress were determined.

Figure IV shows the results of the preliminary test which was made to determine the effect of various lubricants and gaskets upon strain. Lubricant #1 was black rubber-to-metal cement; lubricant #2 was clear rubber cement. Gasket #1 had been used during the Proof Testing; Gasket #2 was of the same dimensions but had not been used previously.

Figures V, VIII, XI, XIV, and XVII show measured and theoretical circumferential strain distributions for one or more pressures. Theoretical curves are based upon equation (3).

Figures VI, IX, XII, XV, and XVIII are plots of out-of-roundness versus circumferential positions.

Figures VII, X, XIII, XVI, and XIX are plots of ring thickness versus circumferential position.

Figures XX-XXVI are a comparison of measured and predicted strains. The experimental points are an average of

III

Results

All results presented in this section were derived from data obtained by the authors.

Figure III is a plot of the data obtained during the compression tests of the aluminum alloy specimens and from which the values of Young's modulus and the yield stress were determined.

Figure IV shows the results of the preliminary test which was made to determine the effect of various lubricants and repeated room strain. Lubricant #1 was black rubber-to-metal cement; lubricant #2 was clear rubber cement. Gasket #1 had been used during the first testing; gasket #2 was of the same dimensions cut and not been used previously.

Figures V, VIII, XI, XIV, and XVII show measured and theoretical circumferential strain distributions for one or more pressures. Theoretical curves are based upon equation (3).

Figures VI, IX, XII, XV, and XVIII are plots of unit-elongation versus circumferential position.

Figure VII, X, XIII, XVI, and XIX are plots of unit-elongation versus meridional position.

Figure XX is a comparison of measured and theoretical strains. The experimental points are an average of

strains read at the 0° and 180° positions, and 90° and 270° positions. The theoretical curves are based upon equation (3).

Figure XXVII shows experimental collapse points plotted on arguments of pressure and the ratio of out-of-roundness to average thickness.

Figure XXVIII is a comparison of experimental collapse pressures with several theoretical predictions. All theoretical curves are based upon equation (4). They differ in that Curve A is plotted for $\sigma_{max} = \sigma_y = 35{,}000$ psi. and $h = h_{ave} = 0.250"$; Curve B is plotted for $\sigma_{max} = 41{,}000$ psi. and $h = h_{ave.} = 0.250"$; Curve C is plotted for $\sigma_{max} = 41{,}000$ psi. and $h = h_{min.} = 0.243"$.

FIGURE III

STRESS STRAIN CURVE

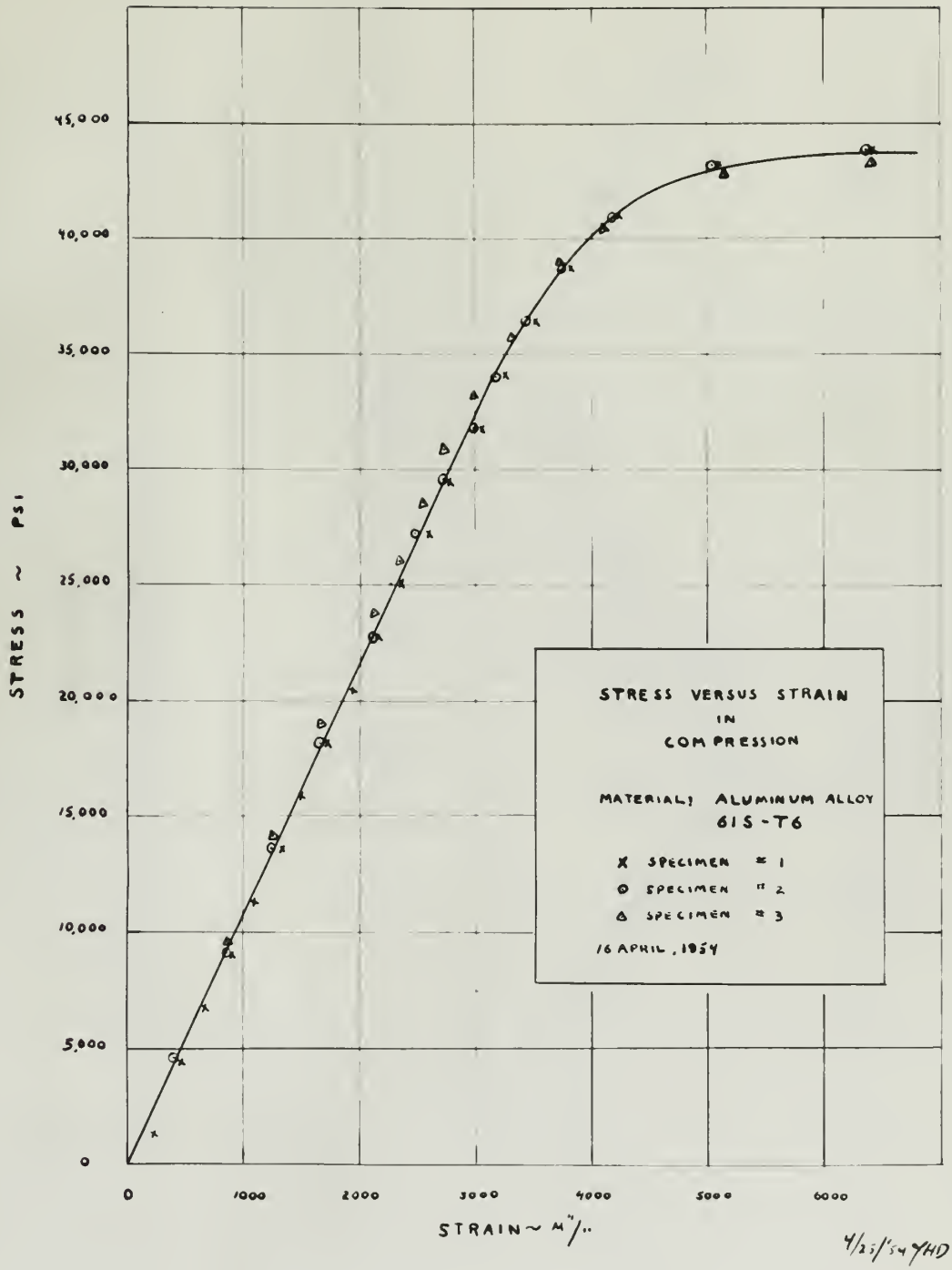

4/25/54 YHD

Figure IV

CIRCUMFERENTIAL STRAIN DISTRIBUTION FOR DIFFERENT LUBRICANTS AND GASKETS
RING NO.-PRELIMINARY TEST

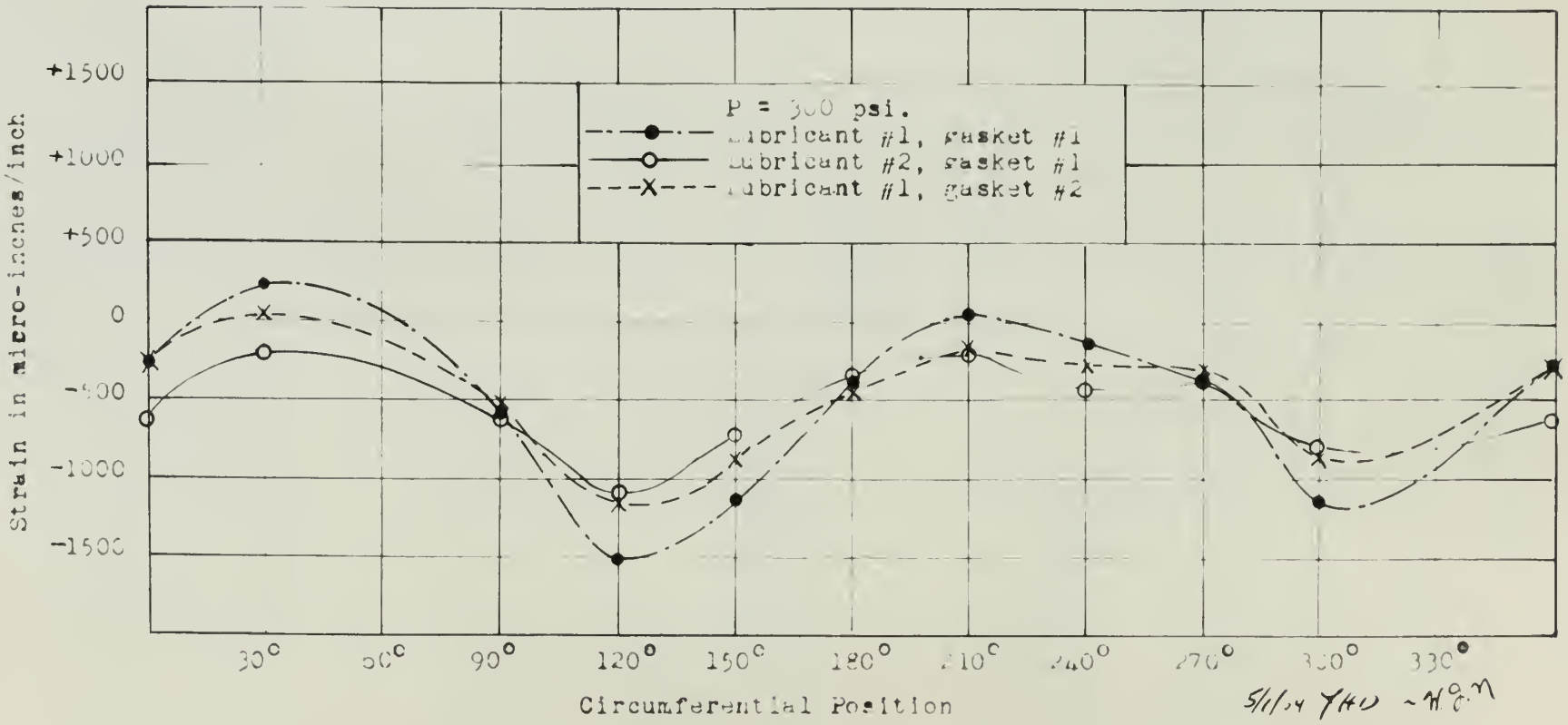

Figure V

CIRCUMFERENTIAL STRAIN DISTRIBUTION ON INNER SURFACE
RING NO. 2 u_o = 0.0118"

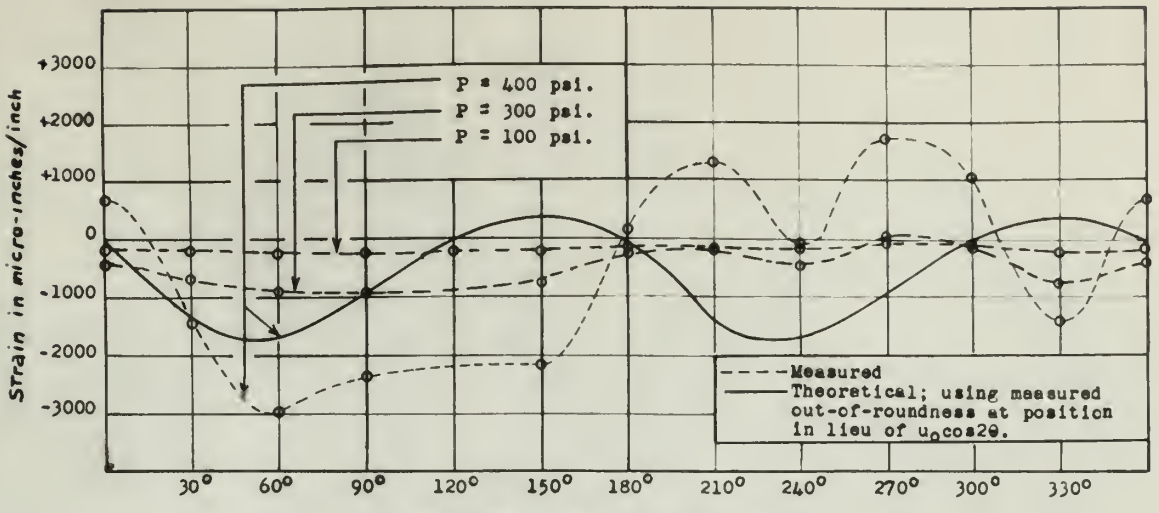

Figure VI

INITIAL CONFIGURATION
RING NO. 2

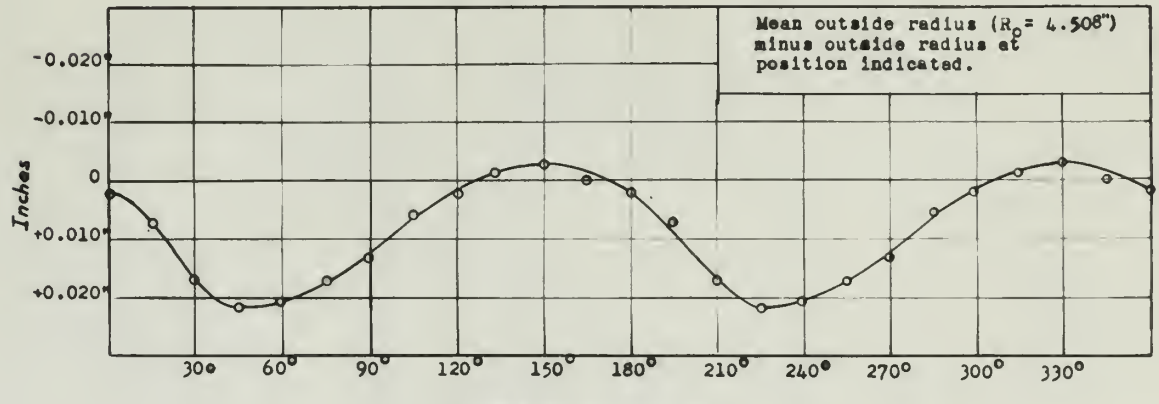

Figure VII

VARIATION IN THICKNESS
RING NO, 2

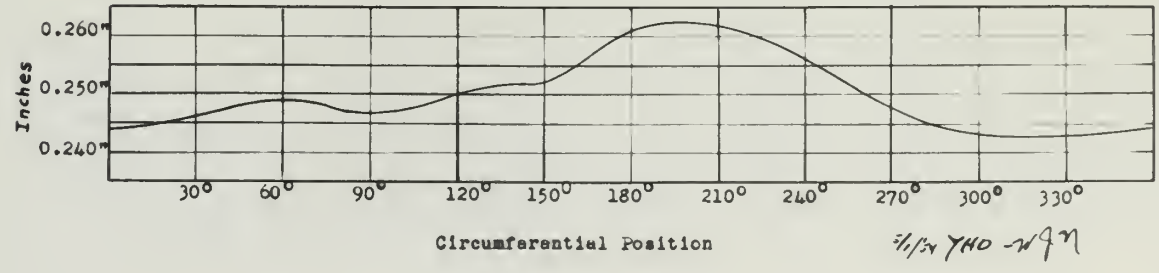

Figure VIII

CIRCUMFERENTIAL STRAIN DISTRIBUTION ON INNER SURFACE
RING NO. 3 u_o = 0.0268"

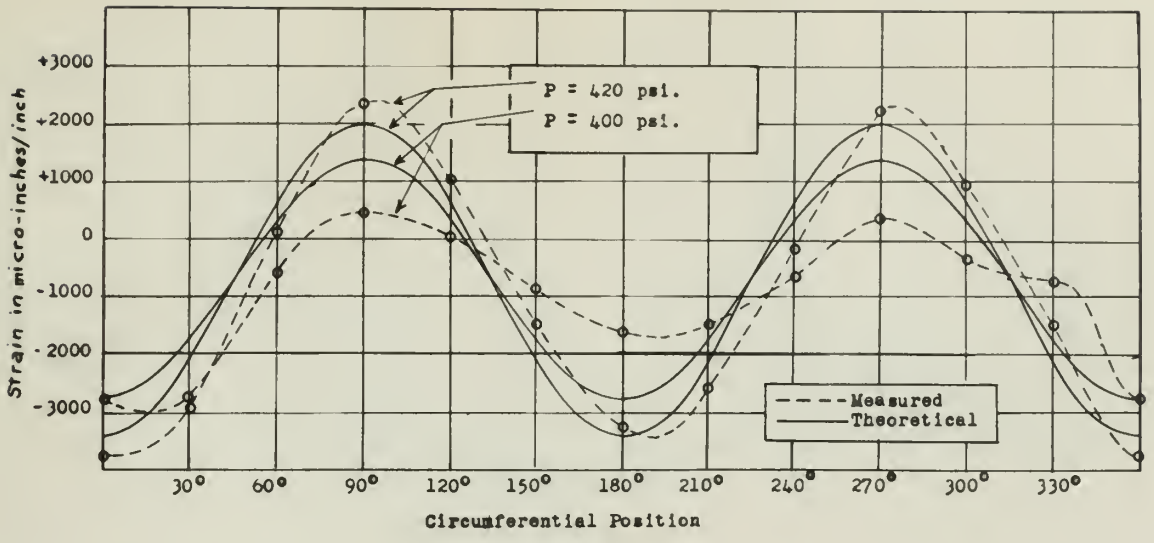

Figure IX

INITIAL CONFIGURATION
RING NO. 3

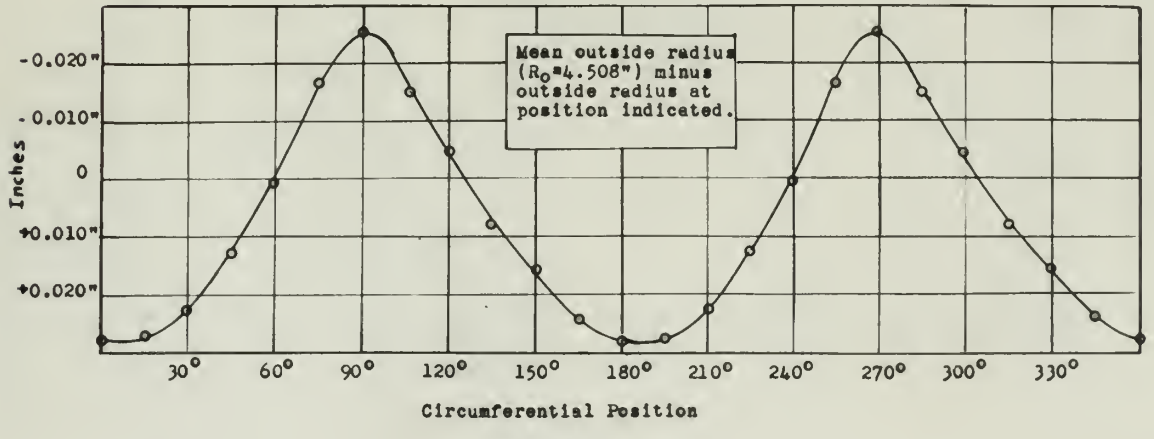

Figure X

VARIATION IN THICKNESS
RING NO. 3

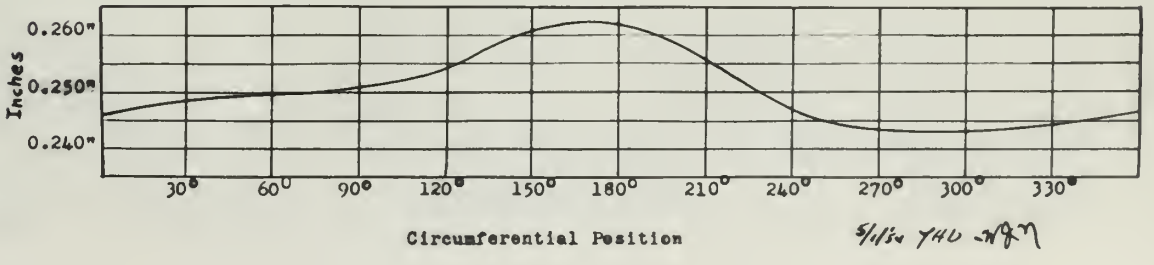

Figure XI

CIRCUMFERENTIAL STRAIN DISTRIBUTION ON INNER SURFACE
RING NO. 5 u_o = 0.0705"

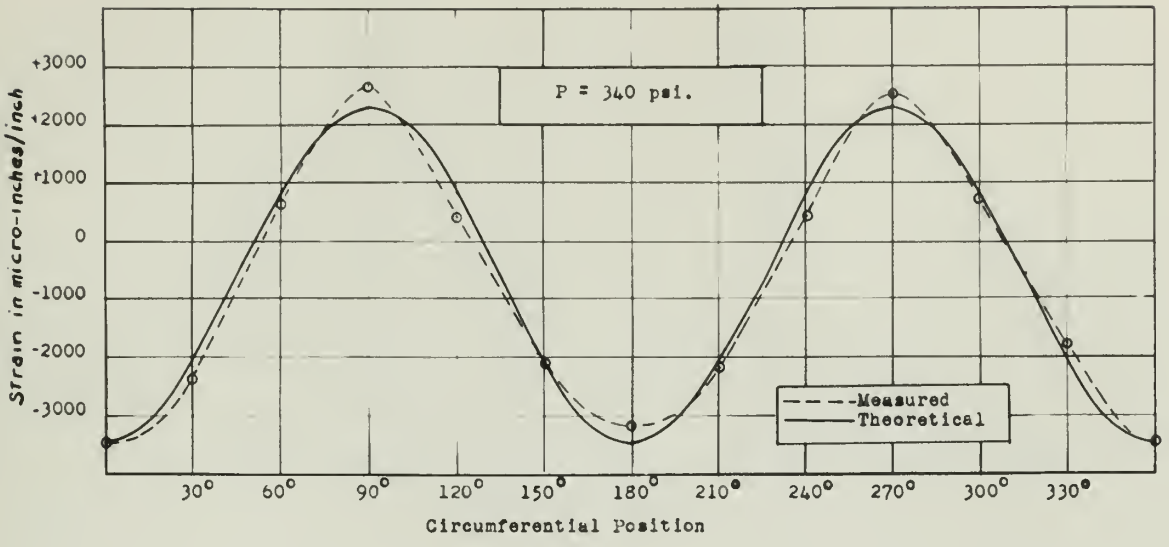

Figure XII

INITIAL CONFIGURATION
RING NO. 5

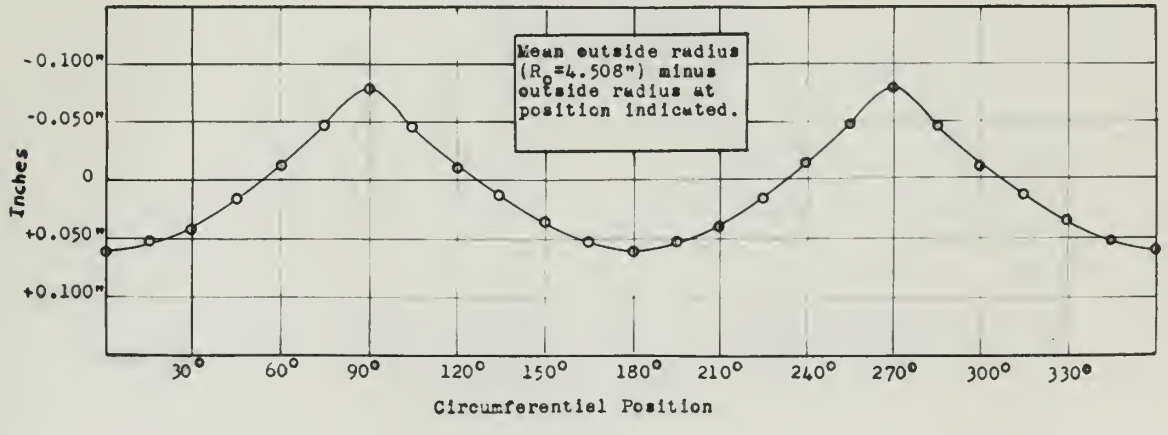

Figure XIII

VARIATION IN THINCKNESS
RING NO. 5

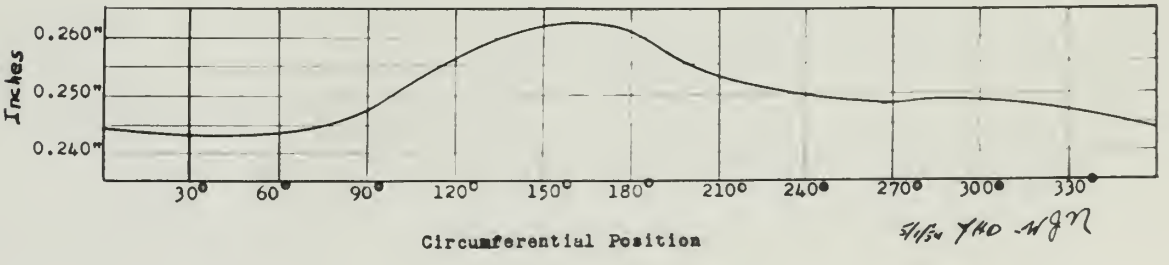

5/1/54 YHO WJM

Figure XIV

CIRCUMFERENTIAL STRAIN DISTRIBUTION ON INNER SURFACE
RING NO. 6 u_o = 0.075"

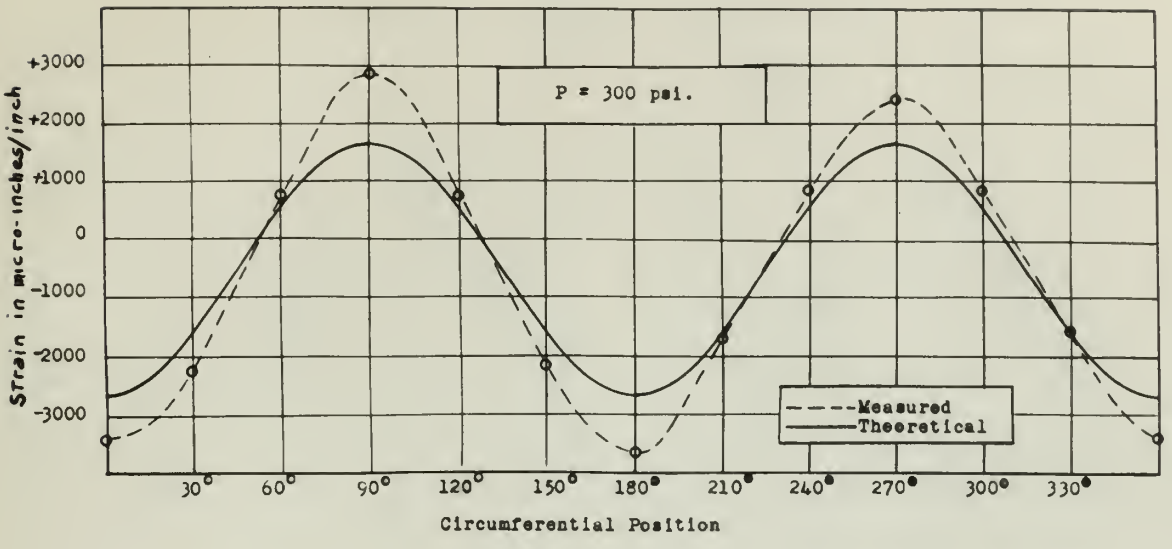

Figure XV

INITIAL CONFIGURATION
RING NO. 6

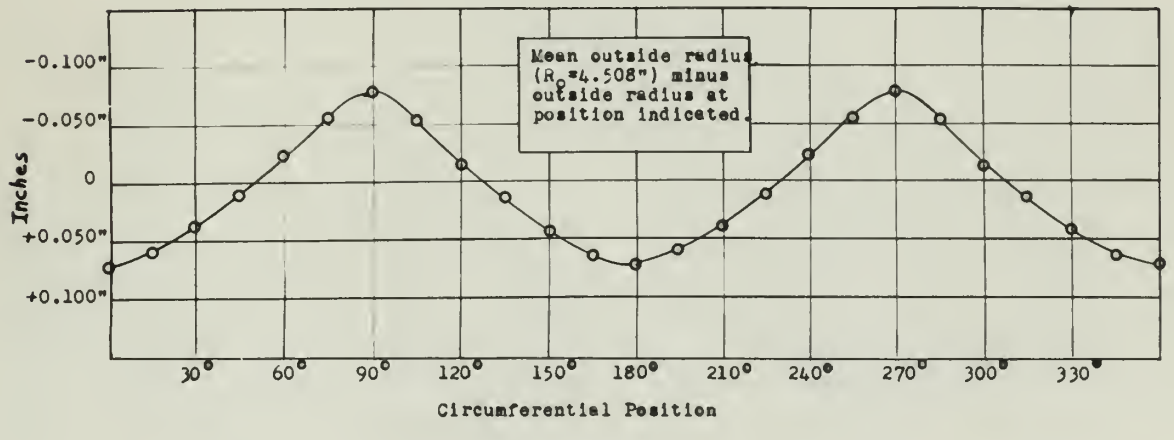

Figure XVI

VARIATION IN THICKNESS
RING NO. 6

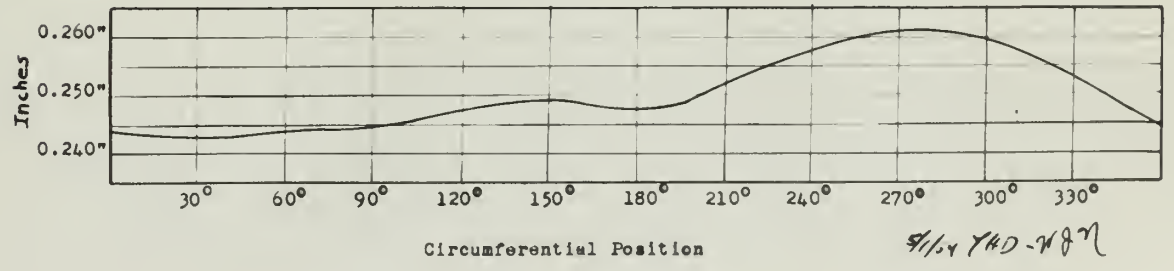

4/1/54 YHD-WJM

Figure XVII

CIRCUMFERENTIAL STRAIN DISTRIBUTION ON INNER SURFACE
RING NO. 7 u_o = 0.1535"

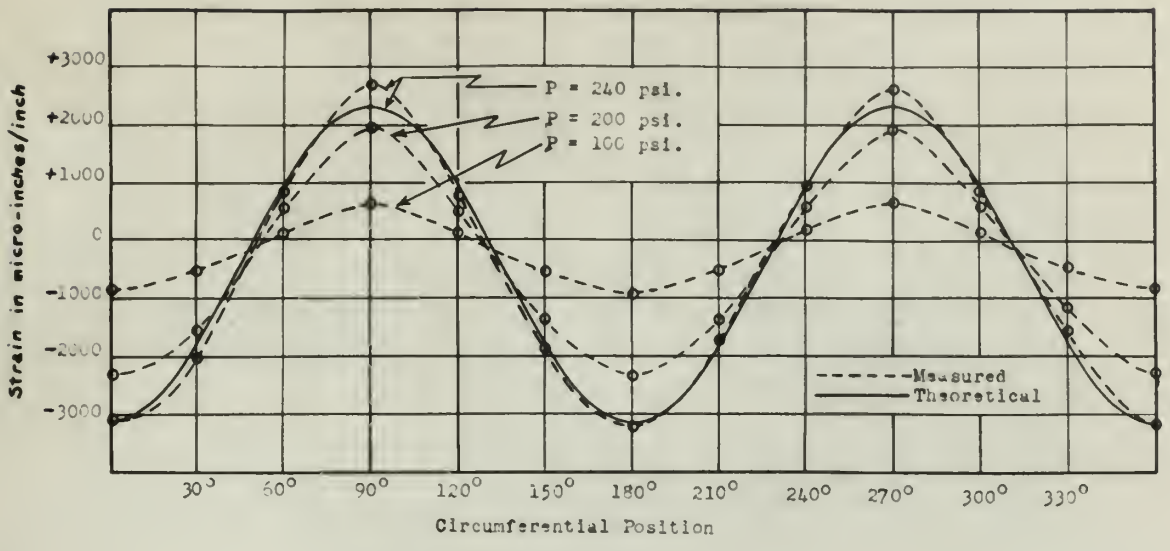

Figure XVIII

INITIAL CONFIGURATION
RING NO. 7

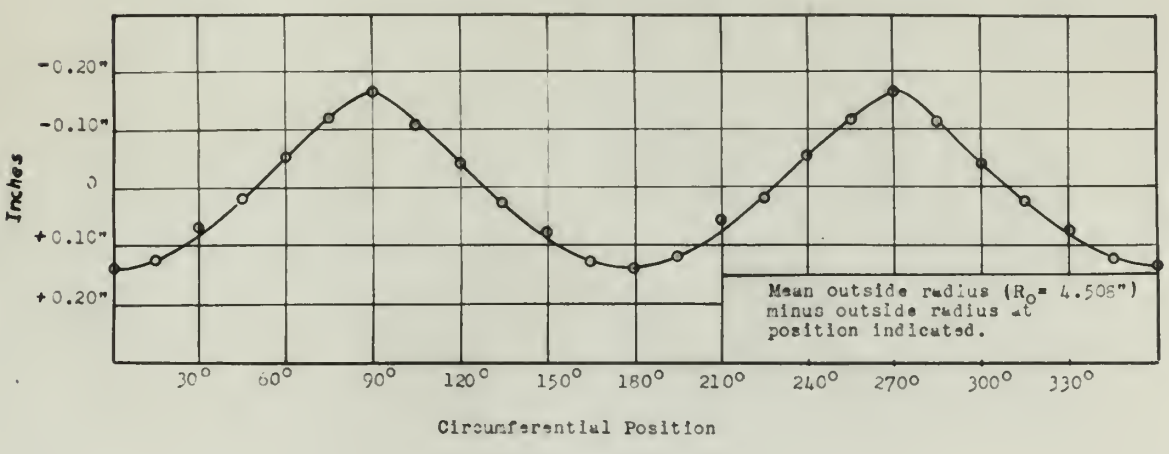

Figure XIX

VARIATION IN THICKNESS
RING NO. 7

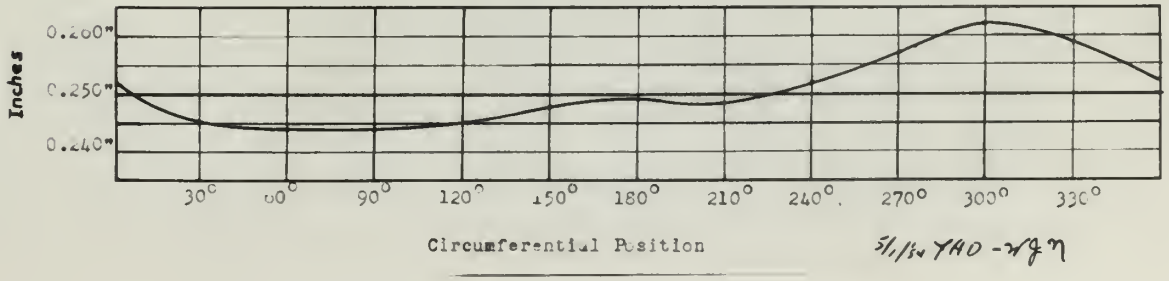

5/1/54 YHO -WJM

Figure XX

COMPARISON OF MEASURED AND THEORETICAL STRAINS
RING NO. 3 u_o = 0.027"

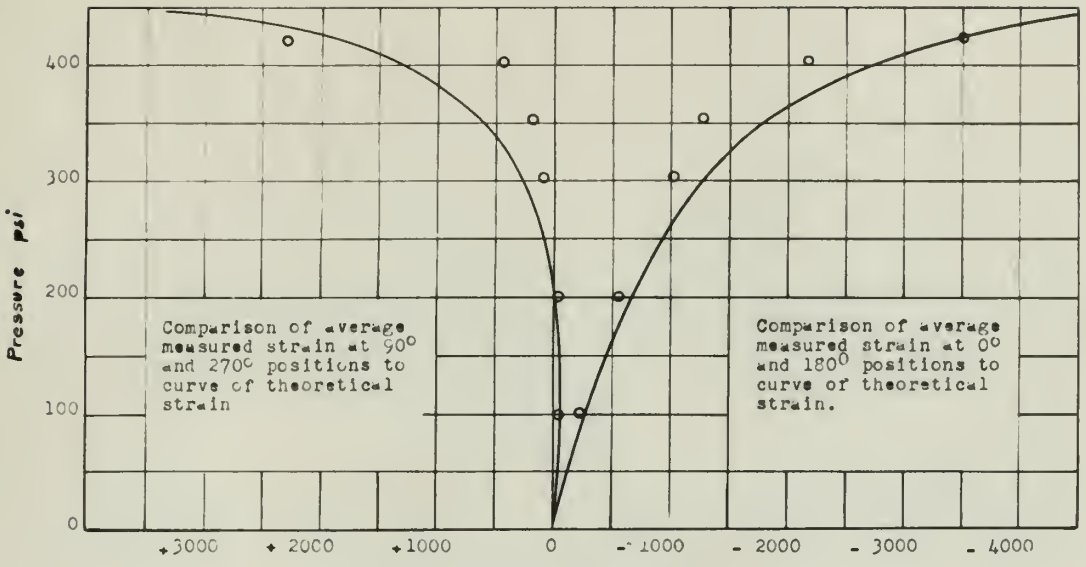

Figure XXI

COMPARISON OF MEASURED AND THEORETICAL STRAINS
RING NO. 4 u_o = 0.048"

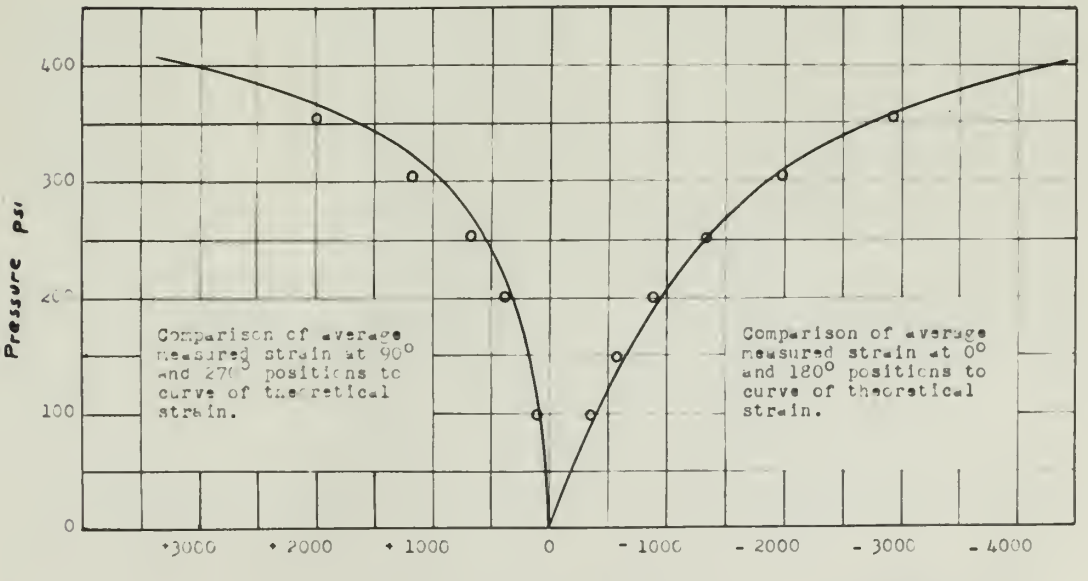

5/1/54 YAD-WGR

Figure XXII

COMPARISON OF MEASURED AND THEORETICAL STRAINS
RING NO. 5 u_o = 0.070"

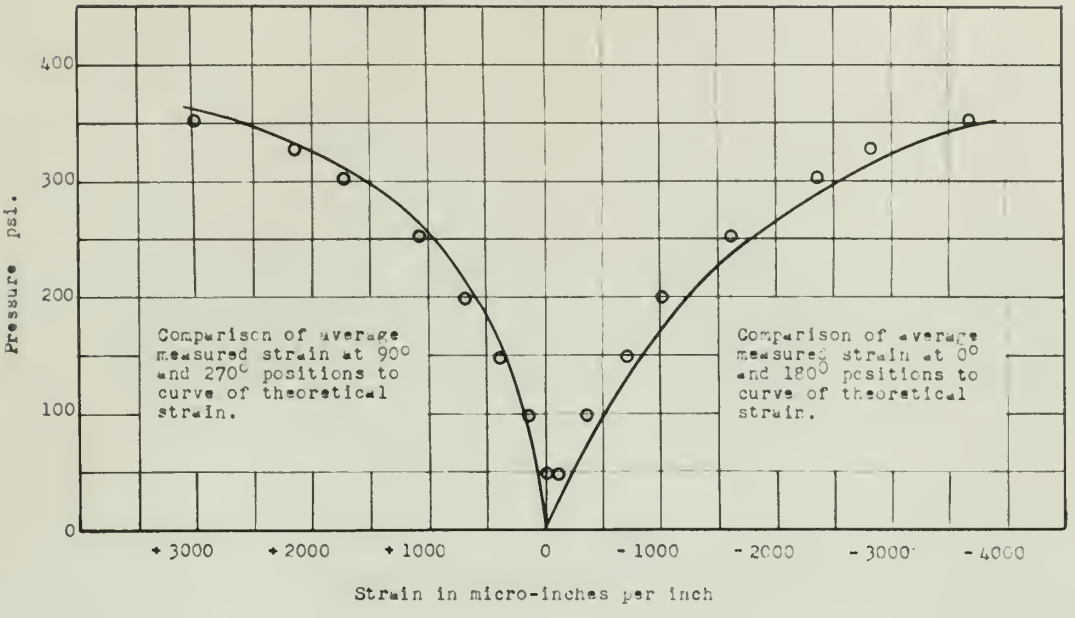

Figure XXIII

COMPARISON OF MEASURED AND THEORETICAL STRAINS
RING NO. 6 u_o = 0.075"

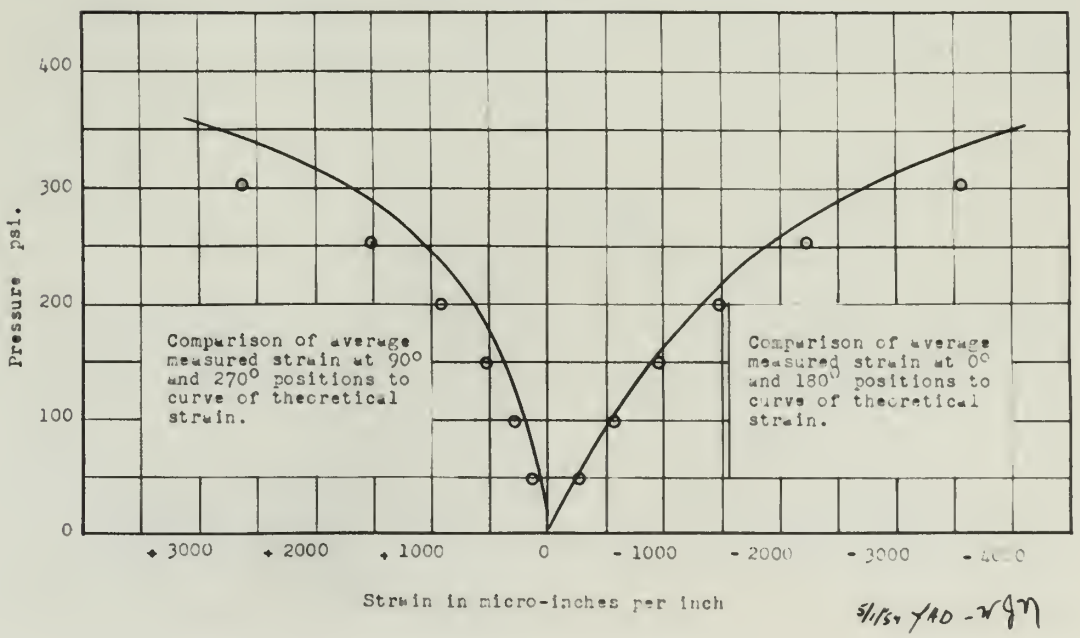

Figure XXIV

COMPARISON OF MEASURED AND THEORETICAL STRAINS
RING NO. 7 u_o = 0.1935"

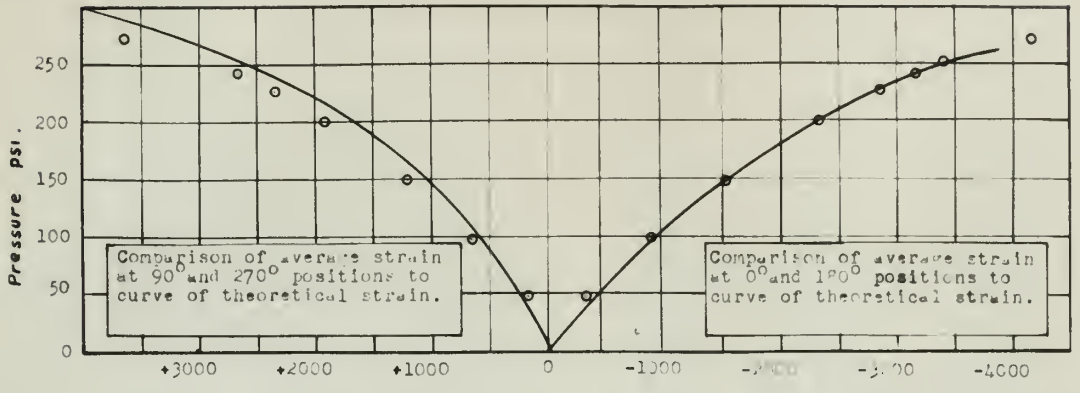

Strain in micro-inches per inch

Figure XXV

COMPARISON OF MEASURED AND THEORETICAL STRAINS
RING NO. 8 u_o = 0.204"

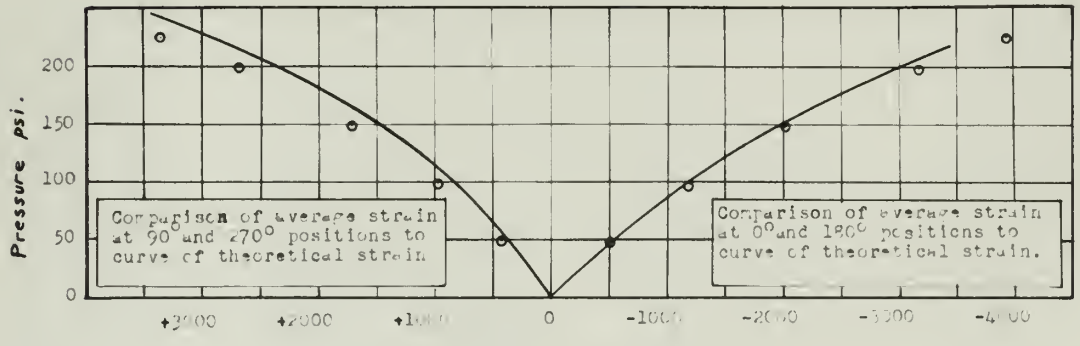

Strain in micro-inches per inch

Figure XXVI

COMPARISON OF MEASURED AND THEORETICAL STRAINS
RING NO. 9 u_o = 0.223"

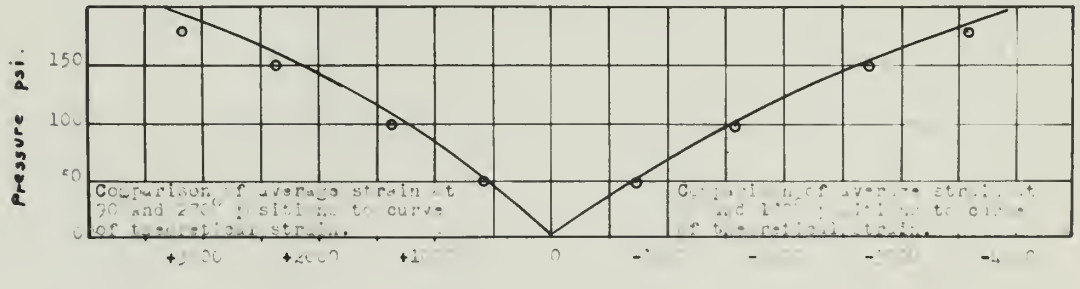

Strain in micro-inches per inch

5/15/54 AD - WQM

Figure XXVII

COMPARISON OF MEASURED AND PREDICTED BUCKLING PRESSURES

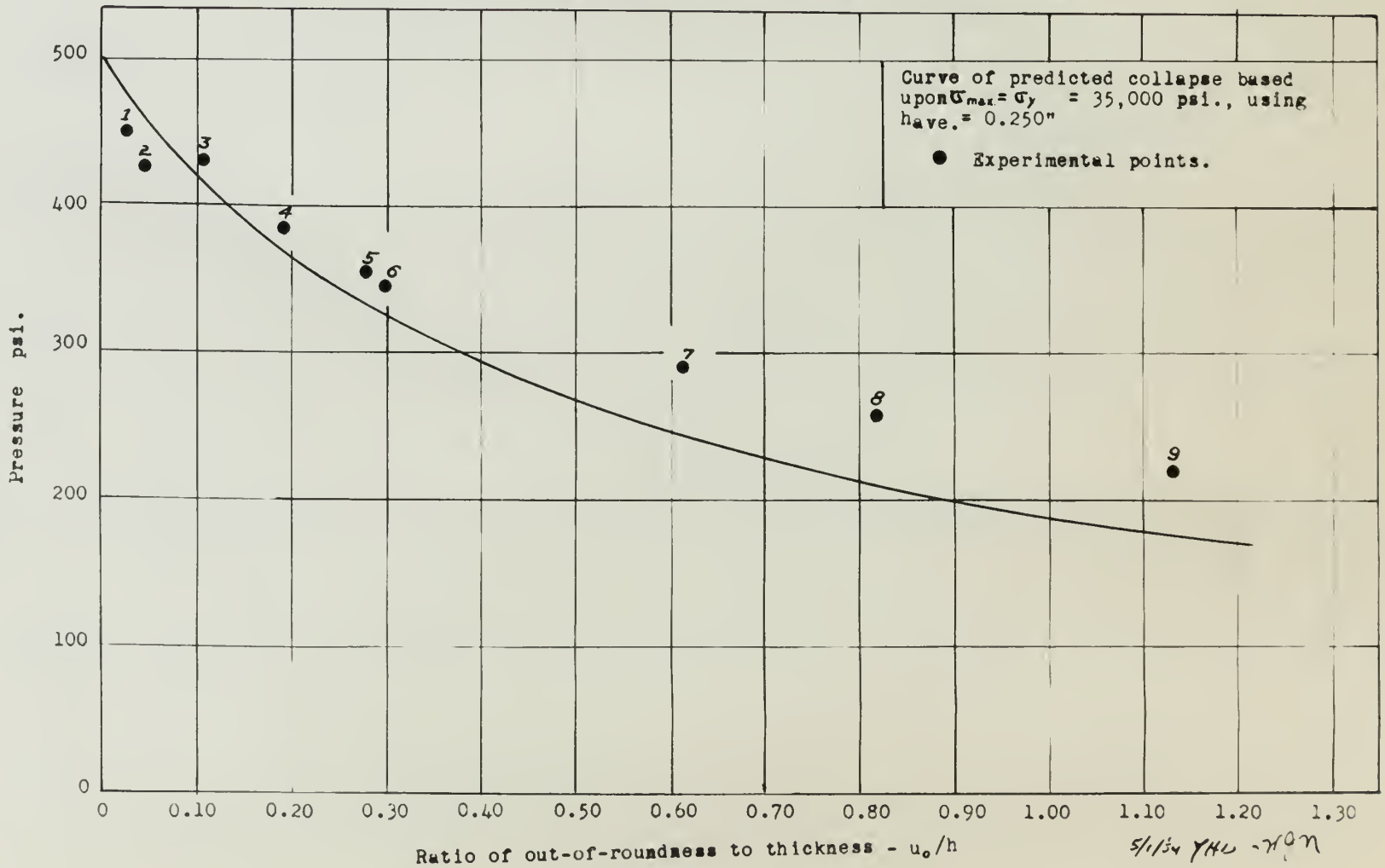

Figure XXVIII

COMPARISON OF MEASURED AND PREDICTED BUCKLING PRESSURES

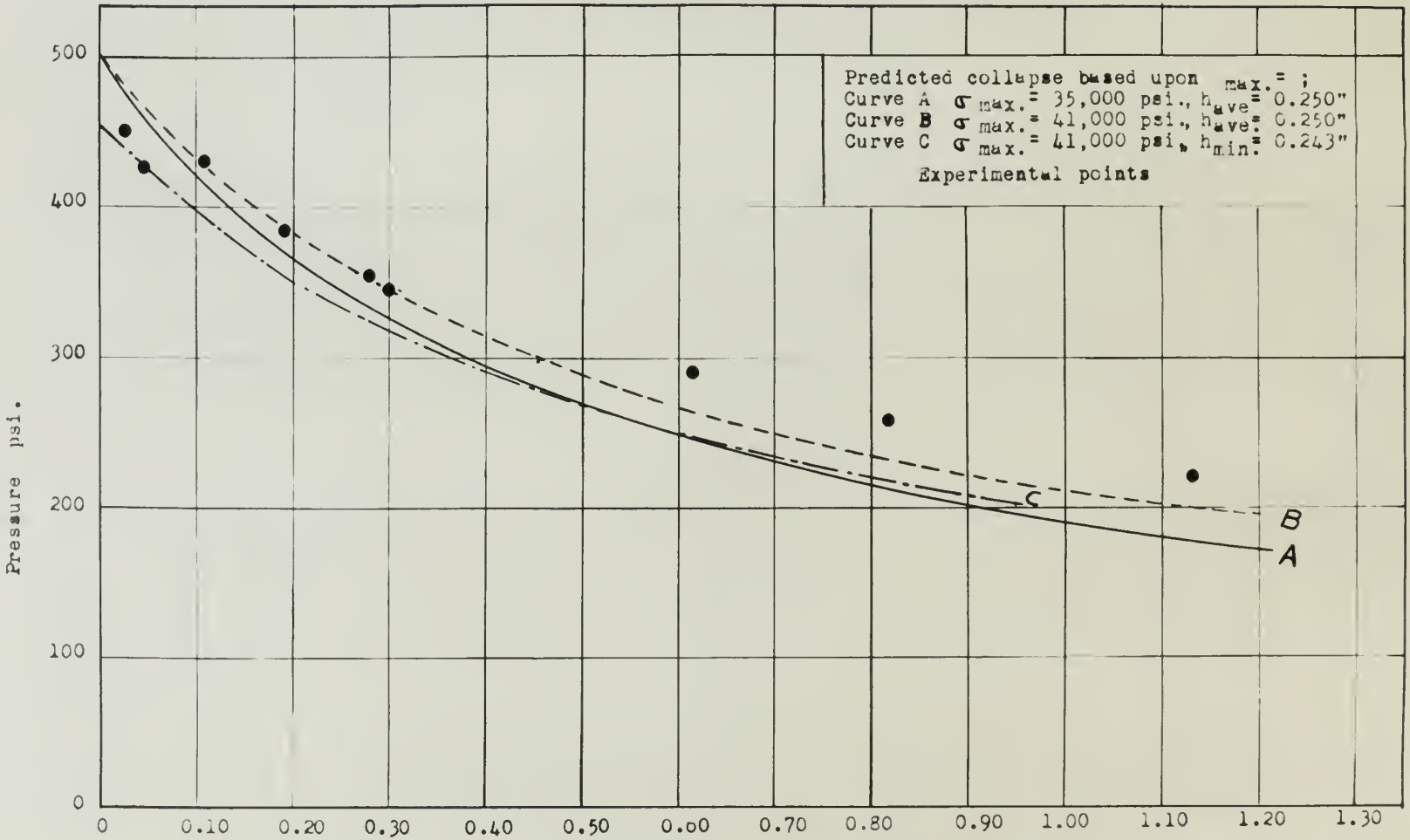

5/1/54 THD -WGM

IV.

DISCUSSION OF RESULTS

Introduction

For convenience and continuity, the experimental results may be grouped in the following sequence:

1. Results of Compression Tests
2. Proof Test Data
3. Circumferential Strain Distributions
4. Maximum Strains
5. Collapse Pressures

This classification is convenient in that the significance of any group depends to some extent upon the interpretation and validity attached to one or more of the preceding groups.

Results of Compression Tests

The results obtained from the compression tests were probably the most significant factors in the correlation of experimental and theoretically predicted quantities.

The data obtained from the tests of the specimens were surprisingly consistent. See Figure III. Values of strain correlate particularly well at high stresses where some deviation might be expected. The possibility of introducing rather significant errors during the resetting of the Huggenberger Tensometers was considered,

IV.

DISCUSSION OF RESULTS

Introduction

For convenience and continuity, the experimental results may be grouped in the following sequence:

1. Results of Compression Tests
2. Proof Coat Tests
3. Circumferential Strain Distributions
4. Bending Strains
5. Collapse Pressures

This classification is convenient in that the significance of any group depends to some extent upon the interpretation and validity attached to one or more of the preceding groups.

Results of Compression Tests

The results obtained from the compression tests were probably the most significant factors in the correlation of experimental and theoretically predicted quantities.

The data obtained from the tests of the specimens were surprisingly consistent. See Figure III. Values of strain correlate particularly well at high stresses where some deviation might be expected. The possibility of introducing further significant errors during the restoring of the Micrometer Extensometers was considered,

but a review of the data indicated that increments of strain before and subsequent to a reset were consistent. That the stress-strain curve shown in Figure III is representative of the alloy from which the rings were manufactured is implied in preceding sections. Appreciating the fact that the proof stress and ultimate strength of aluminum alloy varies considerably with the details of the heat treatment and possibly the original lot number, the authors specified that the specimens be obtained from the length of tubing from which the rings were manufactured and that all rings and specimens be heat treated as a group.

Young's Modulus, as determined from the stress-strain curve, was 10.8×10^6 psi. and can be compared to $E = 10 \times 10^6$ psi., the value generally given in handbooks. In the authors' opinion, Figure III justified the assumption of a linear stress-strain relationship up to a stress of 34,500 psi. and a 0.2% proof stress, designated yield stress, of 35,000 psi. Furthermore, it is to be noted that a very distinct departure from linearity did not occur until a stress of about 41,000 psi. was obtained.

These properties were commensurate with those characteristics considered most desirable in the material from which the rings were made. The existence of a linear stress-strain relationship over a large range of stress

permitted most of the experimental strains to be compared directly with predictions based upon equation (3) without the complication of a decreasing modulus. For extrapolation of the results to steel rings, a plateau corresponding to a true yield stress was desirable. Although the authors did not anticipate such similarity at the time aluminum alloy was selected, the upper portion of the stress-strain curve is in most respects analogous to the compression test curves obtained for mild steel specimens tested by M. L. Pittman, Jr., and V. W. Rinehart (7).

It may be argued that the remainder of the results would have been of no consequence without the stress-strain data. The use of a standard stress-strain curve for aluminum alloy 61S-T6 would have involved an 8% error in Young's Modulus and a 14% error in the proof stress. Furthermore, the shape of the curve above the proof stress is valuable when analyzing the failure of a ring.

Proof Test Data

The authors have stated that the measured strains at a specified pressure were dependent to some extent upon the gasket and the type of lubricant used between the gasket and the Plexiglas surfaces. Figure IV shows this effect quantitatively. Black rubber-to-metal cement has been designated Lubricant #1 and clear rubber cement as

Lubricant #2. Although Lubricant #1 was considered most suitable on the basis of a preliminary investigation which has been described, Lubricant #2 appeared to be a reasonable second choice. The two gaskets were of the same dimensions and material but differed in that Gasket #1 had been used several times before while Gasket #2 had not. Relative to Gasket #2, Gasket #1 was very limber and appeared to have a slick, oily surface.

As shown by Figure IV the largest measured strains were attained with Lubricant #1 and Gasket #1. Lubricant #1, Gasket #2 were next in magnitude of strains while Lubricant #2, Gasket #1 gave the smallest measured strains. Considered as percentages, the differences in strains are quite significant. The authors reasoned that the gasket and lubricant were able to affect the strains by changing the magnitude of the friction force acting at the gasket-Plexiglas interface.

On the basis of the results indicated by Figure IV, the authors elected to use a well broken-in gasket in conjunction with Lubricant #1 for the remainder of the tests since this combination more nearly satisfied the requirement that the ring be completely free of restraint at the edges.

A thorough investigation of the friction force at the

gasket-Plexiglas interface should be a prerequisite for further experimentation based upon this thesis. The objectives of such an investigation should be a consideration of all likely gaskets and lubricants, a comparison of possible combinations with respect to effect upon strains, and a quantitative evaluation of the coefficient of friction characteristic of given combinations of gasket, lubricant and pressure.

Circumferential Strain Distribution

Figures VI, IX, XII, XV, and XVIII show typical out-of-roundness curves. Of the rings shown in this group, all were deformed intentionally with the exception of Ring No. 2, Figure VI. It is significant that the out-of-roundness obtained in Ring No. 2, while purely arbitrary, is very similar to a configuration given by $u_o \cos 2\theta$. The remainder of the plots are characterized by rather steep peaks in the vicinity of the minimum diameter and shallow peaks at points of maximum diameter. It is to be noted that the steep peaks occurred at points where the deforming loads were applied by the loading machine. The configurations are, however, reasonably similar to a cosine curve of the form $u_o \cos 2\theta$.

Figures VII, X, XIII, XVI, and XIX show the variation in thickness versus circumferential position. It is apparent that the relation of thickness and out-of-roundness at a

particular station is completely arbitrary. In general, the difference between minimum and maximum thickness is of the order of 0.02". Since the out-of-round plot is derived from the diameters read to the outer circumference, the corresponding configuration of the neutral axis may be assumed to deviate slightly from that of the plot. Since sections of thickness greater than average were generally opposite sections of less than average, the effect of this deviation upon the measured value of u_o is assumed to be of no consequence except in the circular rings. During a preliminary reduction of data the authors considered the effect which a variation in thickness might have upon the plots of out-of-roundness and predicted strains. The plot of out-of-roundness for Ring No. 2 was altered to a minor extent. The plots for other rings were affected an insignificant amount. Correlation of measured and predicted strains was not improved.

With respect to circumferential strain distributions essentially three types of results were obtained. Figure V shows an arbitrary distribution while Figure XVII shows a well defined cosine distribution. Ring No. 3, Figure VIII, appears to combine some of the characteristics of the first two types.

The arbitrary distribution occurred in those rings

which were essentially circular. The theoretical curve shown in Figure V is a plot of equation (3) with the measured out-of-roundness at a particular position substituted for $u_o \cos 2\theta$ and with $h = h_{ave} = 0.250"$. A point of interest is the fact that the small peaks which are visible at low pressures define a pattern which would seem to persist up to the maximum pressures obtained. The pattern is characterized by a relatively constant strain over 60^o or 90^o of the circumference and a fluctuating strain over the remaining 300^o or 270^o; the fluctuations are a reasonable representation of two cycles of a cosine curve. The fact to be observed is that correlation between out-of-roundness and strain distribution is completely lacking.

Subsequent results demonstrate quite clearly that theoretical and measured strains agree satisfactorily when the initial configuration assumed in equation (3) is actually obtained in the ring. It is possible, then, that the method of measuring out-of-roundness was not sufficiently accurate in the case of Ring No. 2. In appraising the out-of-roundness measurement, it is convenient to visualize the initial configuration of the ring as a series of the form $Ro + u_o \cos 2\theta + u1 \cos 3\theta + u2 \cos 4\theta - - - u_n \cos (n + 2)\theta$. The measurements from which Figure VI

$\mu_0 \cos (\beta + \gamma) \beta$. The measurements from which Figure VI
[illegible] $\mu_0 + \mu_0 \cos 2\theta + \mu_1 \cos 2\beta + \mu_2 \cos 4\beta + \ldots$ -
the initial configuration of the ring as a series of the
out-of-roundness measurements, it is convenient to visualize
the method of measuring out-of-roundness was not entirely
accurate in the case of Ring No. 2. In appraising the
actually obtained in the ring. It is possible, then, that
the initial configuration assumed in equation (2) is
theoretical and measured strains agree satisfactorily when
subsequent results demonstrate quite clearly that
between out-of-roundness and strain distribution is com-
pletely lacking.

are a reasonable representation of two cycles of a cosine
curve. The fact to be observed is that correlation
strain over the remaining 300° or 270°; the fluctuations
over 60° or 90° of the circumference and a fluctuating
pattern is characterized by a relatively constant strain
to persist up to the maximum pressure obtained. The
visible at low pressures define a pattern which would seem
of interest is the fact that the small peaks which are
measured out-of-roundness at a particular position substi-
tuted for $\mu_0 \cos 2\theta$ and with $\lambda = \mu_{max} = 0.250$". A value
shown in Figure V is a plot of equation (2) with the
motion were essentially circular. The theoretical curve

was obtained reflect only those terms of the form $u_0 \cos 2\theta$, $u_2 \cos 4\theta$, $u_4 \cos 6\theta$, etc. It is to be observed that of these terms $u_0 \cos 2\theta$ appears to predominate. Nevertheless, the assumption of a simple contour, $R_0 + u_0 \cos 2\theta$, in equation (3) may not be justified since the effect of odd terms ($u_1 \cos 3\theta$, $u_3 \cos 5\theta$, etc.) is not indicated by Figure VI. On the other hand, the effect of this omission upon the predicted strain distribution is not so serious as might be expected. If a relation corresponding to equation (3) is derived assuming a configuration such as $R_0 + u_1 \cos 3\theta$, it will be found that the maximum bending stress is proportional to $\frac{1}{1-P/P_{crit}}$ where P_{crit} is the buckling pressure of a circular ring into (n+2) lobes. The buckling pressure, P_{crit}, increases rapidly with the number of lobes; thus the value of P_{crit} for a two-lobe collapse is three-eights of P_{crit} for a three lobe collapse and one-fifth of P_{crit} for a four lobe collapse. Consequently even if u_1, u_2, u_3, etc. are comparable in magnitude to u_0 the effect upon the strain distribution will be considerably less since the bending stress is governed by $\frac{1}{1-P/P_{crit}}$. In view of these facts the arbitrary strain distribution appears to be the result of a rather complicated combination of inadequate measure-

ment, variation of thickness, and localized surface irregularities or dents.

It follows, however, that a more thorough investigation of essentially circular rings is warranted. Rings could be machined as circular as possible and to a close tolerance in thickness. If the initial contour were then determined precisely, it would be possible to evaluate the effect of deviations from a basic two lobe pattern such as that given in Figure VI. It is the authors' opinion that under these circumstances the method of measuring out-of-roundness used in this thesis would prove useful as a practical measure, especially at high pressures.

Ring No. 3 appeared to be the borderline case. With reference to Figure VIII it is apparent that the circumferential strain distribution at 400 psi. deviated considerably from the theoretical curve, equation (3) with $h = h_{ave} = 0.250"$. The distribution is not a clearly defined cosine curve, and the magnitude of the strains are generally below the predicted values. On the other hand, at 420 psi. there was a visible deflection of the ring and the strain distribution assumed a form which, except for a 4^{o}-8^{o} phase shift, compared favorably with predicted values. At 400 psi. the deviations from a pure cosine curve are of the same character as the superposition of harmonics upon

a fundamental wave form. Here it is possible to reason that the terms $u_1 \cos 3\theta$, $u_2 \cos 4\theta$, etc. are significant relative to the basic two lobe pattern given by $R_o + u_o \cos 2\theta$. At 420 psi a two lobe strain pattern was clearly predominate; this would be expected since as the pressure approaches P_{crit} for the two lobe collapse pattern, the bending strains become significantly greater than corresponding strains resulting from the superposition of other basic configurations. However, in view of the added complication of the thickness variation and possible localized irregularities the authors do not feel justified in attributing the entire cause of the deviations to an inadequate out-of-round measurement. Again it is suggested that the effect of any deviation from a basic two lobe out-of-round pattern requires further investigation.

The last type of strain distribution, the clearly defined cosine curve, is exemplified by Rings No. 5 and 7, Figures XI-XIII and XVII-XIX. With the exception of Ring No. 6, the plots are typical of the results and correlation observed in Rings No. 4-9. Despite the peaked out-of-roundness curve and the variation in thickness, the correlation of measured and predicted strains is excellent. The manner in which the initial peaks of the strain curve progressively increase in amplitude is clearly demonstrated in Figure XVII. Any deviations from the basic two

lobe pattern were insignificant at all pressures.

The test of Ring No. 6 differed from the others in that the Plexiglas surfaces were coated with black rubber-to-metal cement before the ring was placed in the test chamber. The gasket and outer surface of the ring were coated in the usual manner. This deviation from the usual test procedure was made in order to determine whether or not the friction between the gasket and Plexiglas could be reduced still further. The results of this test are shown in Figure XIV. The correlation of measured and predicted strains should be compared with that obtained in Figure XI since Rings No. 5 and 6 were of comparable out-of-roundness, $u_o = 0.0705"$ and $u_o = 0.075"$ respectively. Where excellent correlation was observed for Ring No. 5, the maximum strains in Ring No. 6 were as much as 40% above the predicted values. This discrepancy cannot be explained by the authors. Were it not for the fact that the results of Rings No. 4, 5, 7, 8, and 9 consistently plotted along the predicted strain curves, it might be assumed that in all cases other than Ring No. 6 a significant restraining force was present at the gasket-Plexiglas interface. The fact that such consistency does exist would imply that the test of Ring No. 6 was faulty in some respect. The results definitely indicate a need for further investigation of the friction force at

the gasket-Plexiglas interface, such as suggested previously.

Maximum Strains

In those rings which were intentionally deformed strain gages were placed at points of maximum (0° and 180°) and minimum (90° and 270°) diameters. The strains at 0° and 180° were averaged and plotted for Rings No. 3-9 on the right side of Figures XX - XXVI. Similarly, the average of the 90° and 270° readings are shown on the left side of the same plots. The theoretical curve is simply a plot of equation (3) with cos 2 θ equal to plus or minus one and $h = h_{ave.} = 0.250"$. The strains at 0° and 180° are particularly important in that they are normally used in the prediction of a collapse pressure; consequently, the strains at these positions are given added consideration.

With the exception of Rings No. 3 and 6, the correlation of measured and theoretical strain is entirely satisfactory. On the pressure scale the compressive strains are generally within a range of $\pm$5-1/2 psi. of the theoretical curve; this was the assumed accuracy of the recorded pressure. The tensile strains always appear below the theoretical curve; if the modulus of elasticity in tension were assumed to be slightly below 10.8×10^6 psi. the tensile strains would also correlate. In view of the consistency noted in Figures XXI, XXII, XXIV, XXV, and XXVI, the authors are inclined to think that this might actually be the case.

the Deeply-Flexible interface, such an undamped flexionary.

Mexican Critters

In these tiny moths were intentionally detected within
eggs were placed at points of maximum (0_o and 180_o) and
minimum (90_o and 270_o) diameters. The strength of 0_o and
180_o were averaged and plotted for ninety 0_o-3 on the
right side of figures II - III. Similarly, the average of
the 90_o and 270_o readings are shown on the left side of the
same plots. The theoretical curve is simply a plot of
equation (3) with the 2θ equal to plus or minus one half
$N = Pure. = 0.250$". The strains at 0_o and 180_o are particularly important in that they are actually used in the interaction of a coiffure resonator; consequently, the strains at these positions are given added consideration.

With the exception of trace B_o. 3 and 9, the correlation of measured and theoretical strain is entirely satisfactory. On the measure scale the oscillatory strains are clearly within a range of $\pm 1\frac{1}{2}$ rel. of the theoretical curve. The cosmic strains clearly meet the planned tolerance of the resonant structure.

In a sense Rings No. 3 and 6 were special cases. As pointed out Ring No. 3 appeared to be the dividing line between configurations in which the two lobe out-or roundness pattern predominated and those which were affected by variations in thickness, harmonics, and/or local irregularities such as a small dent or gouge. Figure XX shows clearly that the measured strains were considerably below the predicted values up to a pressure of 400 psi; at this point the measured strains literally jumped to the theoretical curve. Figure XX tends to substantiate the remarks made previously; that is, in practical cases of out-of-roundness a two lobe configuration derived simply and directly may allow prediction of strains of acceptable accuracy at sufficiently high pressures, but further work is required before complete justification is obtained.

Figure XXIII shows merely that measured strains for Ring No. 6 were larger than the predicted strains over the entire range of pressures. The consistency lends some doubt to the authors' contention that the test may have been faulty.

In conjunction with the considerations of circumferential strain distribution, the results above indicate quite clearly that equation (3) is valid within the qualifications of the derivation; this conclusion is based upon the behavior of

Rings No. 4, 5, 7, 8, and 9 in which the assumption of a configuration $R_o + u_o \cos 2\theta$ was obviously justified.

Collapse Pressure

Figure XXVII shows the collapse pressures of the nine rings plotted versus the ratio of out-of-roundness to average thickness and serves to identify the points shown on Figure XXVIII. The single curve is a plot of equation (4) with σ_{max} = 35,000 psi. Figure XXVIII is more informative in that several variations of equation (4) are plotted; the values of σ_{max} and h which apply to each curve are indicated in the legend.

Foregoing results (see Figure V) indicate that Rings No. 1 and 2 did not assume a two lobe configuration until the ring was in the process of failing completely; if a stable two lobe pattern existed it was possible over a very small range of pressure. Regardless of the cause of the random strain distribution, Figure XXVIII demonstrates clearly that the failure of Rings No. 1 and 2 could have been predicted by equation (4) in which σ_{max} is 41,000 psi and $h = h_{min.} = 0.243"$.

There are two ways in which to view these results. First, it would appear that the minimum thickness, u_o as measured, and the point at which the stress-strain curve departs significantly from linearity are the only factors

constructive to use the 3-D mesh constantly inserted.

Conjugate Gradients

Figure XIII shows the cotangent transform of the unit circle hyperbolic cosine and sine. It should be noticed that the points become closer and closer together as they approach the limits of out-of-consonance at $\pm\infty$. The single curve in a plot of admittance in three several variations of equation (4) are plotted; (4) with $C_{max} = 23,000$ bar. Figure XIII is more instructive on Figure XIII. The single curve in a plot of admittance versus cosine and values to identify the points which are implied in the image.

The values of C_{max} and B which apply to each curve are identified in the image.

Subsequent results (see Figure A) indicate that curve Bc. I and I did not respond a two lobe configuration until the time was in the process of falling completely; it a single two lobe pattern existed it was possible over a very small range of pressure. Regardless of the cause of the lesion atrain distribution, Figure XIII demonstrates clearly that the failure of curve Bc. I and I could have been alleviated by equation (4) to which C_{max} is 47,000 bar and B = C_{min} = 0.333.

There are two ways in which to view these results. First, it would appear that the solution interval, as we have been using it, is too large. Second, the solution interval is adequate, but the solution procedure is inadequate.

to be considered; hence, the use of equation (4) would be justified. This line of reasoning would infer that previous remarks relative to the importance of the basic two lobe configuration are entirely correct and that in practical cases of out-of-roundness one could neglect out-of-round other than that indicated by a simple consideration of diameters. On the other hand it is possible to reason that the variation in thickness was actually not significant; this statement could be based upon the collapse pressure of Rings No. 3, 4, and 5. Then the occurrence of collapse below the predition based upon average thickness would be explained in terms of stress introduced by a superimposed but undetected configuration or by local irregularities. The authors can conclude only that in this case of practical out-or-roundness and arbitrary strain distribution the collapse was predicted by equation (4) using minimum thickness and σ_{max} = 41,000 psi.

Rings No. 3, 4, and 5 differed from Rings No. 1 and 2 in that a clearly defined cosine type strain distribution was observed before failure. In each case the strain peaks corresponded to peaks in the out-of-roundness plot. Furthermore, the progressive failure which occurred in these rings may be contrasted to the rather sudden collapse of Rings No. 1 and 2.

Figure XXVIII shows that Rings No. 3, 4, and 5 collapsed at pressures very near to predictions given by equation (4) with σ_{max} = 41,000 psi and h = h_{ave}. These results seem to justify the argument above that the variation in thickness in itself was not significant and that the behavior of Rings No. 1 and 2 should be explained on the basis of harmonics and/or local irregularities. Nevertheless, the authors' only conclusion is that for rings of u_o/h from 0.10 to 0.30 equation (4), when used with the stress at which marked departure from linearity occurs, will predict quite accurately the failures in those rings where an initial configuration of $R_o + u_o \cos 2\theta$ is predominate.

Rings No. 7, 8, and 9 collapsed at pressures consistently above the predicted collapse pressure. Furthermore, stable configurations were obtained in which the maximum compressive stress was considerably above the yield point. Obviously as u_o increases, the criteria used in computing the collapse pressure becomes more conservative. This result is explained by the fact that the hoop stress upon which the bending stress is superimposed was less at the time yielding occurred in the outer fibers; in addition, the change in stress with respect to pressure was also less in the rings of greater u_o when this yielding began. Then to obtain instability in rings of greater out-of-roundness a larger increase in

pressure was required beyond the point of initial yield in the outer fibers. The authors conclude that for values of u_o/h greater than 0.30 and less than 1.10 the predicted collapse pressures are somewhat conservative but would be considered satisfactory for usual engineering design.

V.

CONCLUSIONS

1. The properties of aluminum alloy 61S-T6 were particularly well adapted to the objectives of this thesis.
2. The most significant problem encountered in the method of experimentation was the reduction of friction at the gasket-Plexiglas interface.
3. The relation for predicted strains in thin rings, equation (3), is valid when the assumed configuration, $R_o + u_o \cos 2\theta$, is obtained.
4. In those cases where the equation for predicted strains is valid and the value of h/D is 0.0285 a failure criteria based upon the stress level in the outer fibers predicts quite accurately the collapse of thin rings in which u_o/h is between 0.10 and 0.30. For values of u_o/h between 0.30 and 1.10 the criteria is somewhat conservative but not to an extent which would be considered over-cautious in engineering design.
5. From the general trend of the experimental collapse pressures as u_o/h decreases, the authors conclude that the collapse pressure predicted for perfectly circular rings by the Levy Formula, $P_{crit} = \frac{3EI}{R^3}$, is valid.

CONCLUSIONS

1. The properties of aluminum alloy 618-T6 were particularly well adapted to the objectives of this thesis.

2. The most significant problem encountered in the method of experimentation was the reduction of friction at the gasket-platelike interface.

3. The relation for predicted stress in thin rings, equation (3), is valid when the assumed configuration, $R_0 + w_0 \cos 2\theta$, is obtained.

4. In those cases where the equation for predicted stress is valid and the value of h/D is 0.0685 a twelve criteria based upon the stress level in the outer fibers predicts quite accurately the collapse of thin rings in which σ_0/s is between 0.10 and 0.30. For values of σ_0/s between 0.30 and 1.10 the criteria advanced conservative but not to an extent which would be considered over-cautious in engineering design.

5. From the general trend of the experimental collapse pressures as σ_0/s increased, all criteria considered the collapse pressure predicted for perfectly circular rings by the Levy formula, $P_{crit} = \frac{3 E I}{R_3}$, is valid.

VI.

RECOMMENDATIONS

1. Aluminum alloy 61S-T6 should be used in any extension of the experimentation described in this thesis.
2. A thorough, quantitative investigation of the friction at the gasket-Plexiglas interface should precede any further use of a test apparatus such as that described herein.
3. An investigation should be made for the purpose of determining the effect of deviations from a basic two lobe pattern as measured in this thesis. The rings to be investigated should be of constant thickness and the initial configuration should be known precisely.
4. A series of rings, machined as circular as possible and to a close tolerance in thickness, should be tested in order to further substantiate the Levy Formula.
5. It is recommended that the scope of this experimentation be extended to include commercial shapes such as I or H sections.

RECOMMENDATIONS

1. Aluminum alloy 61S-T6 should be used in any extension of the experimentation described in this thesis.

2. A thorough, quantitative investigation of the friction at the Heavet-Electrips interface should precede any further use of a test apparatus such as that described herein.

3. An investigation should be made for the purpose of determining the effect of variations from a basic two hole pattern as measured in this thesis. The rivets to be investigated should be of consecutive chronous and the initial configuration should be known previously.

4. A series of tests, assumed as circular as possible and to a close tolerance in thickness, should be tested in order to further substantiate the Duty Formula.

5. It is recommended that the scope of this experimentation be extended to include commercial metres such as I or H sections.

VII.

APPENDIX

APPENDIX.

APPENDIX A

Details of Procedures

Selection of Material for Construction of Rings

Initially the authors considered the possibility of using steel in the manufacture of the rings. A length of centrifugally cast steel tubing of 18" outside diameter and 1-3/4" wall thickness was available. However, the expense of constructing a test apparatus to accommodate steel rings was considered prohibitive in view of the uncertainty of the results. Furthermore, it was felt that the visual test chamber made possible through the use of Plexiglas would be of tremendous advantage during the test phase; this innovation was not considered feasible in the preliminary design of an apparatus to accommodate the pressures necessary to collapse steel rings.

The use of plastics was also given consideration. The various types of plastics were gradually eliminated for one or more of the following reasons:

1. The relatively low modulus of plastics resulted in very low predicted collapse pressures.
2. The ultimate strength was generally low relative to available metals.
3. The extent of a linear stress-strain relationship was limited.

APPENDIX A

Details of Procedures

Selection of Material for Demonstration of Buckle

Initially the writers considered the possibility of using steel in the demonstrator of the study. A length of centrifugally cast steel tubing of 30" outside diameter and 1-3/8" wall thickness was available. However, the expense of manufacturing a test apparatus to accommodate steel alloy was considered prohibitive in view of the uncertainty of the results. Furthermore, it was felt that the visual test phenomena obtained through the use of Plexiglas would be of tremendous advantage during the test phase; this innovation was not considered feasible in the preliminary design of an apparatus to accommodate the pressure necessary to collapse steel alloy.

The use of Plexiglas was also given consideration. The various types of Plexiglas most frequently eliminated for use or more of the following reasons:

1. The relatively low modulus of Plastics tempted in many low buckled original dimensions.

2. The ultimate strength may generally low relative to available metals.

3. The extent of a linear stress-strain relationship was limited.

These considerations indicated that the range of pressures over which useful data could be obtained was very limited, and, further, that the accuracy of the results would be questionable unless extreme precautions were taken in instrumentation.

As noted in Section II, aluminum alloy 61S-T6 appeared to satisfy the requirements of moderate collapse pressures, an essentially linear stress-strain relationship over a considerable range of stresses, and availability.

Manufacture of Rings

As pointed out in Section II the aluminum alloy tubing as received was cut into lengths several times the intended width of the test rings. Alternatively, the rings could have been machined to final dimensions. However, it is rather doubtful that the edges of the finished ring would have remained planar after the ring had been subjected to deformation in a loading machine and a heat treatment. A ring warped in this manner would tend to bind against the plane sides of the annular test chamber within the test apparatus. Consequently, the machining of the rings to the specified width was scheduled as the last operation in the manufacturing process.

The heat treatment of the aluminum alloy was accomplished by the Forge Shop, Boston Naval Shipyard. Specifically, the

These considerations indicated that the range of pressures over which useful data could be obtained was very limited, and, further, that the accuracy of the results would be questionable unless extreme precautions were taken in instrumentation.

As noted in Section II, minutes after SIR-1B appeared to satisfy the requirements of moderate collapse pressure, an essentially linear stress-strain relationship over a considerable range of strains, and availability.

Manufacture of Rings

As pointed out in Section II the aluminum alloy tubing as received was cut into lengths several times the intended width of the test rings. Alternatively, the rings could have been machined to final dimensions. However, it is rather doubtful that the edges of the finished rings would have remained planar after the ring had been subjected to deformation in a loading machine and a heat treatment. A ring warped in this manner would tend eventually find plane sides of the annular test chamber within the test apparatus. Consequently, the machining of the rings to the specified width was scheduled as the last operation in the manufacturing process.

The heat treatment of the aluminum alloy was accomplished by the Boston Naval Shipyard. Specifically, the

solution heat treatment consisted of a two hour soaking period at 970° F followed by a rapid quench in hot water at 180°F. The hot water quench was specified as an additional precaution against residual stresses. Actually the danger of residual stresses was not particularly significant in view of the rather thin thickness of alloy being quenched; nevertheless, the precaution was considered worthwhile since a hot water quench does not reduce the tensile properties appreciably below those obtainable with a cold water quench. The quench was followed by a precipitation heat treatment at 350°F for eight hours. The characteristics of aluminum alloy 61S-T6 as given in reference (5) are:

Tensile Strength	45,000 psi.
Yield Strength	40,000 psi.
E, Young's Modulus	10×10^6 psi.

Upon inspection of the sections after the heat treatment, it was found that the magnitude of the out-of-roundness introduced had not changed by any significant amount.

Instrumentation

The requirements placed upon the type strain gage selected were that the gage be small enough for mounting in the space available and that the gage length be sufficiently short with respect to the strain gradient. The SR-4, type A-7, strain gage satisfied these requirements. The gages

A-7, strain gage installed these requirements. The design
block with respect to the strain gradient. The 24-4, type
selected were that the gage be small enough for mounting in
the space available and that the gage length be sufficiently

Instrumentation

The requirements placed upon the Cyra strain gage
introduced had not changed by any significant amount.
Upon inspection of the sections after the mass stress-
ment, it was found that the magnitude of the out-of-roundness

could be easily mounted within the width of the ring, and, furthermore, a 3/16" gage length was entirely adequate since the predicted stress gradient in the vicinity of points of maximum stress was very small.

A multiple selector switchbox was used to facilitate reading the strain indications. The switchbox was constructed to permit the operator to set the same initial reading on all strain gages.

Design and Manufacture of Test Apparatus

The primary concern of the authors in the initial design of a test apparatus was the application of a uniform pressure on the outer surface of the rings without the introduction of restraining forces on the ring edges. An annular test chamber appeared to be the most suitable in this respect. The annulus was designed such that the tolerance between the surfaces and the edges of the ring would be exceedingly small, i.e., order of 0.001-0.002". This would facilitate sealing and yet the ring would remain "free floating" so to speak. From preliminary calculations based on the Levy formula for the collapse of 9" diameter aluminum rings or the 1/4 inch thickness, it was estimated that the test chamber would be subjected to a pressure of approximately 500 psi. Because Plexiglas is beautifully clear and can be obtained in large thick sheets with polished surfaces, it was decided to design the test annulus with upper and

lower surfaces of this material. This construction would permit visual inspection of collapse and the possibility of obtaining deflection readings. Plexiglas, however, has a low modulus of elasticity and therefore required backing to prevent the surface from deflecting appreciably when subjected to the expected pressures. The top steel web assembly and the bottom steel reinforcing ring as indicated in Figure I were designed for limiting the deflections of the Plexiglas. The hole in the bottom Plexiglas and reinforcing plates was introduced to accommodate strain gage leads. The steel surfaces indicated to be surface ground in Figure I were so designated to provide good contact surfaces between the steel and the Plexiglas. The steel surfaces as received, particularly those of the spacer ring, would not have insured a uniform spacing of the two surfaces forming the annulus.

Although four 3/8" bolts would have been sufficient from considerations of strength alone, it was decided to use sixteen in order to obtain oil tightness.

Originally rubber gasket material was to be used between the spacer ring and the Plexiglas surfaces to prevent oil leakage at the junction of the steel and Plexiglas outside the annulus. However, the rubber gasket would have been compressed in varying amounts around the test apparatus,

depending on the tension in each bolt upon tightening up. It was possible to circumvent this difficulty by using paper of 0.010" thickness.

The pressure tap was designed to accommodate a 1/4" copper tube fitting. The air release tap diametrically opposite was so placed to vent the test chamber while oil was being introduced.

The cathetometer used to take deflection readings was mounted as indicated in Figure II and Photograph No. (4). The heavy brass plug on which the cathetometer is mounted was machined to fit snugly into the thick walled pipe which had been welded into the center of the top web assembly of the test apparatus; the thick-walled pipe was machined true to an axis perpendicular to the surface of the Plexiglas. A bench mark was established on the web assembly to facilitate taking deflection readings.

Proof Test of Apparatus

The objective of this phase of the testing was to solve as completely as possible the many unexpected problems of detail which plague any initial effort. In addition it was desirable to establish a standard test procedure to be used during the remainder of the experimental work.

Of concern to the authors during the design of the

apparatus was the need for an effective seal between the Plexiglas surfaces and the edges of the test ring. Preliminary considerations indicated that the most likely solution would be the use of either a leather or rubber gasket of slightly greater width than the ring. The gasket could be shaped to fold back against the Plexiglas surface when the top assembly was bolted down. See Figure XXIX (a). To facilitate assembly, the gasket could be glued to the outer circumference of the ring prior to insertion in the test chamber.

The following trial gaskets were selected for preliminary investigation:

1. A strip of bicycle tire inner tube cut to 3/4" width, 28" in length, and joined at the ends with rubber cement. Results: Not successful because a secure junction could not be obtained.
2. Rubber electrical tape applied to the outer circumference with the ends lapped.
   Results: Extrusion of the tape between the Plexiglas surfaces and the edges of the ring occurred at pressures of about 400 psi.
3. Leather strip 3/4" wide, 28" in length with junction secured by a special leather cement.
   Results: Not successful because the strength of the junction was unsatisfactory.

appertua was the need for an effective seal between the Plastiline surfaces and the edges of the test tube. Preliminary considerations indicated that the most likely solution would be the use of either a leather or rubber gasket of slightly greater width than the slot. The gasket could be shaped to fold back against the Plastiline surface when the top assembly was pushed down. See Figure XXIX (e). To facilitate assembly, the gasket could be glued to the outer circumference of the rim prior to insertion in the test chamber.

The following trial gaskets were selected for preliminary investigation:

1. A strip of bicycle tire inner tube cut to 3\4" width, 25" in length, and joined at the ends with rubber cement. Results: Not successful because a secure junction could not be obtained.

2. Rubber electrical tape applied to the outer circumference with the edge lapped.
Results: Extrusion of the tape between the Plastiline surfaces and the edges of the rims occurred at pressures of about 400 psi.

3. Leather strip 3\4" wide, 25" in length with junction secured by a special fastener cement.
Results: Not appreciably increased the strength of the junction was unsatisfactory.

FIGURE XXIX

DETAILS OF GASKET

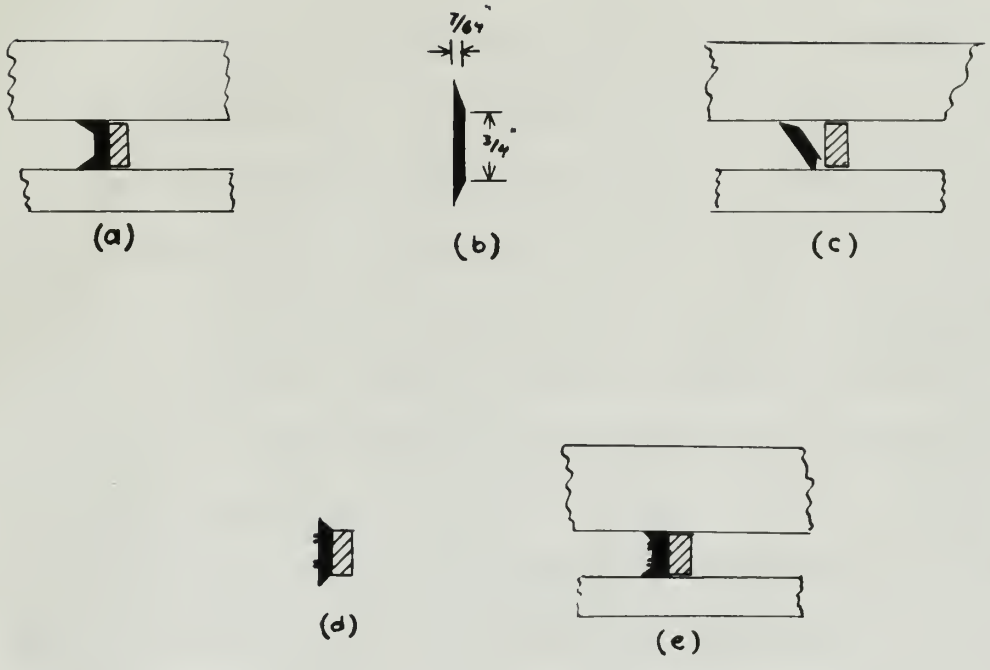

FIGURE XXX

DETAILS OF LUBRICANT TEST

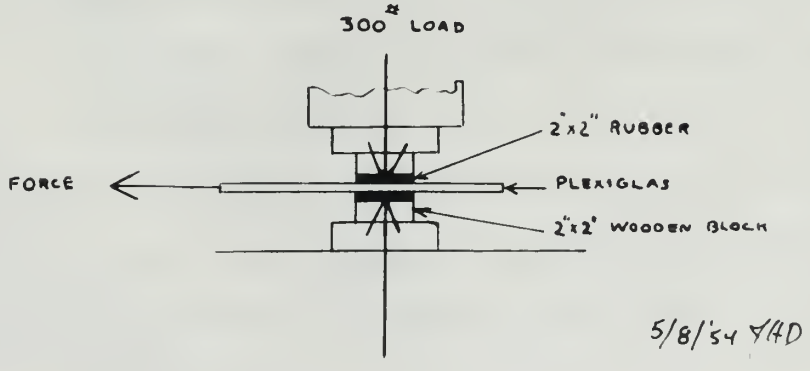

5/8/'54 AHD

4. Truck tire inner tube 9" in diameter cut to 3/4" width with edges beveled as indicated in Figure XXIX(b).

   Results: Successful in holding pressures up to 875 psi.; it is interesting to note that even at this pressure the gasket did not extrude. Pressure was not increased beyond 875 psi. for fear of introducing a permanent set in the top Plexiglas surface. There was no junction difficulty in this particular case because the gasket was continuous.

Further experimentation with gasket No. 4 indicated that the 3/4" width was unnecessary and could be reduced to 1/2". The angle of the bevel was changed to 45°. The procedure for cutting the final gaskets was as follows:

1. Glue a 2" section of rubber tubing around the circumference of an 11" wooden disk attached to a lathe chuck.
2. Place the disk in the lathe and turn at slow speeds. (At high speeds the rubber was torn loose from the wooden disk)
3. Hold a sharp, pointed cutting tool at 45° to the edge of the disk and slowly press the tool into the rubber in much the same manner as if turning down wood.

4. Turn six inner tube 5" in diameter out to 3\4"
width with edge beveled as indicated in figure
XXIX(b).

Result: Successful in holding pressures up to
875 psi.; it is interesting to note that even at
this pressure the gasket did not extrude. Pressure
was not increased beyond 875 psi. for fear of in-
troducing a permanent set in the top Plexiglas
surface. There was no injection difficulty in
this particular case because the gasket was con-
tinuous.

Further experimentation with Gasket No. 4 indicated
that the 3\4" width was unnecessary and could be reduced
to 1\2". The angle of the bevel was changed to 45°. The
procedure for cutting the final gaskets was as follows:

1. Glue a 2" section of rubber tubing around the cir-
cumference of an 11" aspian disk attached to a
lathe chuck.
2. Place the disk in the lathe and turn at slow speeds.
(A high speeds the rubber may tear loose from
the wooden disk)
3. Hold a sharp, pointed cutting tool at 45° to the
edge of the disk and firmly press the tool into
the rubber in such a manner as it bevels
down wood.

4. After the cutting blade has passed completely through the rubber, the tool is removed and inserted 1/2" from the first cut, the inclination being that required to produce a reverse 45° bevel.

Gaskets manufactured as above were glued to the outer circumference of the preliminary test rings with clear or black rubber cement. It was thought that a film of oil between the rubber gasket and the Plexiglas surfaces would be sufficient to lubricate the gasket and permit relatively friction free slipping. The first preliminary test ring was placed in the test chamber. Pressures well above the predicted failure pressure were applied without collapse of the ring. The possibility of passing through the first critical collapse pressure was discounted as a complete explanation because without noticeable restraint such could occur only by a combination of ideal conditions and fortuitious circumstances. The apparatus was repeatedly opened to adjust the gasket and, if possible to determine the cause of the restraint. After numerous trials the ring buckled at approximately 550 psi., well above the predicted collapse pressure.

The second preliminary test ring was similarly tested several times without success. At this point the authors

6. Close the cabinet once you have opened completely.

decided to direct all efforts toward the elimination of the restraining force which prevented the collapse of the rings at reasonable pressures. It was assumed that the restraining force occurred as a result of friction between the rubber gasket and the Plexiglas since without the gasket the rings were found to be completely free when enclosed in the test chamber.

Several types of lubricants were investigated by spreading the lubricant over two rubber 2"x2" squares and sandwiching a piece of Plexiglas between them. A load was applied to the rubber squares by means of wooden blocks placed between the rubber squares and the heads of a loading machine. See Figure XXX. The force necessary to move the Plexiglas under specified loads was observed. The following lubricants were used:

1. Number 40 S.A.E. motor oil.

   Results: Plexiglas could not be moved by a force less than 40 lbs. when a load of 300 lbs. was applied by the loading machine.

2. Silicone Compound DC4.

   Results: Same as No. 1.

3. Vaseline

   Results: Plexiglas could be moved by a force of approximately 8 lbs. when a load of 300 lbs. was applied by the loading machine.

4. Clear rubber cement applied to rubber and oil film on Plexiglas.

   Results: Plexiglas could be moved by a force of approximately 6 lbs. when a load of 300 lbs. was applied by the loading machine.

5. Black rubber-to-metal cement applied to rubber and oil film on Plexiglas.

   Results: Lubricant effective to the extent that the 2" rubber squares would not remain in place under wooden blocks as the load was being applied.

On the basis of the preceding results it was concluded that the black rubber-to-metal cement was the most suitable lubricant. The rubber gasket was cemented to the outer circumference of the preliminary test ring with a large amount of cement. The aluminum ring was then placed in the test apparatus and the top assembly bolted in position. It was noted at this time that the gasket would not remain in position on the aluminum ring but pulled away in the manner indicated in Figure XXIX (c). The top assembly was removed and several strands of light string were passed around the outer circumference of the gasket. See Figure XXIX (d). The beveled edges were observed to fold back uniformily along the surface of the Plexiglas when the ring and gasket were again placed in the test chamber and the top assembly had been positioned and bolted down. See Figure XXIX (e).

4. Clear rubber cement applied to rubber and oil film on Plexiglas.

Results: Plexiglas could be moved by a force of approximately 6 lbs. When a load of 300 lbs. was applied by the loading machine.

3. Black rubber-to-metal cement applied to rubber and oil film on Plexiglas.

Results: Important effective to the extent that the 5" rubber squares would not remain in place under wooden blocks as the load was being applied.

On the basis of the preceding results it was concluded that the clear rubber-to-metal cement was the most suitable lubricant. The rubber gasket was cemented to the outer circumference of the preliminary test ring with a large amount of cement. The aluminum ring was then placed in the test apparatus and the top assembly lofted to position. It was noted at this time that the gasket would not remain in position on the aluminum ring but pulled away in the manner indicated in Figure III (a). The top assembly was removed and several strands of light string were wound around the outer circumference of the gasket. See Figure III (b). The sealed edges were observed to fold back uniformly along the surface of the Plexiglas when the ring and gasket were again placed in the test chamber and the air assembly had been positioned and bolted down. See Figure III (c).

Pressure was applied and the preliminary test ring buckled very close to the predicted collapse pressure.

The test procedure with respect to gasket material, gasket size, and lubrication was thus established. It is worthwhile to note that the best results were obtained when the black cement was applied to the beveled surfaces, the inner surface of the gasket, and the outer surface of the ring. The cement was allowed to dry slightly after application.

In an effort to obtain deflection readings the authors considered testing the rings in two phases. During the first phase clear rubber cement would be used as the lubricant and both deflection readings and strain readings were to be recorded up to the pressure at which collapse was expected. The pressure would then be released and the ring removed for lubrication with the black cement. During the second phase strain readings were to be taken until actual collapse occurred. However, as pointed out previously strains taken during the two phases did not correlate. Furthermore, the cathetometer proved impractical. The third preliminary test ring was strain gaged and tested with various lubricants and gasket material to show that the strains did in fact depend upon these factors. Results of these tests were presented in Figure IV.

pressure was applied and the freshwater part only pushed
very close to the predicted collapse pressure.

The test procedure with respect to pressure application,
gasket size, and lubrication was thus established. It is
worthwhile to note that the best results were obtained when
the black cement was applied to the beveled surfaces, the
inner surface of the gasket, and the outer surface of the
ring. The gasket was allowed to dry slightly after appli-
cation.

In an effort to obtain duplication regarding the surfaces
considered testing the rings in two phases. During the
first phase clear rubber cement would be used as the
lubricant and both deflection readings and strain readings
were to be recorded up to the pressure at which collapse
was expected. The pressure would then be released and the
ring removed for inspection with the black cement. During
the second phase strain readings were to be taken until
normal collapse occurred. However, as carried out pre-
viously strains taken during the two phases did not corre-
late. Furthermore, the permanent flawed imperfect.
The third preliminary test ring was strain gaged and tested
with various lubricants and gasket material to show most
of these tests were presented in Figure IX.
the original ring is first described upon these results.

During the proof testing period oil leakage around the bolt holes was noted. A strip of rubber electrical tape 3/4" in width was glued to the inner circumference of the spacer ring. The edges of this seal folded back toward the center of the test chamber and were pressed tightly against the Plexiglas when pressure was applied. Holes were cut in the electrical tape in way of the pressure tape and air release tape. Little or no oil leakage was observed around the bolt holes throughout the remainder of the tests.

Test of Compression Specimens

Since the value of E, Young's Modulus, and σ_y were of primary importance in the correlation of experimental data with predicted stress distribution and collapse pressure, it was immediately apparent to the authors that the values of E and σ_y for the material used should be determined experimentally rather than relying on handbook values which represent average data at best.

Four 2 1/2" wide semi-circular sections were cut from the original piece of aluminum tubing to provide the material from which tensile specimens were to be machined. The semi-circular sections had to be flattened before machining; therefore, the sections were annealed prior to the flattening process to prevent cracking. Annealing was carried out as recommended by the Metals Handbook (5). To insure a reasonably complete anneal, the semi-circular

To insure a reasonably complete mineral, the semi-circular
carried out as recommended by the Materials Handbook (5).
the distorted process to remove chipping. Sometimes mul
specimens; therefore, the sections were examined prior to
The semi-circular sections may be fractured before
material from which tensile specimens were to be machined.
the original piece of aluminum testing to provide the
four 2 1/2" wide semi-circular sections were cut from
represent average data at best.
permanently rather than relying on handbook values which
of E and C_3 for the material used should be determined re-
of primary importance in the correlation of experimental
data with predicted stress distribution and collapse pressure,
It was immediately apparent to the authors that values

Test of Compression Specimens

Since the value of ν, Young's modulus, and C_3 were

bolt holes throughout the remainder of the tests.
the elastomer when pressure was applied. Holes were put in
release tape. Little or no oil leakage was observed around
centers of the test chamber and were treated slightly wider
sleeve ring. The edges of this seal folded back toward the
3/4" in width was glued to the inner circumference of the
bolt holes was noted. A strip of rubber electrical tape
During the proof testing period oil leakage around the

sections were heated for two hours at 750°F, then slowly cooled (not faster than 50°F per hour) until a temperature of 500° was reached. Below 500°F the rate or cooling was not important and the sections were removed from the furnace and allowed to air cool to room temperature.

The sections were then flattened in a mechanical press. No difficulties were experienced in the flattening operation. Cracks did not occur in the sections and very little spring-back was observed when the upper head of the press was lifted from the sections. From all indications, the aluminum alloy was sufficiently annealed by the process described above.

To obtain uniformity of physical properties in the flattened sections, they were heat treated along with the ring sections as described in the material related to the manufacture of the rings.

Unfortunately the flat bar specimens were not quite as true as the authors had anticipated, and it was feared that appreciable bending stresses might be introduced in the tensile specimens during the application of loads. Initial unfairness could have been eliminated by machining the flat surfaces; however, this procedure would not have been too practical since the original wall thickness of the aluminum tubing was only 0.250". A further reduction in thickness would have increased the difficulty of mounting

of Tensometers. It was then decided to use three compression specimens cut from the flattest portions of the section. Since the length of the specimens required was of the order of 2.5", no appreciable difficulty was experienced in finding planar portions of the sections for this purpose.

Three compression specimens were manufactured by the Department of Mechanical Engineering machine shop. Specification for compression test specimens:

Using the same material from which the rings were manufactured, three specimens are to be cut and milled to the dimensions of 0.84 x 2.53 inches, these dimensions conforming to the proportions of 1 to 3 as recommended by ASTM standards.

The compression specimen test block and two Type A Huggenberger Tensometers were furnished by the Department of Mechanical Engineering, M.I.T. Load was applied to the block by means of a 10,000 pound capacity loading machine.

As recommended by the Metals Handbook, the Tensometers were mounted on opposite sides of the test specimen. The gage points were located symmetrically with respect to the middle of the length of the specimen and not closer to the end of the specimen than a distance approximately equal to the width of the specimen.

It was found necessary to reset the Huggenberger Tensometers at least four times during each specimen run.

Extensometers at least four times during each cycle.

It was found necessary to check the Huggenberger extensometers. It was then decided to use three comparison specimens cut from the flattest portions of the specimen. Since the length of the specimens required was of the order of 7.5", no appreciable difficulty was experienced in finding minor portions of the sections for this purpose.

Three compression specimens were manufactured by the Department of Mechanical Engineering machine shop.

Specification for compression test specimens:

Using the same material from which the rivets were manufactured, three specimens are to be cut and milled to the dimensions of 0.84 x 2.55 inches, these dimensions conforming to the proportions of 1 to 3 as recommended by ASTM standards.

The compression specimen test block and two Type A Huggenberger Tensometers were furnished by the Department of Mechanical Engineering, M.I.T. Load was applied to the block by means of a 10,000 pound capacity loading machine.

As recommended by the Metals Handbook, the Tensometers were mounted on opposite sides of the test specimen. The gage points were located symmetrically with respect to the middle of the length of the specimen and not closer to the end of the specimen than a distance approximately equal to the width of the specimen.

APPENDIX B

Sample Calculations and Summary of Data

Calculation of R_o, Radius to Outer Circumference

The radius to the outer circumference of each ring was measured indirectly by fitting a wire of known diameter around the outer surface of the ring, scribing the wire in position, and then measuring the distance between the scribe marks on a 36" rule.

Then $R_o = \frac{\ell}{2\pi} - d$, where

R_o = radius to outer circumference of the ring in inches.

ℓ = length of wrapper wire measured between scribe marks in inches.

d = diameter of wrapper wire in inches.

Thus for Ring No. 1:

$$R_o = \frac{28.391}{2\pi} - 0.01"$$

$$R_o = 4.509"$$

The value of R_o used in the remaining calculations is the average of all measured radii.

Compression Test

The strains given by opposite Huggenberger Tensometers at a specified load were averaged to avoid errors due to bending. The stress corresponding to this strain was obtained by dividing the load by the original cross sectional area of the specimen.

The following calculation applies in the case of Specimen No. 1 at a load of 4500 lbs.

Data - Specimen No. 1

Load lbs.	Huggenberger No. 2201 Calibration Factor 1040 Rdg.	Rdg	Rdg	Huggenberger No. 2195 Calibration Factor 1051 Rdg	Rdg	Rdg
0	1.50			1.5		
500	1.30	-0.20	-0.20	1.24	-0.26	-0.26
1000	1.09	-0.21	-0.41	1.00	-0.24	-0.30
1500	0.86	-0.23	-0.64	0.74	-0.26	-0.76
2000	0.63	-0.23	-0.87	0.50	-0.24	-1.00
2500	0.43	-0.20	-1.07	0.28	-0.22	-1.22
3000	0.20	-0.23	-1.30	0.05	-0.23	-1.45
Reset	1.50			1.50		
3500	1.33	-0.17	-1.47	1.28	-0.22	-1.67
4000	1.11	-0.22	-1.69	1.04	-0.24	-1.91
4500	0.89	-0.22	-1.91	0.81	-0.23	-2.14

$$\text{Strain} = \frac{\text{Tensometer Reading}}{\text{Calibration Factor}} \text{ in inches/inch}$$

ε_1 = Strain in inches/inch given by Tensometer No. 2201

ε_2 = Strain in inches/inch given by Tensometer No. 2195

ε = Average measured strain in micro-inches/inch

$$\varepsilon_1 = \frac{-1.91}{1040} = -0.001836 \text{ inches/inch}$$

$$\varepsilon_2 = \frac{-2.14}{1051} = -0.002036 \text{ inches/inch}$$

$$\varepsilon = \frac{(-0.001836) + (-0.002036)}{2} \times 10^6 = -1936 \text{ micro-inches/inch}$$

$$\sigma = \frac{L}{txw}$$

σ = stress in psi.

L = load in lbs.

The following calculation applies in the case of

Specimen No. 1 at a load of 4500 lbs.

Date - Specimen No. 1

Engineer in charge Mr. Lang Engineering Lab. 1395

Deflection Meter 1940 Deformation Meter 1931

Load lbs.	Mag.	Deg	Min	Min	Min
0	1.50		1.5		
500	2.30	-0.20	-0.80	1.54	-0.20
1000	1.95	-0.21	-0.41	1.00	-0.29
1500	0.80	-0.23	-0.04	0.74	-0.26
2000	0.05	-0.25	-0.07	0.50	-0.24
2500	0.45	-0.20	-1.07	0.38	-0.22
3000	0.10	-0.27	-1.30	0.05	-0.23
Reset	1.50			1.50	
2500	1.33	-0.17	-1.47	1.38	-0.12
1000	1.11	-0.22	-1.69	1.04	-0.34
4500	0.85	-0.27	-1.31	0.82	-0.23	-2.14

$$\text{Strain} = \frac{\text{Deflection Meter}}{\text{Deformation Factor}} \text{ in inches/inch}$$

$$\varepsilon_1 = \frac{\text{Strain in inches/inch given by Deformation Meter No. 1931}}{}$$

$$\varepsilon_2 = \frac{\text{Strain in inches/inch given by Deformation Meter No. 2195}}{}$$

$$\varepsilon = \text{Average mechanical strain in direction of item}$$

$$\varepsilon_1 = \frac{-1.91}{1940} = -0.000979 \text{ inches/inch}$$

$$\varepsilon_2 = \frac{-2.14}{1931} = -0.000959 \text{ inches/inch}$$

$$\varepsilon = \frac{(-0.000979) + (-0.000959)}{2} \times 10^6 = -1936 \frac{\text{micro-inches}}{\text{inch}}$$

$$\sigma = \frac{P}{A_{TM}}$$

σ = stress in psi.

n = load in lbs.

t = thickness of specimen in inches

w = width of specimen in inches

$$\sigma = \frac{4,500}{(0.201)(0.841)} = 20,500 \text{ psi}$$

The results of the Compression Test calculations are presented as experimental points in Figure III.

Circumferential Strains

Except for the case of Ring No. 2 all predicted circumferential strain distributions were computed directly from equation (3).

$$\epsilon = \frac{P R_o}{E h} + \frac{6 P R u_o h \cos 2\theta}{Eh^3 - 4 P R^3}$$

All factors are defined in SYMBOLS AND ABBREVIATIONS, page vi.

For Ring No. 7, $u_o = 0.1535"$; then for P = 240 psi.

$$\epsilon = \frac{(240)(4.508)}{(0.250)(10.8 \times 10^6)} + \frac{(6)(240)(4.383)(0.1535)(0.250)\cos 2\theta}{(10.8 \times 10^6)(0.250)^3 - (4)(240)(4.383)^3}$$

$\epsilon = (400.7) + (2754.8 \cos 2\theta)$ micro-inches/inch

θ	$\cos 2\theta$	$2754.8 \cos 2\theta$	ϵ
0° & 180°	+1	+2754.8	+3155.5
30° & 210°	+1/2	+1377.4	+1778.1
60° & 240°	-1/2	-1377.4	-976.7
90° & 270°	-1	-2754.8	-2354.1
120° & 300°	-1/2	-1377.4	-976.7
150° & 330°	+1/2	+1377.4	+1778.1

$$C = \frac{4{,}500}{(0.201)(0.1461)} = 30{,}300 \text{ psi}$$

The results of the compressor test calculations are presented as experimental points in Figure III.

Circumferential Stress

Except for the case of Ring No. 2 all predicted circumferential stress distributions were computed directly from equation (3).

$$\epsilon = \frac{2\,n}{3\,r_o} + \frac{b\,i\,x\,N^o\,n\,\cos 2\,\theta}{r_2^2 - i\,\epsilon\,x_2}$$

All factors are defined in SYMBOLS AND ABBREVIATIONS, page vi.

For Ring No. 7, $a^o = 0.1535$"; time for $\gamma = 240$ psi.

$$\epsilon = \frac{(480)(4.304)}{(0.1250)(10.6 \times 10^6)} + \frac{(61)(240)(4.304)(0.1535)(0.250)\cos 2\,\theta}{(10.6 \times 10^6)(0.250)^2 - (4)(1240)(4.304)^2}$$

$\epsilon = (452.7) + (2124.3 \cos 2\,\theta)$ micro-inches/inch

θ	$\cos 2\,\theta$	$2124.8 \cos 2\,\theta$	ϵ
$0^o \equiv 180^o$	+1	+2124.8	+2577.5
$30^o \equiv 210^o$	+1/2	+1062.4	+1515.1
$60^o \equiv 240^o$	-1/2	-1062.4	-609.7
$90^o \equiv 270^o$	-1	-2124.8	-1672.3
$120^o \equiv 300^o$	-1/2	-1062.4	-609.7
$150^o \equiv 330^o$	+1/2	+1062.4	+1515.1

Since ε has been defined as a compression strain the plotted values become:

Circumferential Position	Strain in micro-inches/inch
0° & 180°	-3155.5
30° & 210°	-1788.1
60° & 240°	+976.7
90° & 270°	+2354.1
120° & 300°	+976.7
150° & 330°	-1778.1

The circumferential strain distribution for Ring No. 2 was computed using the measured out-of-roundness at each station instead of $u_o \cos 2\theta$.

$$\varepsilon = \frac{P R_o}{E h} + \frac{6 P R u h}{Eh^3 - 4PR^3} \qquad (5)$$

Data:

Circumferential Position	u	Sign as determined by equation (5)
0° & 180°	0.0075"	-
30° & 210°	0.0800"	+
50° & 230°	0.0125"	+
80° & 260°	0.0065"	+
110° & 290°	0.0045"	-
150° & 330°	0.0125"	-

at P = 400 psi.

Since ε has been defined as a compression strain the plotted values become:

Circumferential Position	Strain in micro-inches/inch
0^o & 180^o	-3155.5
30^o & 210^o	-1788.1
60^o & 240^o	+979.7
90^o & 270^o	+2394.1
120^o & 300^o	+976.7
150^o & 330^o	-1778.1

The circumferential strain distribution for ring No. 2 was computed using the measured out-of-roundness at each station instead of r_o cos 2 θ.

$$\varepsilon = \frac{\beta\, R_o}{E\, H} + \frac{t\, E\, R\, H}{EI_z - \mu R^2 S} \qquad (5)$$

Data:

Circumferential Position	δ	Sign as determined by equation (5)
0^o & 180^o	0.0075"	-
30^o & 210^o	0.0800"	+
50^o & 230^o	0.0125"	+
80^o & 260^o	0.0065"	+
120^o & 290^o	0.0045"	-
150^o & 330^o	0.0125"	-

at P = 400 psi.

$$\varepsilon = \frac{(400)(4.508)}{(0.250)(10.8 \times 10^6)} + \frac{(6)(400)(4.383)(0.250)\,u}{(10.8 \times 10^6)(0.250)^3 - (4)(400)(4.383)^3}$$

ε = 667.85 + 83353.4 u micro-inches/inch

Substituting data:

Circumferential Position	Plotted Strain in micro-inches/inch
0° & 180°	-42.7
30° & 210°	-1334.65
50° & 230°	-1709.77
80° & 260°	-1209.63
110° & 290°	-292.76
150° & 330°	+374.08

A summary of all such calculated values is given in the form of curves, see Figures V, VIII, XI, XIV, and XVII.

Maximum Strains

The maximum strains at specified pressures were computed using equation (3). Cos 2 θ becomes +1 for 0° and 180° positions and -1 for 90° and 270° positions.

$$\varepsilon = \frac{P R_o}{E h} + \frac{6 P R u_o h}{E h^3 - 4PR^3} \qquad (6)$$

$$\varepsilon = \frac{P R_o}{E h} - \frac{6 P R u_o h}{E h^3 - 4 P R^3} \qquad (7)$$

ε for a ring of given u_o is computed from equations (6) and (7) at several increments of pressure. For Ring No. 5, u_o = 0.070"; then at 50 psi.:

$$\varepsilon = \frac{(10.230)(10.0 \times 10^6)}{(4001)(4.302)} + \frac{(10.8 \times 10^6)(0.2301)^3 - 14(4001)(4.302)^3}{(8)(4000)(4.302)(0.2301)(0.2301) \text{ in}}$$

$$\varepsilon = 661.35 + 0323.4 \text{ micro-inches/inch}$$

Summation data:

Circumferential location	In plate-thickness direction
	Focused Stress
D_0 & 180_0	-42.1
30_0 & 210_0	-1234.23
30_0 & 330_0	-1713.11
90_0 & 270_0	-1809.03
150_0 & 330_0	-3825.19
150_0 & 330_0	+3174.00

& tabulate of all such calculated values is given on the following page, see figures A, AIII, XI, XIA, and XAII.

Maximum Stresses

The maximum stresses at specified locations were combined using equation (3). Use 5 @ locations at the 0_0 and 180_0 horizons and -1 for 30_0 and 150_0 positions.

$$\varepsilon = \frac{\beta\, n}{\gamma\, n^0} = \frac{\beta\, M_2 - \gamma\, M_3}{\beta\, \gamma\, \Pi\, n^0\, n} \qquad (6)$$

$$\varepsilon = \frac{\beta\, n}{\delta\, M^0} = \frac{\beta\, M_2 - \gamma\, M_3}{\delta\, \gamma\, \Pi\, n^0\, n} \qquad (7)$$

$n^0 = 0.0410$, given at 30 bar:

and (7) at central locations of diameter. Use step no. 3, & for a kind of given n^0 to computed item equation (6)

ε at 0° and 180°

$$\varepsilon = \frac{(50)(4.508)}{(10.8 \times 10^6)(0.250)} + \frac{(6)(50)(4.383)(0.070)(0.250)}{(10.8 \times 10^6)(0.250)^3 - (4)(50)(4.383)^3}$$

ε = 234.9 micro-inches/inch (Plotted with - sign)

ε at 90° and 270°

$$\varepsilon = \frac{(50)(4.508)}{(10.8 \times 10^6)(0.250)} - \frac{(6)(50)(4.383)(0.070)(0.250)}{(10.8 \times 10^6)(0.250)^3 - (4)(50)(4.383)^3}$$

ε = - 68.0 micro-inches/inch (Plotted with + sign)

Pressure psi.	Plotted value at 0° and 180°	Plotted value at 90° and 270°
50	-234.9	+68.0
100	-507.7	+173.8
150	-834.3	+333.5
200	-1,241.7	+573.9
250	-1,778.1	+943.4
300	-2,539.9	+1,538.2
350	-3,750.7	+2,582.1
400	-6,077.3	+4,741.7

A summary of all such calculated values is given in the form of plots, see Figures XX-XXVI.

Collapse Pressures

The curves of predicted collapse pressures were derived indirectly by first plotting equation (4). Stresses at various pressures were computed for several values of u_o.

$$\varepsilon \text{ at } 0^\circ \text{ and } 180^\circ$$

$$\varepsilon = \frac{(50)(4.308)}{(170.8 \times 10^6)(0.250)} - \frac{(8)(50)(4.303)(0.070)(0.250)}{(170.8 \times 10^6)(0.250)^2 - (4)(50)(4.303)^2}$$

$$\varepsilon = 324.3 \text{ micro-inches/inch (Plotted with - sign)}$$

$$\varepsilon \text{ at } 90^\circ \text{ and } 270^\circ$$

$$\varepsilon = \frac{(50)(4.308)}{(170.8 \times 10^6)(0.250)} - \frac{(8)(50)(4.303)(0.070)(0.250)}{(170.8 \times 10^6)(0.250)^2 - (4)(50)(4.303)^2}$$

$$\varepsilon = -69.4 \text{ micro-inches/inch (Plotted with + sign)}$$

Increment	0° and 180°	90° and 270°
Det.	Plotted values at	Plotted values at
50	-254.9	+68.6
100	-501.7	+173.8
150	-684.3	+233.9
200	-1,241.7	+273.9
250	-1,778.1	+283.4
300	-2,234.9	+1,239.2
350	-3,150.7	+2,302.1
400	-4,111.3	+4,141.7

A summary of all these calculated values is given in the form of plots, see Figures IX-XXVI.

Computer Programs

The output of listings containing numerical values pertaining to various increments are omitted for brevity. Statements at

A cross curve of predicted collapse pressures was then drawn using the values given by the intersection of a single ordinate 35,000 psi. or 41,000 psi. with the curves of stress versus pressure.

To compute one point for stress-pressure curves:

$u_o = 0.050"$, $P = 50$ psi., $h = 0.250"$

$$\sigma = \frac{P R_o}{h} + \frac{6 P R u_o h E}{E h^3 - 4 PR^3}$$

$$\sigma = \frac{(50)(4.508)}{(0.250} + \frac{(6)(50)(0.050)(4.383)(0.250)(10.8 \times 10^6)}{(10.8 \times 10^6)(0.250)^3 - (4)(50)(4.383)^3}$$

$\sigma = 2,090$ psi., maximum compressive stress

Similarly:

Pressure psi.	σ psi.
100	4,431
200	10,609
250	15,005
300	21,139
350	30,737
400	50,206

Values for $\sigma_{max.}$ were computed at several increments of pressure for the following values of u_o: 0.050", 0.100", 0.150", 0.200", and 0.250". The procedure was repeated using $h = h_{min.} = 0.243"$.

The results of these computations are presented as curves, Figure XXXI. Shown in the same Figure are ordinates

A cross curve of tangential cylinder pressure was drawn using the various given BJ Rod Interpolator of 5 single ordinate 35,000 psi. or 47,000 psi. with the curves of stress versus pressure.

To compute one point for stress-intensity curves:

$\sigma^{\circ} = 0.050^{\circ}$, $E = 30 \times 10^{6}$, $\mu = 0.250$

$$\epsilon = \frac{1}{E}\sigma^{\circ} + \frac{\rho}{E}\sigma^{\circ}\mu - 4\mu$$

$$\epsilon = \frac{(50)(4.5061)}{(0.250)} + \frac{(5)(50)(10.050)(6.385)(0.250)(10.8 \times 10^{6})^{3}}{(10.8 \times 10^{6})(10.250)^{3}} - (4)(50)(4.385)^{3}$$

$\epsilon = 5,050$ psi., maximum cylindrical stress

Stiffer:

Pressure psi.	ϵ psi.
100	4,431
200	10,609
250	13,003
300	21,139
350	30,137
400	30,258

Values for $\epsilon_{max.}$ were checked by several trial methods of Pressure for the following values of μ: 0.050", 0.100", 0.150", 0.200", and 0.245". The coordinates were selected using $\mu = \mu_{min.} = 0.245$".

The results of these computations are plotted on [illegible] curves, Figure XXII. Shown in dye also plotted are theoretical

FIGURE XXXI

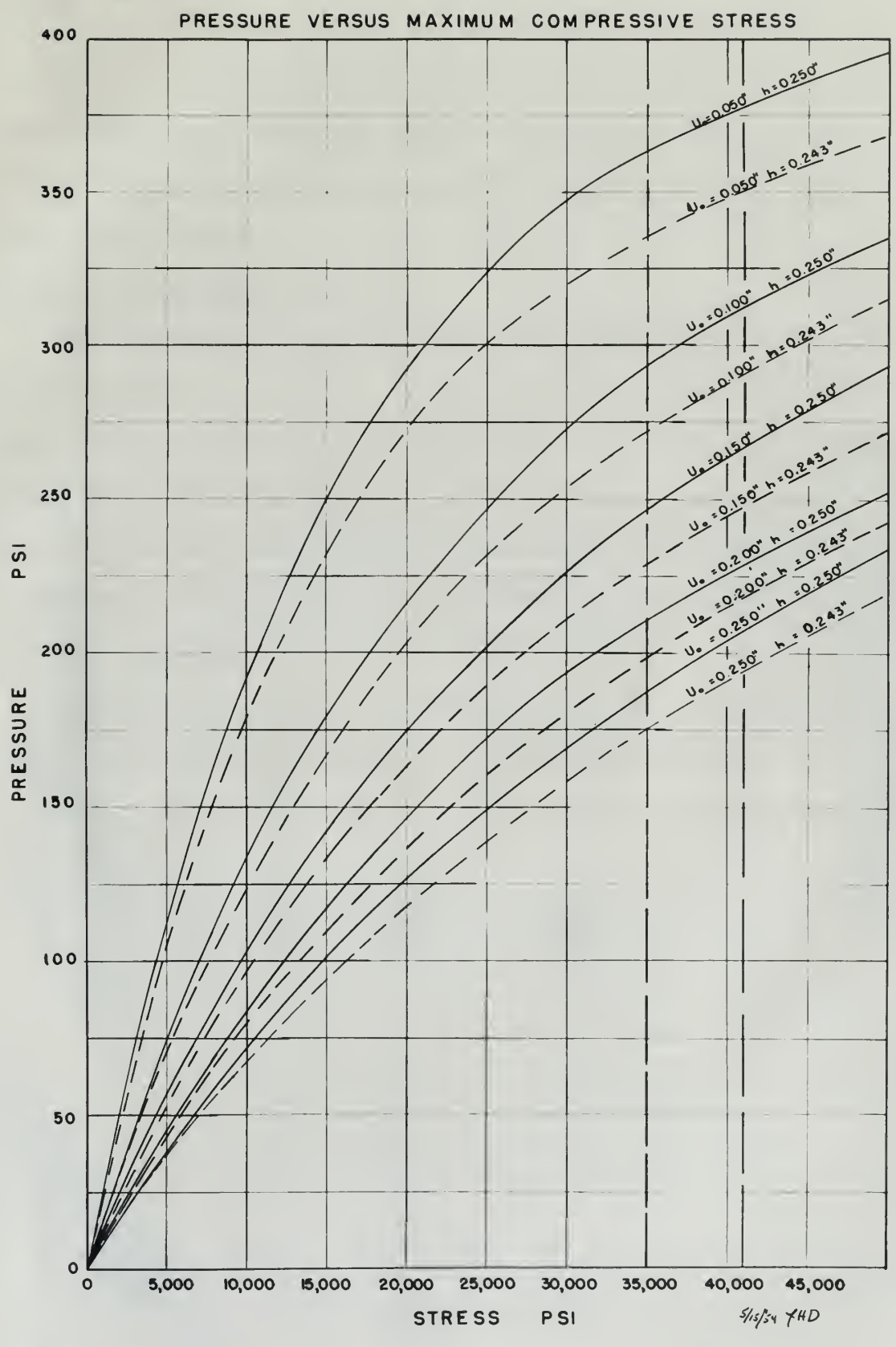
PRESSURE VERSUS MAXIMUM COMPRESSIVE STRESS
PRESSURE PSI
STRESS PSI
0
50
100
150
200
250
300
350
400
0
5,000
10,000
15,000
20,000
25,000
30,000
35,000
40,000
45,000
Uo=0.050" h=0.250"
Uo=0.050" h=0.243"
Uo=0.100" h=0.250"
Uo=0.100" h=0.243"
Uo=0.150" h=0.250"
Uo=0.150" h=0.243"
Uo=0.200" h=0.250"
Uo=0.200" h=0.243"
Uo=0.250" h=0.250"
Uo=0.250" h=0.243"
5/15/54 YHD

at 35,000 psi. and 41,000 psi. The intersection of pressure-stress curve with these ordinates determined the points through which the predicted collapse pressure curves were drawn; see Figures XXVII and XXVIII.

Experimental Strain Readings

The strain data was checked for significant errors by plotting measured strains versus pressure for each strain gage. There were no marked deviations from the fair curves which were drawn through the points. These curves were also used to determine the experimental points shown in the plots of circumferential strain distribution in Figures V, VIII, XI, XIV, and XVII.

The measured values of strain shown in Figures IV and XX-XXVI were taken directly from the original data.

XI-XIX were taken directly from the original data.

The measured values of micrin shown in Figure IX and XI, XIV, and XVII.

Of circumferential strain distribution in Figures V, VIII, used to determine the experimental points shown in the circle motor were taken through the points. These curves must also plotted measured strain values traverse for each blade. There may be noted deviations from the fair curves

Experimental Strain Gradients

The strain data was checked for sufficient circle by drawn per Figures XVII and XVIII.

through which the predicted radiation intensity curves were after some with three ordinates determined for points at 25,000 per. and 47,000 per. The interpretation of measure-

APPENDIX C

Original Data

Table I is a tabulation of the data taken during the test of the three compression specimens.

Table II is a record of the data recorded during the investigation of the effects of lubricants and gasket material upon the strain distribution around the inner circumference of the aluminum rings.

Tables III - XI contain data relating to physical dimensions, circumferential strain distribution, collapse pressures and diametral readings for each ring.

APPENDIX C

Original Data

Table I is a tabulation of the data taken during the year of the three compression specimens.

Table II is a record of the data recorded during the investigation of the effects of lubricants and powder material upon the strain distribution around the circumferences of the plugless rings.

Tables III - XI contain data relating to physical dimensions, circumferential strain distribution, collapse pressure and elemental readings for each ring.

Table I
Data for Stress-Strain Curve in Compression

Load	Specimen #1		Specimen #2		Specimen #3	
lbs.	H#2201	H#2195	H#2201	H#2195	H#2201	H#2195
0	1.50	1.50	1.60	1.58	1.58	1.60
500	1.30	1.24				
1000	1.09	1.00	1.40	0.94	1.26	0.95
1500	0.86	0.74				
2000	0.63	0.50	0.96	0.41	0.82	0.55
2500	0.43	0.28				
3000	0.20	0.05	0.59	0.03	0.37	0.19
Reset to	1.50	1.50	1.55	1.62	1.59	1.49
3500	1.33	1.28				
4000	1.11	1.04	1.05	1.15	1.15	1.06
4500	0.89	0.81				
5000	0.66	0.57	0.62	0.69	0.70	0.60
5500	0.45	0.35	0.45	0.52	0.46	0.35
6000	0.21	0.10	0.22	0.29	0.24	0.10
Reset to	1.50	1.60	1.60	1.55	1.54	1.53
6500	1.30	——	1.36	1.30	1.40	1.43
7000	1.05	——	1.10	1.03	1.11	1.18
7500	0.82	——	0,90	0.80	0.78	0.84
8000	0.56	——	0.65	0.55	0.38	0.40
				Reset to	1.50	1.50
8500	0.25	——	0.35	0.19	1.10	1.07
Reset to	1.50	1.50	1.50	1.60		
9000	1.01	1.12	1.34	1.40	0.11	-0.12
				Reset to	1.47	1.55
9110					0.29	0.10
9500	0.01	0.30	0.54	0.36		
Reset to	1.50	1.50	1.55	1.45		
9630	0.02	0.23				
9650			0.39	-0.15		

Table 1

Data for planning/budgeting in Cameroon

Type	Population	Growth %	Density	Urban %	Urban growth %	Urban density
0	1.00	0.00	1.00	1.00	0.00	1.00
200	1.00	0.00	1.00	1.00	0.00	1.00
400	1.00	0.00	1.00	1.00	0.00	1.00
600	1.00	0.00	1.00	1.00	0.00	1.00
800	1.00	0.00	1.00	1.00	0.00	1.00
1000	1.00	0.00	1.00	1.00	0.00	1.00
1200	1.00	0.00	1.00	1.00	0.00	1.00
1400	1.00	0.00	1.00	1.00	0.00	1.00
1600	1.00	0.00	1.00	1.00	0.00	1.00
1800	1.00	0.00	1.00	1.00	0.00	1.00
2000	1.00	0.00	1.00	1.00	0.00	1.00
2200	1.00	0.00	1.00	1.00	0.00	1.00
2400	1.00	0.00	1.00	1.00	0.00	1.00
2600	1.00	0.00	1.00	1.00	0.00	1.00
2800	1.00	0.00	1.00	1.00	0.00	1.00
3000	1.00	0.00	1.00	1.00	0.00	1.00
3200	1.00	0.00	1.00	1.00	0.00	1.00
3400	1.00	0.00	1.00	1.00	0.00	1.00
3600	1.00	0.00	1.00	1.00	0.00	1.00
3800	1.00	0.00	1.00	1.00	0.00	1.00
4000	1.00	0.00	1.00	1.00	0.00	1.00
4200	1.00	0.00	1.00	1.00	0.00	1.00
4400	1.00	0.00	1.00	1.00	0.00	1.00
4600	1.00	0.00	1.00	1.00	0.00	1.00
4800	1.00	0.00	1.00	1.00	0.00	1.00
5000	1.00	0.00	1.00	1.00	0.00	1.00

Type	Population	Growth %	Density	Urban %	Urban growth %	Urban density
0	1.00	0.00	1.00	1.00	0.00	1.00
200	1.00	0.00	1.00	1.00	0.00	1.00
400	1.00	0.00	1.00	1.00	0.00	1.00
600	1.00	0.00	1.00	1.00	0.00	1.00
800	1.00	0.00	1.00	1.00	0.00	1.00
1000	1.00	0.00	1.00	1.00	0.00	1.00
1200	1.00	0.00	1.00	1.00	0.00	1.00
1400	1.00	0.00	1.00	1.00	0.00	1.00
1600	1.00	0.00	1.00	1.00	0.00	1.00
1800	1.00	0.00	1.00	1.00	0.00	1.00
2000	1.00	0.00	1.00	1.00	0.00	1.00
2200	1.00	0.00	1.00	1.00	0.00	1.00
2400	1.00	0.00	1.00	1.00	0.00	1.00
2600	1.00	0.00	1.00	1.00	0.00	1.00
2800	1.00	0.00	1.00	1.00	0.00	1.00
3000	1.00	0.00	1.00	1.00	0.00	1.00
3200	1.00	0.00	1.00	1.00	0.00	1.00
3400	1.00	0.00	1.00	1.00	0.00	1.00
3600	1.00	0.00	1.00	1.00	0.00	1.00
3800	1.00	0.00	1.00	1.00	0.00	1.00
4000	1.00	0.00	1.00	1.00	0.00	1.00
4200	1.00	0.00	1.00	1.00	0.00	1.00
4400	1.00	0.00	1.00	1.00	0.00	1.00
4600	1.00	0.00	1.00	1.00	0.00	1.00
4800	1.00	0.00	1.00	1.00	0.00	1.00
5000	1.00	0.00	1.00	1.00	0.00	1.00

Type	Population	Growth %	Density	Urban %	Urban growth %	Urban density
0	1.00	0.00	1.00	1.00	0.00	1.00
200	1.00	0.00	1.00	1.00	0.00	1.00
400	1.00	0.00	1.00	1.00	0.00	1.00
600	1.00	0.00	1.00	1.00	0.00	1.00
800	1.00	0.00	1.00	1.00	0.00	1.00
1000	1.00	0.00	1.00	1.00	0.00	1.00
1200	1.00	0.00	1.00	1.00	0.00	1.00
1400	1.00	0.00	1.00	1.00	0.00	1.00
1600	1.00	0.00	1.00	1.00	0.00	1.00
1800	1.00	0.00	1.00	1.00	0.00	1.00
2000	1.00	0.00	1.00	1.00	0.00	1.00
2200	1.00	0.00	1.00	1.00	0.00	1.00
2400	1.00	0.00	1.00	1.00	0.00	1.00
2600	1.00	0.00	1.00	1.00	0.00	1.00
2800	1.00	0.00	1.00	1.00	0.00	1.00
3000	1.00	0.00	1.00	1.00	0.00	1.00
3200	1.00	0.00	1.00	1.00	0.00	1.00
3400	1.00	0.00	1.00	1.00	0.00	1.00
3600	1.00	0.00	1.00	1.00	0.00	1.00
3800	1.00	0.00	1.00	1.00	0.00	1.00
4000	1.00	0.00	1.00	1.00	0.00	1.00
4200	1.00	0.00	1.00	1.00	0.00	1.00
4400	1.00	0.00	1.00	1.00	0.00	1.00
4600	1.00	0.00	1.00	1.00	0.00	1.00
4800	1.00	0.00	1.00	1.00	0.00	1.00
5000	1.00	0.00	1.00	1.00	0.00	1.00

Table II
Strain Data for Preliminary Test Ring

Lubricant #2 Gasket #1 — Strains in Micro-inch per inch at Positions indicated

Pressure psi	0°	30°	60°	90°	120°	150°	180°	210°	240°	270°	300°	330°
0	7000	7000	7000	7000	7000	7000	7000	7000	7000	7000	7000	7000
99	6820	6920	——	6800	6695	6800	6890	6900	6830	6875	6780	——
200	6615	6830	——	6600	6375	6580	6765	6800	6660	6750	6570	——
303	6375	6800	——	6385	5920	6270	6660	6790	6580	6630	6215	——
403	6120	7650	——	6190	5200	5690	6510	7010	6780	6540	5630	——

Lubricant #1 Gasket #1

Pressure psi	0°	30°	60°	90°	120°	150°	180°	210°	240°	270°	300°	330°
0	7000	7000	7000	7000	7000	7000	7000	7000	7000	7000	7000	7000
99	6770	6900	——	6815	6680	6760	6855	6890	6850	6885	6765	——
200	6530	6870	——	6650	6285	6460	6700	6840	6770	6785	6480	——
303	6270	7100	——	6400	5500	5875	6635	7055	6860	6610	5870	——

Lubricant #1 Gasket #2

Pressure psi	0°	30°	60°	90°	120°	150°	180°	210°	240°	270°	300°	330°
0	7000	7000	7000	7000	7000	7000	7000	7000	7000	7000	7000	7000
99	6760	6880	——	6850	6700	6760	6840	6880	6860	6905	6790	——
200	6520	6810	——	6670	6350	6500	6700	6800	6735	6800	6550	——
303	6260	6840	——	6460	5840	6120	6550	6820	6730	6695	6150	——
403	6070	7430	——	6150	4810	5305	6450	7345	7180	6540	7240	——

Table III
Dimensions and Strain Data for Ring #1

Angle	h in.	b in	Strains in micro-inches per inch at pressures indicated: 0	99	200	303	403	453
0°	0.247	0.444	11,000	10,780	10,610	10,500	10,270	10,120
30°	0.250	0.445	11,000	10,805	10,670	10,515	10,285	10,160
60°	0.253	0.445	11,000	10,850	10,680	10,460	10,305	10,215
90°	0.261	0.444	11,000	10,860	10,640	10,370	10,200	10,120
120°	0.261	0.445	11,000	10,820	10,590	10,310	10,090	9,970
150°	0.256	0.444						
180°	0.247	0.445	11,000	10,860	10,790	10,790	10,730	10,710
210°	0.242	0.446	11,000	10,830	10,750	10,670	10,545	10,460
240°	0.243	0.445	11,000	10,805	10,560	10,255	9,910	9,730
270°	0.243	0.444	11,000	10,800	10,480	10,120	9,830	9,715
300°	0.246	0.444	11,000	10,870	10,700	10,530	10,470	10,430
330°	0.248	0.445	11,000	10,840	10,705	10,605	10,530	10,460

Collapse Pressure = 450 psi

Outside Radius = 4.509"

Diameter readings in inches

0-180°	9.012	90-270°	9.038
15-195°	9.008	105-285°	9.035
30-210°	9.008	120-300°	9.031
45-225°	9.016	135-315°	9.032
60-240°	9.027	150-330°	9.033
75-255°	9.035	165-345°	9.026

Table IV

Dimensions and Strain Data for Ring #2

Angle	h in.	b in.	Strains in micro-inches per inch at pressures indicated 0	99	200	303	403
0°	0.244	0.448	11,000	10,820	10,690	10,590	11,670
30°	0.246	0.447	11,000	10,810	10,605	10,320	9,550
60°	0.249	0.448	11,000	10,780	10,520	10,100	8,030
90°	0.247	0.448	11,000	10,765	10,475	10,090	8,640
120°	0.250	0.448	11,000	———	———	———	———
150°	0.252	0.448	11,000	10,800	10,580	10,250	8,850
180°	0.261	0.448	11,000	10,885	10,770	10,755	11,160
210°	0.262	0.448	11,000	10,850	10,750	10,840	12,335
240°	0.256	0.448	11,000	10,825	10,650	10,555	10,930
270°	0.247	0.448	11,000	10,920	10,885	11,040	12,720
300°	0.243	0.448	11,000	10,905	10,840	10,895	12,030
330°	0.243	0.448	11,000	10,790	10,540	10,220	9,580

Collapse Pressure = 425 psi

Diameter readings in inches.

0–180°	9.020	90–270°	9.042
15–195°	9.030	105–285°	9.027
30–210°	9.050	120–300°	9.020
45–225°	9.060	135–315°	9.013
60–240°	9.057	150–330°	9.010

Outside radius = 4.510"

Table V

Dimensions and Strain Data for Ring #3

Angle	h in.	b in	Strains in micro-inches per inch at pressures indicated 0	99	200	303	353	403	423
0°	0.246	0.444	9,000	8,745	8,450	7,940	7,690	6,225	5,230
30°	0.249	0.443	9,000	8,730	8,385	7,830	7,550	6,280	6,080
60°	0.249	0.445	9,000	8,840	8,640	8,475	8,390	8,450	9,150
90°	0.251	0.444	9,000	8,950	8,960	9,130	9,240	9,480	11,360
120°	0.254	0.443	9,000	8,895	8,840	8,930	8,980	9,040	10,010
150°	0.261	0.444	9,000	8,815	8,640	8,460	8,360	8,180	7,520
180°	0.262	0.445	9,000	8,750	8,460	8,035	7,775	7,405	5,760
210°	0.256	0.445	9,000	8,770	8,490	8,070	7,830	7,530	6,410
240°	0,247	0.444	9,000	8,840	8,660	8,490	8,410	8,355	8,860
270°	0.243	0.445	9,000	8,940	8,940	9.060	9,110	9,370	11,220
300°	0.243	0.445	9,000	8,755	8,520	8,360	8,410	8,660	9,920
330°	0.244	0.445	9,000	8,850	8,735	8,650	8,570	8,280	7,530

Collapse Pressure = 430 psi.

Diameter readings in inches.

Outside Radius = 4.510"

0-180°	9.072	90-270°	8.965
15-195°	9.071	105-285°	8.986
30-210°	9.061	120-300°	9.007
45-225°	9.041	135-315°	9.032
60-240°	9.017	150-330°	9.047
75-255°	8.983	165-345°	9.064

Table 5

Dimensional and Elastic Data for Steel

Dimensions in micro-inches per inch at temperatures indicated

Temp. °F	E in psi	0	200	400	600	800	1000
-400°	0.314	0.000	6,212	6,010	7,090	7,820	8,530
0°	0.312	0.000	6,212	6,010	7,090	7,820	8,530
32°	0.310	0.000	6,212	6,010	7,090	7,820	8,530
68°	0.308	0.000	6,212	6,010	7,090	7,820	8,530
100°	0.306	0.000	6,212	6,010	7,090	7,820	8,530
200°	0.304	0.000	6,212	6,010	7,090	7,820	8,530
300°	0.302	0.000	6,212	6,010	7,090	7,820	8,530
400°	0.300	0.000	6,212	6,010	7,090	7,820	8,530
500°	0.298	0.000	6,212	6,010	7,090	7,820	8,530
600°	0.296	0.000	6,212	6,010	7,090	7,820	8,530
700°	0.294	0.000	6,212	6,010	7,090	7,820	8,530
800°	0.292	0.000	6,212	6,010	7,090	7,820	8,530
900°	0.290	0.000	6,212	6,010	7,090	7,820	8,530
1000°	0.288	0.000	6,212	6,010	7,090	7,820	8,530
1100°	0.286	0.000	6,212	6,010	7,090	7,820	8,530
1200°	0.284	0.000	6,212	6,010	7,090	7,820	8,530
1300°	0.282	0.000	6,212	6,010	7,090	7,820	8,530
1400°	0.280	0.000	6,212	6,010	7,090	7,820	8,530
1500°	0.278	0.000	6,212	6,010	7,090	7,820	8,530

Coefficient of Linear Expansion = 7.03 micro-inches per inch per °F

Poisson's ratio for Steel = 0.30

Density of Steel = 0.283 lbs/cu. in.

Table VI

Dimensions and Strain Data for Ring #4

Angle	h in.	b in	Strains in micro-inches per inch at pressures indicated 0	99	150	200	252	303	353	378
0°	0.261	0.445	7,000	6,670	6,460	6,170	5,720	5,140	4,260	3,340
30°	0.254	0.446	7,000	6,765	6,600	6,410	6,140	5,800	5,340	4,910
60°	0.251	0.446	7,000	6,900	6,850	6,855	6,925	7,090	7,420	7,810
90°	0.246	0.444	7,000	7,080	7,170	7,350	7,670	8,180	9,025	9,950
120°	0.249	0.444	7,000	6,880	6,860	6.880	6,955	7,110	7,425	7,820
150°	0.246	0.444	7,000	6,740	6,600	6,390	6,115	5,700	5,105	———
180°	0.244	0.445	7,000	6,630	6,400	6,045	5,580	4,900	3,900	———
210°	0.244	0.445	7,000	6,720	6,550	6,340	6,090	5,770	5,390	———
240°	0.245	0.445	7,000	6,950	6,940	7,015	7,150	7,470	8,000	———
270°	0.248	0.444	7,000	7,120	7,215	7,420	7,690	8,205	7,980	———
300°	0.255	0.444	7,000	6,855	6,790	6,775	6,760	6,820	6,950	———
330°	0.262	0.444	7,000	6,710	6,570	6,345	6,100	5,680	5,135	———

Collapse Pressure = 383 psi

Outside Radius = 4.506"

Diameter readings in inches

0-180°	9.102	90-270°	8.910
15-195°	9.099	105-285°	8.953
30-210°	9.069	120-300°	9.006
45-225°	9.028	135-315°	9.047
60-240°	8.986	150-330°	9.075
75-255°	8.940	165-345°	9.097

Table VI

Displacements and Strain Data for Ring #4

Station	0	45	90	135	180	225	270	315
Displacements in micro-inches per inch of original radius								
δ_r								
δ_θ								
$\gamma_{r\theta}$								
ϵ_r								
ϵ_θ								
ϵ_1								
ϵ_2								
ϵ_{max}								
ϵ_{min}								
ϵ_{oct}								
τ_{max}								
σ_{oct}								
σ_{eff}								

Octahedral strains = $\epsilon_{oct} = \frac{\sqrt{2}}{3}\sqrt{(\epsilon_1-\epsilon_2)^2+(\epsilon_2-\epsilon_3)^2+(\epsilon_3-\epsilon_1)^2}$

Table VII

Dimensions and Strain Data for Ring #5

Angle	h	b	Strains in micro-inches per inch at pressures indicated								
	in.	in.	0	49	99	150	200	252	303	328	353
0°	0.244	0.444	9,000	8,910	8,625	8,290	7,880	7,390	6,630	6,120	5,250
30°	0.243	0.441	9,000	8,870	8,650	8,400	8,100	7,750	7,260	6,960	6,455
60°	0.243	0.444	9,000	8,860	8,860	8,880	8,930	9,030	9,280	9,495	9,880
90°	0.247	0.445	9,000	9,020	9,175	9,415	9,720	10,140	10,800	11,245	12,100
120°	0.256	0.445	9,000	8,925	8,890	8,890	8,925	9,000	9,170	9,295	9,580
150°	0.262	0.444	9,000	8,875	8,695	8,470	8,210	7,900	7,470	7,200	6,760
180°	0.261	0.443	9,000	8,850	8,605	8,260	7,860	7,360	6,650	6,200	5,380
210°	0.253	0.445	9,000	8,900	8,710	8,470	8,215	7,880	7,430	7,130	7,595
240°	0.250	0.445	9,000	8,930	8,910	8,920	8,960	9,030	9,200	9,320	9,590
270°	0.248	0.444	9,000	8,955	9,100	9,330	9,600	9,990	10,625	11,060	11,905
300°	0.249	0.44 5	9,000	8,900	8,885	8,915	8,965	9,075	9,320	9,530	9,965
330°	0.247	0.445	9,000	8,920	8,765	8,560	8,340	8,090	7,710	7,485	7,115

Collapse Pressure = 365 psi.

Diameter readings in inches

Outside Radius = 4.508"

0-180°	9.138	90-270°	8.856
15-195°	9.122	105-285°	8.923
30-210°	9.097	120-300°	8.994
45-225°	9.046	135-315°	9.041
60-240°	8.985	150-330°	9.086
75-255°	8.920	165-345°	9.122

Table XII

Dimensions and Shapes of Some Typical Ore Bins

Ore bins in advance-tunnel and level-tunnel locations

Width	H	U	Ø	I.50	900	252	300	348	343
8'	0.444	9,420	8,424	8,424	1,860	1,410	4,620	6,120	5,250
10'	0.444	9,420	8,424	8,424	1,860	1,410	4,620	6,120	5,250
12'	0.444	9,420	8,424	8,424	1,860	1,410	4,620	6,120	5,250
14'	0.444	9,420	8,424	8,424	1,860	1,410	4,620	6,120	5,250
16'	0.444	9,420	8,424	8,424	1,860	1,410	4,620	6,120	5,250
18'	0.444	9,420	8,424	8,424	1,860	1,410	4,620	6,120	5,250
20'	0.444	9,420	8,424	8,424	1,860	1,410	4,620	6,120	5,250
22'	0.444	9,420	8,424	8,424	1,860	1,410	4,620	6,120	5,250
24'	0.444	9,420	8,424	8,424	1,860	1,410	4,620	6,120	5,250
26'	0.444	9,420	8,424	8,424	1,860	1,410	4,620	6,120	5,250
28'	0.444	9,420	8,424	8,424	1,860	1,410	4,620	6,120	5,250
30'	0.444	9,420	8,424	8,424	1,860	1,410	4,620	6,120	5,250
32'	0.444	9,420	8,424	8,424	1,860	1,410	4,620	6,120	5,250
34'	0.444	9,420	8,424	8,424	1,860	1,410	4,620	6,120	5,250
36'	0.444	9,420	8,424	8,424	1,860	1,410	4,620	6,120	5,250
38'	0.444	9,420	8,424	8,424	1,860	1,410	4,620	6,120	5,250
40'	0.444	9,420	8,424	8,424	1,860	1,410	4,620	6,120	5,250

Specifications and Dimensions for Steel Bins

8'-0"	0.444	5,420	4,424	4,424	1,860	1,410	4,620	6,120	5,250
10'-0"	0.444	6,420	5,424	5,424	1,860	1,410	4,620	6,120	5,250
12'-0"	0.444	7,420	6,424	6,424	1,860	1,410	4,620	6,120	5,250
14'-0"	0.444	8,420	7,424	7,424	1,860	1,410	4,620	6,120	5,250
16'-0"	0.444	9,420	8,424	8,424	1,860	1,410	4,620	6,120	5,250
18'-0"	0.444	10,420	9,424	9,424	1,860	1,410	4,620	6,120	5,250
20'-0"	0.444	11,420	10,424	10,424	1,860	1,410	4,620	6,120	5,250
22'-0"	0.444	12,420	11,424	11,424	1,860	1,410	4,620	6,120	5,250
24'-0"	0.444	13,420	12,424	12,424	1,860	1,410	4,620	6,120	5,250
26'-0"	0.444	14,420	13,424	13,424	1,860	1,410	4,620	6,120	5,250
28'-0"	0.444	15,420	14,424	14,424	1,860	1,410	4,620	6,120	5,250
30'-0"	0.444	16,420	15,424	15,424	1,860	1,410	4,620	6,120	5,250
32'-0"	0.444	17,420	16,424	16,424	1,860	1,410	4,620	6,120	5,250
34'-0"	0.444	18,420	17,424	17,424	1,860	1,410	4,620	6,120	5,250
36'-0"	0.444	19,420	18,424	18,424	1,860	1,410	4,620	6,120	5,250
38'-0"	0.444	20,420	19,424	19,424	1,860	1,410	4,620	6,120	5,250
40'-0"	0.444	21,420	20,424	20,424	1,860	1,410	4,620	6,120	5,250

Specifications and Dimensions for Steel Bins

Standard Deviation = 4.4508

Table VIII
Dimensions and Strain Data for Ring #6

Angle	h in	b in	Strains in micro-inches per inch at pressures indicated 0	49	99	150	200	252	303
0°	0.244	0.444	9,000	8,740	8,460	8,105	7,580	6,850	5,580
30°	0.243	0.445	9,000	8,780	8,560	8,290	7,945	7,475	6,725
60°	0.244	0.445	9,000	8,960	8,950	8,970	9,080	9,290	9,770
90°	0.244	0.445	9,000	9,155	9,340	9,610	10,035	10,690	11,860
120°	0.248	0.445	9,000	8,990	8,990	9,020	9,120	9,315	9,760
150°	0.249	0.445	9,000	8,830	8,600	8,340	8,005	7,540	6,825
180°	0.247	0.445	9,000	8,720	8,390	7,975	7,445	6,670	5,305
210°	0.252	0.445	9,000	8,840	8,685	8,490	8,240	7,885	7,310
240°	0.257	0.445	9,000	8,995	9,015	9,075	9,200	9,410	9,890
270°	0.261	0.445	9,000	9,100	9,230	9,430	9,770	10,330	11,410
300°	0.260	0.444	9,000	8,990	8,980	9,010	9,115	9,330	9,860
330°	0.253	0.444	9,000	8,870	8,705	8,520	8,280	7,950	7,410

Collapse Pressure = 345 psi.

Outside Radius = 4.506"

Diameter readings in inches

0-180°	9,158	90-270°	8.858
15-195°	9.134	105-285°	8.908
30-210°	9.093	120-300°	8.986
45-225°	9.038	135-315°	9.042
60-240°	8.968	150-330°	8.910
75-255°	8.905	165-345°	9.142

Table IX
Dimensions and Strain Data for Ring #7

Angle	h in.	b in	Strains in micro-inches per inch at pressures indicated 0	49	99	150	200	226	242	273	288
0°	0.252	0.444	9,000	8,695	8,160	7,510	6,700	6,230	5,890	4,920	3,775
30°	0.245	0.444	9,000	8,850	8,465	8,010	7,460	7,180	6,960	6,375	5,850
60°	0.244	0.443	9,000	9,020	9,130	9,280	9,550	9,735	9,880	10,300	10,655
90°	0.244	0.444	9,000	9,140	9,630	10,210	10,950	11,380	11,700	12,725	14,110
120°	0.245	0.444	9,000	8,990	9,110	9,260	9,500	9,660	9,770	10,150	10,450
150°	0.248	0.443	9,000	8,850	8,460	8,130	7,630	7,340	7,140	6,590	6,090
180°	0.249	0.444	9,000	8,685	8,090	7,460	6,635	6,140	5,790	4,760	3,510
210°	0.248	0.444	9,000	8,790	8,485	8,110	7,660	7,420	7,260	6,810	6,465
240°	0.252	0.444	9,000	9,010	9,150	9,290	9,570	9,750	9,900	10,355	10,780
270°	0.257	0.444	9,000	9,230	9,680	10,200	10,910	11,330	11,620	12,570	13,590
300°	0.262	0.443	9,000	8,985	9,130	9,295	9,560	9,710	9,815	10,210	10,575
330°	0.259	0.442	9,000	8,800	8,520	8,220	7,820	7,585	7,430	7,025	6,730

Collapse Pressure = 290 psi

Outside Radius = 4.508"

Diameter readings in inches.

0-180°	9.293	90-270°	8.679
15-195°	9.259	105-285°	8.793
30-210°	9.155	120-300°	8.929
45-225°	9.052	135-315°	9.067
60-240°	8.905	150-330°	9.168
75-255°	8.775	165-345°	9.265

| | | |

Table X

Dimensions and Strain Data for Ring #8

Angle	h in.	b in	Strains in micro-inches per inch at pressure indicated 0	49	99	150	200	226	242	252
0°	0.263	0.445	9,000							
30°	0.260	0.444	9,000	8,660	8,240	7,690	6,935	6,570	6,250	5,940
60°	0.253	0.445	9,000	9,075	9,165	9,325	9,600	9,770	9,900	10,050
90°	0.250	0.445	9,000	9,400	9,930	10,635	11,580	12,200	12,705	13,260
120°	0.248	0.444	9,000	9,110	9,310	9,650	10,170	10,530	10,810	11,110
150°	0.249	0.445	9,000	8,730	8,440	8,100	7,620	7,360	7,185	7,040
180°	0.246	0.445	9,000	8,470	7,800	6,955	5,820	5,070	4,385	3,540
210°	0.244	0.445	9,000	8,680	8,260	7,710	7,040	6,630	6,330	6,050
240°	0.243	0.446	9,000	9,080	9,215	9,430	9,790	10,040	10,230	10,440
270°	0.244	0.445	9,000	9,440	10,010	10,775	11,810	12,520	13,110	13,860
300°	0.247	0.445	9,000	9,075	9,220	9,460	9,835	10,080	10,275	10,465
330°	0.257	0.444	9,000	8,675	8,310	7,835	7,240	6,870	6,585	6,320

Collapse Pressure = 257 psi

Outside Radius = 4.509"

Diameter readings in inches

0-180°	9,386	90-270°	8.571
15-195°	9.341	105-285°	8.686
30-210°	9.207	120-300°	8.847
45-225°	9.066	135-315°	9.026
60-240°	8.879	150-330°	9.167
75-255°	8.659	165-345°	9.286

| | | |

Table XI
Dimensions and Strain Data for Ring #9

Angle	h in.	b in	Strains in micro-inches per inch at pressures indicated. 0	49	99	150	180	200
0°	0.248	0.443	9,000	8,290	7,425	6,260	5,380	4,560
30°	0.244	0.444	9,000	8,570	8,055	7,390	6,910	6,495
60°	0.244	0.444	9,000	9,150	9,395	9,780	10,120	10,410
90°	0.243	0.444	9,000	9,620	10,430	11,490	12,320	13,130
120°	0.244	0.443	9,000	9,190	9,435	9,820	10,140	10,420
150°	0.252	0.444	9,000					
180°	0.261	0.444	9,000	8,290	7,415	6,280	5,430	4,630
210°	0.261	0.445	9,000	8,640	8,220	7,670	7,285	6,960
240°	0.258	0.444	9,000	9,160	9,390	9,745	10,040	10,310
270°	0.251	0.445	9,000	9,570	10,310	11,275	12,025	12,750
300°	0.249	0.443	9,000	9,180	9,440	9,850	10,200	10,520
330°	0.250	0.443	9,000	8,650	8,215	7,645	7,260	6,930

Collapse Pressure = 220 psi

Outside Radius = 4.510"

Diameter readings in inches.

0-180°	9.532	90-270°	8.401
15-195°	9.452	105-285°	8.549
30-210°	9.254	120-300°	8.798
45-225°	9.021	135-315°	9.042
60-240°	8.794	150-330°	9.259
75-255°	8.575	165-345°	9.447

Table 11

Dimensions and Section Data for Plate Girders

Girder Spacing = 6'-0" Span = 60'-0"

Plate	t in.	d in.	Ag in.²	I in.⁴	Sx in.³	rx in.	Ix/Ag in.²	Ix/Ag in.²
				Girders not Interconnected			Girders Interconnected	
				Dead Load Only			Dead Load + Live Load	
0°	0.625	60.000	37.500	9,000.0	300.0	15.492	9,000.0	9,000.0
	0.750	60.000	45.000	9,000.0	300.0	14.142	9,000.0	9,000.0
30°	0.625	60.000	37.500	8,202.8	273.4	14.815	8,202.8	8,202.8
	0.750	60.000	45.000	8,378.8	279.3	13.636	8,378.8	8,378.8
45°	0.625	60.000	37.500	7,340.0	244.7	13.993	7,340.0	7,340.0
	0.750	60.000	45.000	7,580.0	252.7	12.910	7,580.0	7,580.0
60°	0.625	60.000	37.500	6,477.5	215.9	13.144	6,477.5	6,477.5
	0.750	60.000	45.000	6,720.0	224.0	12.192	6,720.0	6,720.0
75°	0.625	60.000	37.500	6,000.0	200.0	12.649	6,000.0	6,000.0
	0.750	60.000	45.000	6,240.0	208.0	11.785	6,240.0	6,240.0
90°	0.625	60.000	37.500	5,962.5	198.8	12.649	5,962.5	5,962.5
	0.750	60.000	45.000	6,202.5	206.8	11.785	6,202.5	6,202.5

Girder Spacing = 8'-0" Span = 60'-0"

Plate	t in.	d in.	Ag in.²	I in.⁴	Sx in.³	rx in.	Ix/Ag in.²	Ix/Ag in.²
				Girders not Interconnected			Girders Interconnected	
				Dead Load Only			Dead Load + Live Load	
0°	0.625	60.000	37.500	9,000.0	300.0	15.492	9,000.0	9,000.0
	0.750	60.000	45.000	9,000.0	300.0	14.142	9,000.0	9,000.0
30°	0.625	60.000	37.500	8,202.8	273.4	14.815	8,202.8	8,202.8
	0.750	60.000	45.000	8,378.8	279.3	13.636	8,378.8	8,378.8
45°	0.625	60.000	37.500	7,340.0	244.7	13.993	7,340.0	7,340.0
	0.750	60.000	45.000	7,580.0	252.7	12.910	7,580.0	7,580.0
60°	0.625	60.000	37.500	6,477.5	215.9	13.144	6,477.5	6,477.5
	0.750	60.000	45.000	6,720.0	224.0	12.192	6,720.0	6,720.0
75°	0.625	60.000	37.500	6,000.0	200.0	12.649	6,000.0	6,000.0
	0.750	60.000	45.000	6,240.0	208.0	11.785	6,240.0	6,240.0
90°	0.625	60.000	37.500	5,962.5	198.8	12.649	5,962.5	5,962.5
	0.750	60.000	45.000	6,202.5	206.8	11.785	6,202.5	6,202.5

Girder Spacing = 10'-0" Span = 60'-0"

Plate	t in.	d in.	Ag in.²	I in.⁴	Sx in.³	rx in.	Ix/Ag in.²	Ix/Ag in.²
				Girders not Interconnected			Girders Interconnected	
				Dead Load Only			Dead Load + Live Load	
0°	0.625	60.000	37.500	9,000.0	300.0	15.492	9,000.0	9,000.0
	0.750	60.000	45.000	9,000.0	300.0	14.142	9,000.0	9,000.0
30°	0.625	60.000	37.500	8,202.8	273.4	14.815	8,202.8	8,202.8
	0.750	60.000	45.000	8,378.8	279.3	13.636	8,378.8	8,378.8
45°	0.625	60.000	37.500	7,340.0	244.7	13.993	7,340.0	7,340.0
	0.750	60.000	45.000	7,580.0	252.7	12.910	7,580.0	7,580.0
60°	0.625	60.000	37.500	6,477.5	215.9	13.144	6,477.5	6,477.5
	0.750	60.000	45.000	6,720.0	224.0	12.192	6,720.0	6,720.0
75°	0.625	60.000	37.500	6,000.0	200.0	12.649	6,000.0	6,000.0
	0.750	60.000	45.000	6,240.0	208.0	11.785	6,240.0	6,240.0
90°	0.625	60.000	37.500	5,962.5	198.8	12.649	5,962.5	5,962.5
	0.750	60.000	45.000	6,202.5	206.8	11.785	6,202.5	6,202.5

APPENDIX D

Literature Citations

(1) J. M. MONCRIEFF, "The Practical Column Under Central or Eccentric Loads", Transactions of the American Society of Civil Engineers, Vol. XLV, 1901, pp. 334-431.

(2) M. LEVY, "Buckling of Circular Rings and Tubes Under Uniform External Pressure", J. Math Pure et Appl. (Liouville), Vol. 10, No. 3, 1884, pp. 5.

(3) A. P. BORESI, Thesis submitted at University of Illinois, 1952.

(4) S. P. TIMOSHENKO, "Strength of Materials", Part II, Second Edition, August 1941, D. Van Nostrand Company, Inc., 250 Fourth Avenue, New York, pp. 101 - 103, 216 - 224.

(5) "Metals Handbook", 1948 Edition, pp. 109-111, 822.

(6) D. A. POLYCHRONE, "On the Buckling of Intermittently Supported Plates", Doctor of Science Thesis, M.I.T., 1949, pp. 64-73.

(7) M. L. PITTMAN and V. W. RINEHART, "On Providing Uniform Edge Compression Loads for Wide Flat Plates", N.A. Thesis, 1954.

APPENDIX D

Literature Citations

(1) M. BOUDRILLET, "The Practical Column Under Central or Eccentric Loads", Transactions of the American Society of Civil Engineers, Vol. XIV, 1901, pp. 339-431.

(2) M. LEVY, "Buckling of Circular Rings and Tubes Under Uniform External Pressure", J. Math Pure et Appl. (Liouville), Vol. 10, No. 3, 1884, pp. 5.

(3) A. P. BORESI, Theory Advanced at University of Illinois, 1952.

(4) S. P. TIMOSHENKO, "Strength of Materials", Part II, Second Edition, August 1941, D. Van Nostrand Company, Inc., 250 Fourth Avenue, New York, pp. 101 - 103, 218 - 224.

(5) "Metals Handbook", 1948 Edition, pp. 109-111, 822.

(6) D. A. DUNLOPBROWN, "On the Buckling of Internittently Supported Plates", Doctor of Science Thesis, M.I.T., 1949, pp. 64-73.

(7) E. L. PITTMAN and V. R. RIEMHART, "On Providing Uniform Edge Compression Loads for Wide Flat Plates", T.A. Thesis, 1954.